WL-TR-91-3126

TURBULENCE MODELING

A. L. Laganelli
UNISTRY Associates, Inc.
129 North Eagle Road
Havertown, PA 19083

S. M. Dash
Science Applications, International Corp.
501 Office Center Drive, Suite 420
Fort Washington, PA 19034

October 1991

Final Report for Period: 10 May 1991 – 10 October 1991

Approved for Public Release; Distribution is Unlimited.

FLIGHT DYNAMICS LABORATORY
WRIGHT RESEARCH AND DEVELOPMENT CENTER
WRIGHT-PATTERSON AIR FORCE BASE, OH 45433-7542

REPORT DOCUMENTATION PAGE

Form Approved
OMB No. 0704-0188

1. REPORT DATE *(DD-MM-YYYY)*	2. REPORT TYPE	3. DATES COVERED *(From - To)*
October 1991	FINAL	10 May 91 - 10 Oct 91

4. TITLE AND SUBTITLE

Turbulence Modeling

5a. CONTRACT NUMBER
F33615-91-C-3002

5b. GRANT NUMBER

5c. PROGRAM ELEMENT NUMBER

6. AUTHOR(S)

Anthony L. Laganelli – UNISTRY Associates, Inc.

Sanford M. Dash – Science Applications, International Corp.

5d. PROJECT NUMBER

5e. TASK NUMBER

5f. WORK UNIT NUMBER

7. PERFORMING ORGANIZATION NAME(S) AND ADDRESS(ES)

UNISTRY Associates, Inc.
129 North Eagle Road

Science Applications, Int'l Corp
501 Office Center Dr Ste 420

8. PERFORMING ORGANIZATION REPORT NUMBER

UA-TR-91-03

9. SPONSORING / MONITORING AGENCY NAME(S) AND ADDRESS(ES)

Flight Dynamics Laboratory
Wright Research and Development Center
Wright-Patterson Air Force Base, OH 45433-7542

10. SPONSOR/MONITOR'S ACRONYM(S)

WRDC/FIMG

11. SPONSOR/MONITOR'S REPORT NUMBER(S)

WL-TR-91-3126

12. DISTRIBUTION / AVAILABILITY STATEMENT

Approved for Public Release; distribution is unlimited

13. SUPPLEMENTARY NOTES

14. ABSTRACT

An investigation of the embodied physics in turbulence closure models was made that focused on compressible turbulent flows, boundary layer and free shear layers, including wall effects such as roughness, blowing, curvature. A hybrid k-3 turbulence model was selected that consists of the standard two-equation model for the outer layer and a one-equation model for the inner viscous layer. This model was chosen due to its success in analyzing compressible flows including interactions, as well as the experience base using k-e models to treat a wide range of engineering problems, while also being adaptable to industrial codes. The baseline model will consider the Sarkar and Zeman compressible-dilatation terms together with the hybrid k-e turbulence model.

A phase II building-block approach is recommended that provides a "dial-a-model" menu from a matrix of turbulence closure coefficients generated from the baseline compressible hybrid k-e model and a multi-zone Navier-Stokes solver. A direct result of this effort will be the technology transfer to the government/industrial sector and the commercialization of a "Turbulence-Tutorial." The tutorial will consist of a boundary layer code, turbulence models, and a database adaptable to a PC to provide researchers/teachers/students with guidance to explore turbulence issues.

15. SUBJECT TERMS

16. SECURITY CLASSIFICATION OF:			17. LIMITATION OF ABSTRACT	18. NUMBER OF PAGES	19a. NAME OF RESPONSIBLE PERSON
a. REPORT	b. ABSTRACT	c. THIS PAGE			AFRL/VA
UNCLASSIFIED	UNCLASSIFIED	UNCLASSIFIED	SAR	78	19b. TELEPHONE NUMBER *(include area code)* 937-255-1871

Standard Form 298 (Rev. 8-98)
Prescribed by ANSI Std. 239.18

TABLE OF CONTENTS

TABLE OF CONTENTS (Continued)

LIST OF TABLES

LIST OF FIGURES

1.0 INTRODUCTION AND SIGNIFICANCE OF PROBLEM

During the past two decades, a significant amount of effort has been directed toward developing methodologies for turbulence closure of the time-averaged Navier-Stokes (N-S) equations. Several workshops have been held to address issues concerning turbulence modeling. These issues consisted of the use of simple models to predict complex flows that are three-dimensional in nature, computational efficiency of higher order models, test database for model validation, and the degree of accuracy of higher order models over simple models to predict complex flow experienced in engineering design. The most noted consisted of the AFSOR/HTTM-Stanford Conference (Kline, et al,1982) on complex turbulent flows. This conference followed an earlier conference (1968) that extended the limited two-dimensional, incompressible work to include compressibility, curvature, mass transfer, separation, and secondary motion. More recently, several workshops have been held on the subject matter relative to application to the National AeroSpace Plane (NASP) program (NASP, 1989 - 1991) as well as Cornell University (Lumley, 1990) that led to a continuation of the Stanford effort (Bradshaw, et al, 1-91). This recent work considered a more complete range of test cases with a focus on compressible flows that included shock/boundary layer interactions.

In general, the techniques that have been developed to date have been based on two-dimensional, incompressible, fundamental parallel shear flows. These techniques have subsequently been extended to three-dimensional, compressible, complex flowfields and have been shown to be inadequate and usually without generality. While advances have been made in numerical algorithms to aid the turbulence modeler and facilitate computer storage, full Reynolds stress solutions is still considered long range. Accordingly, generalization of existing techniques based on low-speed turbulence models and physical evidence appears capable of meeting near term requirements for the design process and will be the focus of this review.

Several recent papers have appeared in the literature that have essentially reviewed the state-of-the-art in turbulence modeling and have formed the basis of this investigation. These include the work of Rodi (1-91) and Chen and Patel (1988) who introduced a hybrid model that consists of the standard k- ε equations for the outer part of the boundary layer and a one-equation model with standard empirical description of the length scale (ε) for the near wall region.

Compressibility effects were examined by Rubesin (1-89), Viegas and Rubesin (6-91), Cousteix, et al (1-91), Situ and Schetz (6-91), and Dash (6-91). Compressibility corrections appeared to improve the spreadrate predictions of unconfined flows but did not work as well as turbulence models without the corrections for boundary layer flows.

A critical evaluation of two-equation models for near wall turbulence was presented by Speziale, et al (6-90) and an excellent examination of several turbulence

models was made by Menter (June, 1991) for attached and separated flows. In the latter paper, the models of Baldwin and Barth (1-91 and 8-90), Johnson and King (11-85), Baldwin and Lomax (1978), and Wilcox (11-88) were examined. Wilcox (1-91 and 6-91) presents an historical review of the k-ω two- equation model as well as progress in hypersonic turbulence modeling. The later paper also included a critique of compressible effects.

Horstman (6-91) compared several hypersonic flow cases using a standard k-ε model, the Rodi (1-91) hybrid model, and the k-ε model with variations of compressible effects using the work of Rubesin (6-90) and Verong and Coakley (1-87) for correction to the turbulent length scale. To examine the effects of the individual modifications in the compressible model, Horstman provided solutions with the Rubesin correction alone and with the length scale correction alone. When compared to the standard k-ε compressible model, the length scale correction had a significant impact on heat transfer in the reattachment region as well as controlling the separation length.

Turbulence models that have received wide spread attention are the k-ε models which were developed for incompressible flows. The apparent limitation in the k-ε models lies with the ε transport equations intrinsic behavior approaching solid boundaries (viscous, near wall region). Accordingly, bridging techniques (wall functions) have been adapted to accommodate the viscous thin-layer region where steep gradients exist. However, the use of the law of the wall and the assumption that turbulent quantities can be expressed in terms of the wall shear velocity fail under severe pressure gradient flows since the near wall region is not controlled by wall shear stress.

An examination of two-equation models with low Reynolds number techniques was made by Patel et al, (1985) for incompressible flows which indicated that improvements were required for damping in order to develop a more generalized turbulence model. Shih (8-90) reviewed this work together with direct simulation (DNS) of the Reynolds stresses (Mansour et al, 1988) and proposed a modification of the pressure transport term of the k-equation as well as a length scale correction to account for the asymptotic behavior of the dissipation rate to be $\varepsilon \sim 0\ (y^2)$ near the wall.

Table I provides a hierarchy of turbulence models which has expanded upon the summaries of Dash (6-91) as well as Rubesin (1-89). Dash noted that with current-generation main-frame computers (CRAY-2, for example), a grid-resolved, steady 3D flowfield solution using a two-equation turbulence model in an efficient PNS solver can require over twenty-four hours of CPU time, depending on grid requirements and complexity of thermochemistry. Accordingly a practical viewpoint is required to meet near-term work required for use in advanced CFD codes. Turbulence modeling at the two-equation level meets this requirement.

TABLE 1 HIERARCHY OF TURBULENCE MODELS

LARGE-EDDY SIMULATION	SOLVES LARGE-SCALE USING 3D MESH WITH TIME-AND-SPACE RESOLUTION WITH B.C.'S THAT ARE TRANSIENT OR PERIODIC
SECOND-ORDER CLOSURE (COMPRESSIBLE)	DONALDSON ET AL.; ONE-POINT/ONE-TIME MOMENT EQUATION–DISSIPATION/DIFFUSION/PRESSURE STRAIN/NEAR WALL CORRECTIONS/EXTRA COMPRESSIBLE TERMS/GEOMETRIC TERMS
REYNOLDS STRESS MODELS (INCOMPRESSIBLE)	LAUNDER ET AL.; ELIMINATES BOUSSINESQ/ISOTROPIC ASSUMPTION–SEVERAL PDE'S FOR TURBULENCE STRESS TENSOR $(\overline{u'_i u'_j})$
GENERALIZED EXTENSIONS OF TWO-EQUATION MODELS	• ALGEBRAIC REYNOLDS STRESS (HANJALIC ET AL., k-ε WITH NON-ISOTROPIC CORRECTIONS) • MULTI-SCALE (HANJALIC/k-ε AND WILCOX/k-$\tilde{\omega}$) • SPEZIALE/k-τ, WHICH IS A k-$\tilde{\omega}$ TYPE–AN ISOTROPIC, TIME DERIVATIVE INTRODUCES LAG BETWEEN RESPONSE OF STRESS AND MEAN MOTION

TABLE 1 HIERARCHY OF TURBULENCE MODELS (CONTINUED)

TWO-EQUATION MODELS

$(k-\varepsilon, k-\tilde{\omega}, k-\tau, k-w)$,

$v=\sqrt{k}$, and $\ell=\ell(k,\varepsilon)$

- LAG EFFECTS ACCOUNTED FOR, $v=\sqrt{k}$, $\ell=\ell(k,\varepsilon)$:

  $(k-\varepsilon)$ RODI,LOUNDER, SPEZIALE, ET AL.
  $(k-\tilde{\omega})$ SAFFMAN, WILCOX, ET AL.
  $(k-\tau)$ SPAZIALE, ET AL.
  $(k-w)$ SPALDING

- AD-HOC EXTENSIONS FOR CURVATURE AND COMPRESSIBILITY

- k-ε (INCOMPRESSIBLE) WALL FUNCTIONS: CHIEN, LAM-BREMHORST,SHIH, DUTOYA-MICHARD,HASSID-POREH,LAUNDER-SHARMA, HOFFMAN, GORSKI, CHEN, ETC.

- k-ε (INCOMPRESSIBLE) BRIDGING TECHNIQUES WITH VAN-DRIEST DAMPING: DASH, CHIENG-LAUNDER, VIEGAS-RUBESIN

- COMPRESSIBLE MODIFICATIONS: DASH, SARKER, ET AL., ZEMAN, WILCOX, SPEZIALE, ET AL.

- TWO-LAYER MODELS $(v=\sqrt{k}, \ell=\ell(k))$: FEATURE TWO EQUATION k-ε FOR THE OUTER LAYER AND A ONE-EQUATION MODEL FOR LENGTH SCALE WITH k EQUATION FOR INNER LAYER:

  PATEL, ET AL. (WITH WOLFSHTEIN), AND RODI (WITH NORRIS-REYNOLDS) IACOVIDES-LAUNDER (WITH VAN DRIEST): INCOMP.

  HORSTMAN(WITH RODI AND RUBESIN EXTRA COMP.TERMS):COMP.

TABLE 1 HIERARCHY OF TURBULENCE MODELS (CONTINUED)

ONE-AND ONE-HALF MODEL $R_T = k^2/\nu\varepsilon$	• FEATURES COUPLING OF k-ε EQUATIONS INTO A TRANSFRORMED VARIABLE (R_T) AND ELIMINATES THE NEED FOR A LENGTH SCALE: BALDWIN-BARTH

ONE-EQUATION MODEL
$v = \sqrt{k}$, $\ell = \ell(k)$
	• LAG EFFECTS ACCOUNTED FOR
	• USE TURBULENT k-ε PDE AND ALGEBRAIC LENGTH SCALE
	  • WOLFSHTEIN AND NORRIS-REYNOLDS (USE LENGTH SCALE WITH DAMPING BASED ON VELOCITY OF TURBULENCE KINETIC ENERGY)
	  • GOLDBUG INTRODUCED TWO TIME-SCALES TO DETERMINE LARGE/SMALL EDDY LENGTH SCALES

ONE-HALF EQUATION MODEL $v = \sqrt{k_m}$, $\ell = \ell(k_m)$, $k_m = \sqrt{-\overline{u'v'}_m}$ $k_m = \sqrt{-\overline{u'v'}_m\ \rho_m/\rho}$	• DOES NOT USE FIELD EQUATION; PROVIDES ODE TO INTRODUCE LAG BETWEEN TURBULENCE AND MEAN MOTION (STREAM DIRECTION) WHILE IN NORMAL DIRECTION TURBULENCE/MEAN MOTION IN EQUILIBRIUM: JOHNSON-KING: CONSIDERS NON-EQUILIBRIUM EFFECTS IN OUTER LAYER JOHNSON-COAKLEY: INCLUDES A DENSITY RATIO IN VELOCITY SCALE FOR COMPRESSIBLE EFFECTS

TABLE 1 HIERARCHY OF TURBULENCE MODELS (CONTINUED)

ALGEBRAIC EDDY VISCOSITY MODELS (ZERO EQUATION) $\nu = u_\tau$, $\ell = \ell(u_\tau)$

- NO LAG HISTORY EFFECTS

  BOUSSINESQ ASSUMPTION $\rho\overline{u'v'} = \mu_\tau \partial\bar{u}/\partial y$

  ISOTROPIC $\overline{u'u'} = \overline{v'v'} = \overline{\omega'\omega'}$

- BALDWIN-LOMAX/CEBECI-SMITH: BOUNDARY LAYERS
- TING-LIBBY/DONALDSON-GREY: FREE SHEAR LAYERS
- CEBECI-SMITH INTRODUCE PRESSURE GRADIENT, BLOWING, AND ROUGHNESS VIA DAMPING COEFFECIENT WHERE VARIATIONS OF SAME ADOPTED IN HIGHER LEVEL MODELS

As noted in Table I, direct numerical simulation (solves the full/non-averaged Navier-Stokes equation) and large eddy simulation represent the most complete physics for resolving flow characteristics; however, these methodologies are restricted to simulation of simplistic shear flows at low Reynolds numbers. Second-order closure have not demonstrated invariance with fixed coefficients, and their inclusion into advanced computer codes would not permit solutions of realistic flow problems on current generation computers.

Reynolds stress and generalized extensions of two-equation models (such as algebraic Reynolds stress models) have eliminated the Boussinesq/isotropic assumptions but still require several partial differential equations for the stress tensor, or require multiple scales, or modifications to closure constants to allow for more physics. The degree of complexity of these models together with computational time have not shown to be significantly better than the simpler two-equation models.

The remainder of Table I shows the standard two-equation models currently used in the scientific community, variations of these models that have been adapted to handle near-wall conditions, compressibility, and curvature as well as several recent lower order models that have shown successes for a variety of complex flows. As previously noted, the most popular two-equation model is the k-ε model where ad-hoc extensions have been made to include compressibility and curvature. In order to eliminate numerical difficulties of integration (of dissipation) to the wall, bridging techniques (van Driest), wall-functions (low-Reynolds number techniques) and one-equation models (hybrid models) have been adopted to accommodate length scales for the near-wall region. In the latter models, the use of kinetic energy has been used for the velocity scale.

A one and one-half equation model, so named in as much as it retains characteristics of the field equations (k-ε), has recently been developed (Baldwin and Barth, 1-91) that couples the k-ε equations through a transformed variable ($R_T = k^2/\upsilon\varepsilon$) that eliminates need for a length scale (but introduces damping similar to the hybrid models above). Finally, one-equation models that account for lag effects and use the kinetic energy field equation for the velocity scale, variations that include two-time-scales, a one-half model that uses an ordinary differential equation to introduce lag between turbulence and mean motion, and the popular algebraic eddy viscosity models complete the table.

While many successes have been shown for unit problems, i.e., individual effects of pressure gradient, mass transfer, roughness, non-isoenergetic flow etc., within the incompressible or compressible flow state, coupling of these effects has not been demonstrated. A turbulence model utilized for a generalized flow problem must be able to produce the "simpler" unit level problem as well as the coupling effects in order to fully embody the physics in the model and provide agreement with data that would not be fortuitous or due to error cancellation. In attempting to meet this objective,

consideration to Reynolds stress models featuring algebraic, one- equation, and two-equation models will be made relative to velocity and length scale characteristics.

1.1 Program Objectives

The objectives of the proposed program is to investigate the embodied physics of several popular turbulence closure models in order to determine the feasibility of developing universality capable of providing near term solutions to engineering design problems. The model should include compressibility, wall conditions such as roughness, mass transfer, and pressure gradient/curvature and be applicable to both the boundary layer and free shear-layer flows. While the focus is on parallel shear-layer flows, a secondary objective was to examine flows experiencing separation and interactions. The module selected with appropriate modifications should be adaptable to state of the art multizonal Navier-Stokes solvers used in the industrial community. A roadmap to achieve these objectives which can be accomplished in a Phase II program will be investigated.

1.2 Report Organization

The report has been organized into six sections and appendices. This introduction (Section 1) provides an introduction of the turbulence modeling methodologies and issues, and is followed by Section 2 that examines several turbulence models with the pertinent physics that delineate reasons why the models work for various flow conditions. Section 3 provides a recommendation for a turbulence closure model that can be used in a multizonal PNS solver (Section 4) and encompass sufficient generality to handle a large body of geometric/flow engineering problems. A road map is provided in Section 5 that describes how the recommended turbulence model can be generalized through a building block approach to handle unit level as well as coupling of unit level problems subject to compressible flow conditions. A compressible flow database will be outlined for this approach. Finally, Section 6 assesses the results of the Phase I investigation as well as outlines a technical approach for a Phase II program to obtain a generalized turbulence model capable of solving a large class of practical engineering problems.

Appendices are also provided that list details of the turbulence models examined during this program.

2.0 TURBULENCE MODEL REVIEW

This review contains subject matter that can be found in a number of texts (or papers) but is repeated for completeness in order to provide background concerning the turbulence scales of length and velocity and why variations in the choice of these scales can solve a number of turbulent flow states.

The review focussed on models that employ the Boussinesq criteria that the stress-strain law for time-averaged turbulent flow is analogous to viscous fluids. The eddy viscosity function can be expressed in terms of length (ι) and velocity (u) scales such as

$$\mu_t = \iota u$$

The length and velocity scales can be obtained via algebraic functions involving properties of the mean flow and geometry or from differential equations for one or more properties of the turbulent motion. When ι and u are determined in terms of an algebraic form of the mean motion, the models are referred to as zero-equation. When ι is determined algebraically and u is found from a solution to the turbulent kinetic energy transport equation, the model is referred to as a one-equation model. When both ι and u are determined from transport equations, the model is considered a two-equation model

The Boussinesq criteria allows for

$$\tau = \rho \overline{u' v'} = \mu_t \, \partial u/\partial y$$

where μ_t is a property of the local state of turbulence (becomes effective only when there is motion) and is not a property of the fluid. Prandtl proposed a formulation for the eddy viscosity (mixing length hypothesis), namely

$$\mu_t = \iota^2 \left| \frac{\partial u}{\partial y} \right| \rho$$

where ι the mixing-length, is algebraically prescribed and is characteristic of the mean free path of molecules (kinetic theory of gases). The eddy viscosity implies a gradient-type diffusion.

Prandtl later proposed a model that employed the turbulence kinetic energy as the characteristic velocity scale, such that

$$\mu_t = \rho \, k^{1/2} \, \iota$$

where ι is again prescribed algebraically and k requires a solution of a differential equation of turbulent energy transport. Kolmogorov proposed two independent properties to represent the eddy viscosity (see Wilcox description, 1-91) that consisted of turbulence energy k and a characteristic frequency of the motion. For this situation, the eddy viscosity is written as

$$\mu_t = \rho\, k/f$$

where comparison to the Prandtl model allows for $\iota = k^{1/2}/f$ and both k and f (which is ω in the k- ω models) are determined by differential equations of transport.

Several modifications have been made to these basic models. One of the more notable modifications is due to van Driest who introduced a damping factor, such that

$$\mu_{eff} = \mu_L + \mu_t = \mu_L + \rho\, \iota^2_m \left|\frac{\partial u}{\partial y}\right|$$

where

$$\iota_m = k\, y\, [1 - \exp(-y^+/A^+)]$$

for $u^+ = u_\tau y/\upsilon$ and $A^+ = 26$. An effective viscosity is defined that allows for both laminar and turbulent contributions where the latter includes a damping function whose effect is experienced in the near wall region ($y^+ < A^+$).

The above represent a basic formulation from which eddy viscosity models are developed. What follows will be a discussion on variations of length and velocity scales that have been recently reinvestigated and applied to a variety of complex flows. The Cebeci-Smith (1974) and Baldwin-Lomax (1978) zero-equation models are considered as standards from which other turbulence models can be judged. Because the Cebeci-Smith model embodies significant physics for wall bounded parallel shear flows that include pressure gradient, mass transfer, and compressibility, details of this model will be given. Modifications to include rough wall effects based on the work of Laganelli (1-75) and independently discovered (for incompressible flow) by Krogstad (6-91) will also be addressed. The reason for this development is to incorporate techniques suggested by Cebeci-Smith (1974) and Laganelli (1-75 and 12-89) together with the scales of velocity and length as provided in more recent work which are based on the Prandtl-Kolmogorov concept. These techniques will encompass wall conditions for curvature, mass transfer, and roughness.

2.1 Zero-Equation Turbulence Models

2.1.1 Cebeci-Smith (C-S) Model

The Cebeci-Smith turbulence model is a two-layer model consisting of the Prandtl mixing length (inner-layer) and the Clauser model (for the outer-layer). The inner region can be expressed as

$$-\rho \overline{u'v'} = \rho \iota^2 (\partial u/\partial y)^2 = \rho \nu_{mi} (\partial u/\partial y) \tag{1}$$

where

$$\nu_{mi} = \iota^2 |\partial u/\partial y| \tag{2}$$

Introducing the dimensionless groups $u^+ = u/u_\tau$, $y^+ = u_\tau y/\upsilon_w$, $\iota^+ = u_\tau \iota/\upsilon_w$ and $A^+ = u_\tau A/\upsilon_w$, together with the van Driest damping function, the eddy viscosity becomes

$$\nu_{mi} = k^2 (y^+)^2 [1 - \exp(-y^+/A^+)^2] \; |\partial u^+/\partial y^+| \, \nu_w \tag{3}$$

The outer region is expressed as

$$\nu_{m_o} = 0.0168 \; \delta^* U_e \gamma_0 \tag{4}$$

where γ_0, the Klebanoff intermittency factor, is defined as

$$\gamma_0 = [1 + 5.5 (y/\delta)^6]^{-1} \tag{5}$$

The strain gradient $|\partial u/\partial y|$ can be expressed as $|\partial u/\partial y + \partial v/\partial x|$ for two-dimensional problems. The non-dimensional parameter A^+ can be a function of pressure gradient as well as wall conditions (surface roughness and mass transfer). For smooth walls without pressure gradients, the parameter has been determined to be $A^+ = 26$.

The van Driest damping functions is based on Stokes flow for an infinite flat plate undergoing a simple harmonic oscillation where the amplitude of motion diminishes from the wall by the factor $e^{-y/A}$. The constant A depends upon the frequency of oscillation and the fluid viscosity. By fixing the plate relative to the fluid (which now

oscillates), a factor $(1 - e^{-y/A})$ is applied to the fluid oscillation to account for wall damping effects.

In order to accomodate compressiblity, curviture, and mass transfer effects, C-S modified the damping coefficient A^+ such that

$$A^+ = 26 \frac{1}{N} (\rho_w/\bar{\rho})^{1/2} (\bar{\mu}/\mu_w) \qquad (6)$$

- $\frac{1}{N}$: pressure gradient & mass transfer contribution
- $(\rho_w/\bar{\rho})^{1/2}$: compressible contribution
- $(\bar{\mu}/\mu_w)$: incompressible value

Details of this development are provided in Appendix A. In equation (6), the average properties $\bar{\rho}$ and $\bar{\mu}$ are usually chosen to be local values of ρ and μ. the compressible term has been shown to be a valuable contribution for treating non-adiabatic wall conditions.

Further modifications have been made to the C-S model to incorporate wall roughness (see Appendix A) by introducing a vortex generating factor to the mixing length as suggested by van Driest; namely

$$\iota_m^+ = \kappa y^+ [\, 1 - \exp(-y^+/26) + \exp(-60y^+/k_r^+)] \qquad (7)$$

However, the above does not allow reoughness heights to grow for $k_r^+ > 60$ where the viscous sublayer would be eradicated and is in conflict with experimental data. In order to allow the damping factor to be in excess of unity, an incrumental factor due to roughness is introduced such that

$$D_{kr} = [\, 1 + k_r^+/30y^+] \exp(-2.3y^+/k_r^+) \qquad (8)$$

and the damping becomes

$$D = D_{smooth} + D_{kr} \qquad (9)$$

where D_{kr} is the sole means of introducing roughness effects.

The turbulent viscosity coefficients is transitioned from the inner to the outer layer about a switch y_c point defined as follows

$$\mu_t = \begin{cases} \mu_{ti} \text{ @ } y < y_c \\ \mu_{to} \text{ @ } y > y_c \end{cases} \qquad (10)$$

where y_c is the smallest value of y where $\mu_{ti} = \mu_{to}$.

2.2 Characteristic Scales of Turbulence Modeling

In the previous section, it was noted that zero-equation models provided length and velocity scales using prescribed algebraic discriptions. One-equation models used the turbulent kinetic energy field equation for the velocity scale ($k^{1/2}$) and an algebraic prescription for the length scale. Two-equation turbulence models required field equations for both the velocity ($k^{1/2}$) and length ($k^{3/2}/\varepsilon$) scales. Here, the length scale has the characteristics required by Kolmogorov (i.e. $\iota = k^{1/2}/f = k^{3/2}/\varepsilon$ where $f = \omega = \varepsilon/k$) and ε is determined by the dissipation rate equation

$$\nu_t = C_\mu f_\mu k^2/\varepsilon \qquad (11)$$

In the above equation, the damping term f_μ is critical for mean flow predictions and must have the correct asympototic dependence as $y \to 0$ in order for $\nu_t \sim 0\ (y^3)$.

since $k^{3/2}/\varepsilon$ is a characteristic length scale of energy containing eddies $\sim 0\ (\iota)$ and the length scale $k^{3/2}/\varepsilon \sim 0\ (y^3)$, a modification to the eddy viscosity is required to allow for $k^{3/2}/\varepsilon \sim 0\ (y)$. For this situation, the damping term f_μ must be on the order of y for ν_t to be correct and approach unity away from the wall. The scaling requirements are as follows

$$\begin{aligned} &k \sim 0\ (y^2),\ \varepsilon \sim 0\ (1),\ \tau \sim 0\ (y^2),\ f_\mu \sim 0\ (y) \\ &\overline{u'u'} \sim 0\ (y^2),\ \overline{u'v'} \sim 0\ (y^3),\ \frac{\partial u}{\partial y} \sim 0\ (1) \\ &\text{then}\ \ \nu_t \sim 0\ (y^3) \end{aligned} \qquad (12)$$

Appendix H provides a further discussion of scaling issues.

An examination of the C-S model shows that

$$-\rho\,\overline{u'v'} = \rho\,\nu_t \frac{\partial u}{\partial y} = \rho\,(\kappa\, y\, D)^2 \left|\frac{\partial u}{\partial y}\right| \frac{\partial u}{\partial y} \sim o\ (y^4)$$

where as the theory of kinematics shows $-\rho\,\overline{u'v'} \sim 0\ (y^3)$ and could be $\sim 0\ (y^4)$ if all fluctuating quantity correlations were used. Here, we note that the C-S model would yield $-\rho\,\overline{u'v'} \sim 0\ (y^2)$ without damping and would provide an incorrect asymptotic behavior at the wall.

The Baldwin-Lomax (B-L) model, see Appendix B for details, has similar features that are more avantages. Specifically, the B-L model eliminates the outer length scale requirement of boundary layer thickness and uses the magnitude of the vorticity vector as opposed to shear strain for velocity scale.

The diagram below depicts the characteristics of the C-S and B-L models. For attached boundary layer flow, both C-S and B-L models provide adequate solutions to compressible flow problems (modest curvature). The B-L model is shown to have a maximum wake function (y ω D) at y/δ of approximately 60% where the wake factor reaches a maximum (representative of the velocity scale). The turbulent viscosity is shown for the inner and outer regions with the switch point at y_c/δ. When flow separation is experienced, the wake provides a double "hump" where the first hump exceeds the wake function maximum value at y/δ of 0.6. Here, the turbulent viscosity can yield values on order of magnitude less at the switch point than values attained for attached flow conditions.

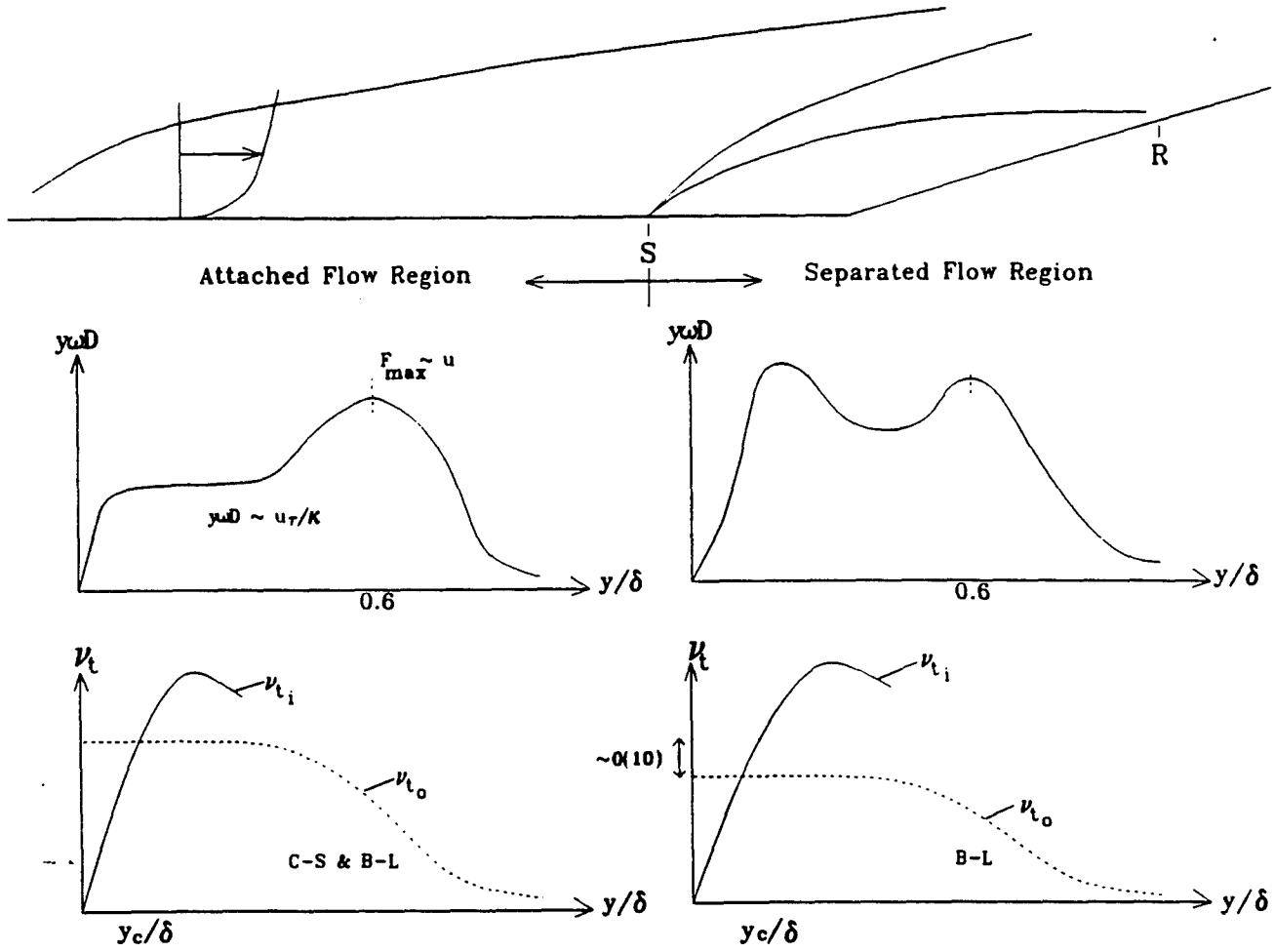

Both C-S and B-L models have been shown to be deficient for separated flows. This is a consequence of strong pressure gardients where separation can cause the shear stress to change sign. Moreover, use of law of the wall relations and turbulence equations based on wall shear stress fail since the near-wall region is not controlled by u_τ. Finally, the constants C_{cp} and C_{KLEB} in Table B.1 have been shown to be a function of compressibility, wall temperature, and skin-friction.

2.3 One-Half Equation Model: Johnson and King (J-K)

The Johnson and King (11-85) model is a non-equilibrium eddy viscosity model that is formulated with an algebraic eddy-viscosity relation and an ordinary differential equation (ODE) based on a simplified turbulent kinetic energy field equation. This equation is based on the distribution of maximum turbulent shear stress which controls the outer layer and ensures lag effects between stress/strain terms. Appendix C provides details for this model.

The inner and outer-layer eddy viscosity relations are expressed as

$$\nu_{ti} = \kappa\, y\, D_{j\text{-}k}\, (\overline{u' v'}_m)^{1/2} \tag{13}$$

and

$$\nu_{to} = \sigma\,(x)\,(0.0168)\, u_e \delta^* \gamma_0 \tag{14}$$

The term σ (x) represents an unknown modeling parameter (history effects) which is solved by the ODE, Eq (9) in Table C.1, and is adjusted to satisfy the relation

$$\nu_t = \frac{(\overline{u' v'}_m)^{1/2}}{(\partial u/\partial y)_m}\, \overline{(u' v'}_m)^{1/2} \tag{15}$$

which can also be expressed as

$$\nu_t = C\, \iota_m\, k_m^{1/2} \tag{16}$$

where the constant C and the length scale ι_m will be addressed for comparitive purposes relative to one-equation and two-equation turbulence models. Further discussion concerning the J-K model and will be provided.

2.4 Characteristics of One-Equation Models

One-equation turbulence models were developed in order to incorporate histroy effects of the turbulent structure. This is a consequence of the inability of the turbulent viscosity to follow sudden changes in the flow structure such as shock/boundary layer interactions and transition from smooth walls to walls featuring roughness or blowing. The eddy viscosity is prescribed as $\nu_t = \nu_t$ (k,ι) where the turbulent kinetic energy k is solved with a transport equation. A closure relationship for the dissipation rate is required such that $\varepsilon = \varepsilon$ (k, ι, ν) where the length scale ι is prescribed

The inner and outer-region dissipation rate ate given as

$$\varepsilon \sim \nu\, k/\iota^2 \tag{17}$$

and

$$\varepsilon \sim k^{3/2}/\ell \tag{18}$$

where a composite of two regions gives

$$\varepsilon = (C_2\, k^{3/2}/\ell)(1 + C_3\, R_T) \tag{19}$$

for

$$R_T = k^{1/2}\, \ell/\nu \tag{20}$$

In the above, as y --> 0, R_T --> 0, and $R_T << C_3$ giving $\varepsilon = C_2\, C_3\, \nu\, k/\ell^2$. On the other hand as y --> ∞, $R_T >> 1$ and $\varepsilon = C_2\, k^{3/2}/\ell$.

The eddy viscosity is expressed as

$$\nu_t = C_4\, k^{1/2}\, \ell\, D \tag{21}$$

where the damping term D is expressed as

$$D = 1 - \exp\,[-C_5\, k^{1/2}\, y/\nu] \tag{22}$$

and the length scale is given as

$$\ell = \begin{cases} \kappa\, \ell @\ y \le y_c \\ C_6 \delta @\ y \ge y_c \end{cases} \tag{23}$$

A number of variations have appeared for the definition of of the length scale in the inner and outer regions of the boundary layers. These variation are presented in Appendix D for the Norris and Reynolds (1975) model, Appendix E for the Goldberg (6-91) model, and Appendix F for the Baldwin and Barth (1-91) model.

2.5 Two-Equation Turbulence Models

The two-equation transport model for turbulent kinetic energy (k) and its dissipation rate (ε) have been formulated to define appropriate velocity and length scales that zero-equation models must specify in an ad-hoc manner. These equations therefore provide a bases for examining more complex flow fields. It is beyond the scope of this paper to give details of the field equation development; accordingly, only a discussion of the results of the models will be provided.

The conservation equations for a turbulent compressible flow field are derived by expressing the dependent variables as a sum of mean and fluctuating quantities. The results are ensemble averaged with the N-S equations (with variable fluid properties)

together with a total energy equation. The instantaneous velocities and temperatures can be mass-weighted averaged using the Favre technique (see Cebeci and Smith, 1974) which provides terms similar to the incompressible counterpart. For the compressible situation, density and pressure are ensemble averaged without weighting.

The momentum equation can be multiplied by the instantaneous velocity which is subsequently ensemble averaged to provide an equation for the kinetic energy of turbulent fluctuations. The dissipation rate of turbulent kinetic energy (ε) can be expressed in analogy to the turbulent kinetic energy format that provides the k-ε turbulent transport equations. These field equations which are provided in a number of references stated above will be expressed in terms of mean flow quantities. The Appendix (G and H) of this report provides the conservation equations, transport equations and constitutive relations for the k-ε two-equation model (Wilcox, 6-91) as well as the k-ε two-equation model (Speziale et al, 6-90). The latter retains the fluctuating quantities for the purpose of discussion for embodied physics. The resulting field equations are:

$$\frac{Dk}{Dt} = \nabla \cdot (\nu + \frac{\nu_t}{\sigma_k}) \nabla k + \wp - \varepsilon = \tilde{E}_k \tag{24}$$

$$\frac{D\tilde{E}}{Dt} = \nabla \cdot (\nu + \frac{\nu_t}{\sigma_\varepsilon}) \nabla \tilde{\varepsilon} + C_1 f_1 \frac{\tilde{\varepsilon}}{k} \wp - c_2 f_2 \frac{\tilde{\varepsilon}^2}{k} + E_\varepsilon + E \tag{25}$$

$$D(\ )/D_t = \partial(\ )/\partial_t + \vec{U} \cdot \nabla$$

where

$$\nu_t = C_\mu f_\mu k^2/\tilde{\varepsilon}$$

$$\wp = \nu_t \left(\frac{\partial \bar{u}_i}{\partial x_j} + \frac{\partial \bar{u}_j}{\partial x_j}\right)\frac{\partial \bar{u}_j}{\partial x_j} - \frac{2}{3}\nu_t \left(\frac{\partial \bar{u}_k}{\partial x_k}\right)^2 \tag{26}$$

$$\tilde{\varepsilon} = \varepsilon + D_E ; \ \varepsilon = \nu \overline{\frac{\partial u'_i}{\partial x_j} \cdot \frac{\partial u'_i}{\partial x_j}} \tag{27}$$

$$E_k = C_D f(M_t) \rho \varepsilon \tag{28}$$

$$E_\varepsilon = f(M_t)$$

The functional form of the turbulent Mach number $f(M_t)$ has several prescriptions, (Dash, 6-91), (Sarkar et al, 11-89), (Zeman,2-90), and (Wilcox, 6-91).

The standard high Reynolds number form of the k-ε field equations provides for the following definitions:

The constants

$$\sigma_k = 1.0,\ \sigma_\varepsilon = 1.3,\ C_1 = 1.44,\ C_2 = 1.92,\ C_\mu = 0.09$$

The functions

$f_1 = f_2 = f_\mu = 1$, represent wall functions for low Re flows

$E_k = E_\varepsilon = O$, represents compressibility corrections

$E = O$, source term to dissipation

$D_\varepsilon = O$, correction to dissipation

(29)

The eddy viscosity is given by equation (11).

As previously noted the two most popular two-equation turbulence models consist of the Jones and Launder (2-72) k- ε model and the Saffman (1970) and Wilcox (1-91 and 6-91) k-ω type. The common field equation of the two-equation models is the turbulent kinetic energy (TKE) equation, eq. (24). The rate of dissipation of TKE (ε) is determined from field equations that are similar to the TKE transport equation. The relationship of the velocity and length scales with eddy viscosity are given as

$$\mu_t = C_\mu f_\mu \rho\, k^{1/2}\, \iota = C_\mu f_\mu \rho\, k^2/\varepsilon = C_\mu f_\mu \rho\, k/\omega \qquad (30)$$

for

$$\iota = k^{1/2}/\omega\ ,\ \omega = \varepsilon/k$$

where f_μ and C_μ have been previously defined and ω is the specific dissipation rate.

The standard k- ε model has been used to predict a wide variety of flows that include jets, wakes, mixing layers, boundary layer (attached and separated), and flows experiencing wall mass transfer and roughness. Due to its inherent limitation with the ε transport equation behavior approaching solid boundaries, wall techniques have been required to provide solutions to a wide range of engineering problems. Since

ad-hoc techniques are required for the near-wall region which can be numerically stiff in turbulent boundary layer flows, alternate forms of two-equation models have been sought. These include the k-ω model of Wilcox (1-91), the k-W model of Spalding (11-82) and the kτ model of Speziale et al (6-90). The latter two models are essentially variations of the Wilcox k-ω model. Appendix G and H of this report provide the field equations, constitutive relations, conservation of mass, momentum and energy as well as closure coefficients for these models.

As noted in the introduction, a position on choice of turbulence closure modeling is required in order to meet near-term goals of providing design resolution to practical engineering problems. Turbulence modeling at the two-equation level meets this requirement. The k- ε two-equation model has been clearly the most used and has developed an extensive experience base to meet the challenges of many complex flow problems. This experience base also includes the adaptation of the k- ε models into multizone PNS solvers which has not been demonstrated by the k-ω type. Moreover, coupling of unit level problems has been demonstrated by the k- ε type with proper use of wall techniques, whereas the k-ω type require boundary condition adjustments (usually with log-law relations to account for wall effects (roughness and blowing for example) which can present problems under compressible flow conditions.

With the recent success of the two-layer models that incorporate the standard k-ε model and one-equation model for length scale in the near-wall region thereby eliminating difficulty of the ε equation in approaching solid wall boundaries, it is our position that the k-ε two-equation type model can meet near-term goals.

It will be demonstrated that a hybrid model that features the standard k-ε field equations for the outer layer and a one-equation model for the inner near-wall region provides the correct asymptotic behavior for dissipation and eliminates numerical stiffness problems. The experience base with use of other wall techniques as well as adapting corrections for compressibility and curvature provide the capability to treat a wide class of engineering problems that include free shear layer, mixing layers, and wall bounded flows including separation subject to compressible flow conditions.

Table II provides a comparison of the J-K model together with the C-S model and the N-R model. Since the Rodi hybrid model is based on the N-R one-equation model for the length scale in the near wall region, it has been added for comparison. The inner-layer eddy viscosity has been structured in terms of fluctuating components in order to make a one to one comparison of all models. Three distinctive variations occur in length and velocity scales that are the underlying reasons why the J-K and Rodi hybrid models have had demonstrated success in both incompressible and compressible flow. The most important is the choice of velocity scale. The C-S model

Table II. COMPARISON OF TURBULENCE MODEL LENGTH/VELOCITY SCALES

C-S	J-K	N-R	RODI TWO-LAYER
$\mu_{t_i} = \rho \ell^2 \left\lvert \frac{\partial u}{\partial y} \right\rvert$	$\mu_{t_i} = \kappa y D_{J-K} (-\overline{u'v'}_m)^{1/2} \rho$	$\mu_{t_i} = C_\mu k^{1/2} \ell_\mu \rho$	μ_{t_i} same as N-R with
$\ell = \kappa y [1 - \exp(-y^+/A^+)]$	$D_{J-K} = \left[1 - \exp\left(\frac{U_D y}{\nu}/A^+\right)\right]$	$k = \frac{1}{2}[(\overline{u}')^2 + (\overline{v}')^2]$	$\epsilon = \frac{k^{3/2}}{C_\ell y}\left(1 + \frac{5.3}{R_T}\right)$
$y^+ = U_\tau y/\nu$	$U_D = (-\overline{u'v'}_m)^{1/2}$	$\ell_\mu = C_\ell y [1 - \exp(-C_3 R_T)]$	
$A^+ = 26$	$A^+ = 17$	$R_T = \sqrt{k}\, y/\nu$	
$\frac{\partial u}{\partial y} = \left(\frac{-\rho \overline{U'V'}}{\rho \ell}\right)^{1/2}$		k from field equation $C_3 = 25/A_\mu A^+$	
		$A^+ = 26$	
		$50.5 < A_\mu < 70$	
$\mu_{t_i} = \rho \kappa y (-\overline{u'v'})^{1/2} (1 - e^{-y^+/A^+})$	$\mu_{t_i} = \rho \kappa y (-\overline{u'v'}_m)^{1/2} (1 - e^{-\frac{U_D y}{\nu}/A^+})^2$	$\mu_{t_i} = C_\mu C_\ell k^{1/2} y (1 - e^{-\frac{25 R_T}{A_\mu A^+}}) \rho$	IBID with ϵ
	$(-\overline{U'V'}_m)$ solved along path of max shear stress from KE transport equation	k solved by KE transport equation $\epsilon = \frac{k^{3/2}}{C_\ell y}\left(1 + \frac{5.3}{R_T}\right)$	
$\mu_{t_o} = 0.0168 \rho \delta^* U_e \gamma_o$	$\mu_{t_o} = \sigma(x)\,(.0168)\,\rho U_e \delta^* \bar{\gamma}_o$	μ_{t_o} by turbulent KE transport equation using ϵ above	μ_{t_o} by solution to k-ϵ field equations

Variations in the switch point locations are prescribed in the models.

uses the wall shear stress velocity (u_τ) while the J-K and N- R use a variation on the Prandtl concept. The J-K model uses $(-\overline{u'v'}_m)^{1/2}$ while the N-R uses $(k)^{1/2}$ where k is the sum of the square of the stress-strain diagonal components i.e.1/2 $[(\overline{u'})^2 + (\overline{v'})^2 + (\overline{w'})^2]$. A variation in the damping coefficient A^+ also exists as well as the exponent of the damping term (i.e., J-K uses a power of 2, while the other features a power of unity). This was required to allow for damping to adjust to ~0 (y) instead of ~ 0 (y^2), note the power of unity on the length scale κy. With reference to eqs (15) and (16), a comparison between the length scales of the N-R and J-K models can be made. Here, ι_m compares directly with the N-R ι_μ, eq D-2, with the velocity scales as described above. Variations in the constants are also noted. It would be interesting to re-examine the J-K model with the correct value for the damping coefficient A^+ (=26) and allow for $(\kappa y D)^2$ as developed in the zero-equation and one equation models.

The elegance of the J-K model is provided in the combination of the use of a turbulence energy term for the velocity scale in the inner-layer and the parameter $\sigma(x)$ which is determined from an ODE for maximum Reynolds shear stress in the outer-layer. The outer layer solution uses an ODE while the N-R model uses a turbulent kinetic energy field equation with a modified Kolmogorov term for dissipation. Since the characteristic scales are based on maximum shear conditions, wall effects such as pressure heat- transfer, and drag are reasonably predicted. However, details of the shear layer structure cannot be obtained by the J-K model as would be provided by the N-R model and to a greater extent by the Rodi hybrid model.

2.6 Higher Order Steady State Turbulence Models

Beyond the two-equation level, a broad spectrum of turbulence model have been formulated to remedy fundamental deficiencies such as Boussinesq gradient transport hypothesis $-\rho\overline{u'v'} = \mu_\tau \frac{\partial u}{\partial y}$ and the assumption of isotropy. The simplest remedy for removing the isotropy assumption can be performed at a two-equation level with significant additional algebra and is called Algebraic Reynolds Stress (ARS) model. Such models were first formulated in the mid-to-later seventies at Imperial College and have been predominately employed for vortical turbulent flows such as corner flow and V/STOL jets. Until quite recently, all ARS work has emphasized incompressible flows. In the recent work of Burr and Dutton (1-90) at the University of Illinois, ARS models have been extended to highly compressible flows with a primary emphasis on NASP-oriented flow problems.

The next class of higher-order turbulence models are multi-scale models which distinguish between turbulent producing large eddies and turbulent dissipating small eddies. These are four equation models which solve for the turbulent kinetic energy of the large and small eddies and turbulent dissipation rates for the transfer from large to

small scale in addition to the basic dissipation rate. Several models have been formulated as extensions for the k-ε model with pioneering work in this area again performed at Imperial College (Hanjalic and Launder) and more recently by Kim and Chen (1-88) at the University of Alabama/Huntsville. This work too has focused on incompressible flows. Attempts to deal with compressible flows are provided by Adol-Hamid and Wilmoth (6-87), NASA/LRC, using the compressibility-correction to the k-ε model of Dash et. al (8-75). Section 3.3 addresses compressible issues.

Multi scale work with the k-ω model has also been performed as described by Wilcox in several recent AIAA Journal articles (11-88 and 7-90). Multiscale models serve to eliminate the Boussinesq approximation since they compute the Reynolds Stress directly.

Next in the hierarchy of higher order models are the Reynolds-Stress models which solve partial differential equations for $\overline{u' u'}$, $\overline{v' v'}$, $\overline{w' w'}$, and $\overline{u' v'}$ in conjunction with a dissipation rate equation. These models have focussed primarily on incompressible flows until quite recently. The new models of Sarker et. al (6-90) at NASA/LARC and Zeman (2-90) at Stanford are compressible extensions of conventional Reynolds-Stress models which use Favre (density-weighted) averaging to account for density fluctuations. The basic compressible models do not account for observed compressibility effects and must be supplemented by modifications to the dissipation rate equation (compressible-dissipation extension) to properly account for observed compressibility effects.

The most sophisticated of the steady state turbulence models are full second-order closure models which solve partial equations (pde's) for all second-order correlated terms such as $\overline{\rho u'}$, . . . , $\overline{h' u'}$, . . . , etc. Third-order correlations are expressed as sums of the 2nd-order correlations. The leading proponent of this work has been Donaldson (1966) at ARAP. Early issues involved the use of algebraic length scale equation which has since been remedied. Such models lost momentum in conclusions drawn in 1982 AFOSR/Stanford Turbulence Model Conference where the claimed "invariance" of coefficients was questioned and refuted. For flows with multi-component species, the number of pde's can be overwhelming making such methodology highly impractical.

3.0 TURBULENCE MODEL RECOMMENDATIONS

3.1 Standard High Reynolds Number k-ε Model

As previously noted, our position on choice of a turbulence closure model is the standard two-equation k-ε model and its subsequent modifications to treat a wide range of engineering problems. The extensive experience base generated by these models should provide a level of generality with proper definitions for closure constants (or parameters) together with near-wall terms to handle multiple flow states. Moreover, the versatility of the models and adaptation to existing industrial codes allows for robust transfer of the methodology.

Two-equation models also provide other obvious features over lower-level models. This includes the use of better physics in the field equations to handle the outer layer region where accelerated flows, severe pressure gradients, and mass transfer (diffusion) can have an impact. Details of the turbulence structure are provided which can help provide insight for a wall function modeling. The models are not computationally intensive and are readily adaptable to current industrial codes.

Equations (24) through (29) presented the generalized two-equation model with and without modifications. Table III has been structured to show how these modifications have been made to the standard high Reynolds number equations. These modifications include near wall techniques, compressible corrections, and geometric (curvature) corrections. Each of these modifications will be discussed. The closure constants that are recommended for the standard k-ε model were acquired from incompressible experiments of free turbulent flows that include free shear layers (jets) as well as confined mixing layers. These same constants have been recommended for boundary layer flows. The relative merit of these constants in flows subject to wall bounded flows which has necessitated wall damping functions requires further investigation relative to compressible effects..

3.2 Near-Wall Techniques

Four levels of near-wall techniques have been characterized as wall functions, bridging techniques using van Driest damping, low Reynolds number techniques, and hybrid techniques. The hybrid techniques actually feature two-layer models that incorporate the standard k-ε model in the outer layer with a one-equation model for the inner layer. Wall functions use law of the wall equations to match a grid point usually taken at the edge of the viscous sublayer with no attempt to resolve the sublayer region. This point is then used as a boundary condition for the outer region for the k-ε equations. Modified versions of the k-equation are also used at this point to solve for the kinetic energy as opposed to setting its value. Wall shear stress velocity is taken as the characteristic velocity. These techniques have the advantage of not encountering numerical problems (no grid points) in the sublayer and can save computational time. However, they require ad-hoc techniques between the wall and

Table III. TWO-EQUATION k-ϵ MODEL VARIATIONS

$$\frac{Dk}{Dt} = \nabla \cdot \left(\nu + \frac{\nu_t}{\sigma_k} \right) \nabla k + \rho - \tilde{\epsilon} + E_k$$

$$\frac{D\tilde{\epsilon}}{Dt} = \nabla \cdot \left(\nu + \frac{\nu_t}{\sigma_\epsilon} \right) \nabla \tilde{\epsilon} + C_1 f_1 \rho - C_2 f_2 \frac{\tilde{\epsilon}^2}{k} + E + E_k$$

$$\nu_t = C_\mu f_\mu k^2 / \tilde{\epsilon}$$

$$\tilde{\epsilon} = \epsilon + D_E$$

STANDARD HIGH Re k-ϵ MODEL

$\sigma_k = 1, \sigma_\epsilon = 1.3, C_1 = 1.44, C_2 = 1.92,$ & $C_\mu = 0.09$

$f_1 = f_2 = f_\mu =$ unity,	Low Re Wall Functions
$E_k = E_\epsilon = 0$,	Compressible Corrections
$D_\epsilon = 0$,	Correction to Dissipation
$E = 0$,	Source Term

COMPRESSIBLE CORRECTIONS
- DASH
- SARKAR et al
- ZEMAN
- RUBESIN
-
-

GEOMETRIC CORRECTIONS
- AXISYMMETRIC
- STREAMWISE CURVITURE
- SWIRL
- VORTICAL
-
-

NEAR WALL TECHNIQUES

WALL FUNCTIONS
- Spalding-Launder
- Chieng-Launder
- Viegas-Rubesin
- Gorski
-
-

BRIDGING TECHNIQUES (Van Driest)
- Dash et al
- Arora et al
-
-

LOW REYNOLDS TECHNIQUES
- Jones-Launder
- Chien
- Lam-Bremhorst
- Launder-Sharma
- Shih
-
-

HYBRID TECHNIQUES
- Iacavides-Launder (Van Driest)
- Patel et al (Wolfshtein)
- Rodi (Norris-Reynolds)
-
-

grid first point which do not have established physics. Moreover, use of law of the wall relations has been demonstrated to be inadequate for complex flows where inaccuracies affect turbulence quantities as well as mean flow properties.

A second approach uses bridging techniques between the wall and grid point at the edge of the viscous sublayer with consideration to multiple layers in between. Here, the van Driest damping functions are applied to provide algebraic relations to solve for the flow conditions. While this method provides better physics, the phenomena is linear and does not account for lag between the stress and mean flow properties. An advantage of this technique however, is the ability to incorporate wall conditions such as roughness, blowing, and pressure gradients through modifications of the van Driest damping function (or coefficient). This has been demonstrated by Aurora et al (11-82) as well as Cebeci-Smith (see Appendix A).

The third technique considers use of the field equations extended to the wall with low Reynolds number techniques that require damping function adjustments to the constants, as well as to the dissipation term. In some instances, the addition of a source term to the dissipation has been used. These techniques provide better physics and have been shown to predict transitional boundary layer flow as well as re-laminarization. In some cases, a non-physical form of dissipation is solved within the viscous sublayer requiring a modified kinetic energy equation to balance the dissipation. As in the van Driest technique, exponential damping is used to compensate errors for the new ad-hoc technique which do not allow for the eddy viscosity to correctly asymptote to the wall (i.e. it does not have an O (y^2) behavior). These techniques also offer opportunities to investigate wall conditions of roughness, blowing,and curvature through the damping terms or damping coefficients. One interesting aspect of the low Reynolds number methods is the choice of velocity scales which use both the wall shear velocity as well as a velocity based on kinetic energy.

The fourth technique considers a hybrid method that uses the standard k-ε model in the outer layer of a two-layer model and a one-equation model for the inner layer. This approach has shown recent success for both incompressible and compressible flows to treat severe pressure gradient regions. Moreover, the one-equation model eliminates the difficulty of the limitation of the dissipation to approach solid boundaries and provides for techniques to treat roughness, mass transfer, curvature, and transition. The technique used by Rodi (1-91) for incompressible flow and extended to compressible flow by Horstman (6-91) uses the one-equation model of Norris-Reynolds (see Appendix D) and will be the candidate methodology for a generalized turbulence model.

3.2.1 RODI Hybrid Model

The Rodi model (1-91) combines the k-ε transport equations with a one-equation length scale model for the near wall region. The rationale and features of this model

have been discussed. Table IV provides the model characteristics. The bulk of the shear layer is determined by the k-ε equations. As evidenced by this review, a number of variations have been used for the damping functions for the one-equation, length scale as well as the matching criteria for the inner/outer layers. It has been demonstrated that the use of the N-R one-equation model provides results for incompressible flow that are consistent with low Reynolds k-ε models, and have been shown to be better for flows with adverse pressure gradients. Moreover, the recent work of Horstman (6-91) has shown that the Rodi hybrid model provides resolution to compressible 2D/3D shock/boundary layer interactions for supersonic and hypersonic conditions.

The standard high Reynolds number k-ε model is used for the bulk of the shear region away from the wall and calculates the distribution of eddy viscosity from (see eq. (11)).

$$\upsilon_t = C_\mu k^2/\varepsilon$$

The near wall region is formulated by a one-equation model whose length scale is prescribed by Equations (D-1) through (D-4). It should be noted that the length scales ι_μ and ι_ε are the same in the log-law region when the coefficient C_μ is chosen as the square of $\overline{u'v'}/k$ under equilibrium conditions. In the near wall regions, gradients require that ι_μ and ι_ε be different and a reduction in ι_μ can be tailored after the van Driest formulation with a proper definition of velocity scales. The N-R model provides for such a function.

Several other phenomena make the Rodi model attractive for potential universality. This includes the ability to provide wall conditions such as blowing, roughness, and curvature using the damping coefficients (C_3 in Equations (D-2) and (D-8)) as developed by C-S, Rodi (1984), and Laganelli (1-75), as well as handle adverse pressure gradient and compressible flow conditions. In essence, the two-layer model appears capable of providing solutions of coupled problems. Another attractive feature is that the model considers a modified version of the Kolmogorov function and provides for correct length scale where $\iota \propto y$ at the wall. Finally, since the transport equations are being used, details of the flow structure can be obtained that are not available with lower order models.

3.3 Compressible Modifications

The k-ε model was originally, formulated from a purely incompressible viewpoint. Its inability to deal with high Mach number compressibility effects was first made evident at the 1972 NASA Free Shear Flow Conference (NASA-72) where its performance versus the classic isoenergetic/single-stream shear layer data showed no decrease in mixing with increasing Mach number, whereas the data indicated a

Table IV. RODI TWO-LAYER (RTL) TURBULENCE MODEL (from Horstman, 6-91)

The two-equation $k - \epsilon$ turbulence model is expressed as

$$\frac{D\rho k}{Dt} = \mu_t\left[S_{ij}S_{ij} - \frac{2}{3}\,\mathrm{div}\,\bar{u}^2\right] - \frac{2}{3}\rho k\,\mathrm{div}\,\bar{u} - \rho\epsilon + \text{diffusion} + \text{LRT} \qquad (1)$$

$$\frac{D\rho\epsilon}{Dt} = \frac{\epsilon}{k}\left[C_1\mu_t\left(S_{ij}S_{ij} - \frac{2}{3}\,\mathrm{div}\,\bar{u}^2\right) - C_1\frac{2}{3}\rho k\,\mathrm{div}\,\bar{u}\right] - C_2 f_2 \rho\frac{\epsilon^2}{k} + \text{diffusion} + \text{LRT} \qquad (2)$$

$$S_{ij} = u_{i,j} + u_{j,i} \qquad (3)$$

$$\mu_t = C_\mu \rho k^2/\epsilon \qquad (4)$$

where LRT refers to the low Reynolds number terms used near solid surfaces. The values used for the constants were $C_1 = 1.44$, $C_2 = 1.92$, and $C_\mu = 0.09$.

The second model used here is the two-layer model developed by Rodi and his co-workers For this model the ϵ equation is replaced by an analytical expression near the wall. In the wall region this model determines the eddy viscosity from the relation

$$\mu_t = f_\mu C_\mu \rho\sqrt{k}\, L \qquad (5)$$

$$f_\mu = 1 - \exp(-0.0198\, R_y) \qquad (6)$$

$$R_y = \rho\sqrt{k}\, y/\mu \qquad (7)$$

where y is the normal distance to the wall. The dissipation rate ϵ is given by

$$\epsilon = \frac{k^{3/2}}{L}\left(1 + \frac{13.2}{\rho\sqrt{k}\, L/\mu}\right) \qquad (8)$$

The length scale L is assumed proportional to the distance from the wall, i.e., $L = C_r y$. The wall region model is matched with the full $k - \epsilon$ model at a distance from the wall where $R_y = 150$ ($f_\mu \approx 0.95$). At this location the eddy viscosity given by Eqn. 4 is equated to Eqn. 5 to determine the proportionality constant C_r. For typical shock-wave/boundary-layer interaction flows solved here C_r varied from 0.8 to 9.0 at various locations in the flow field. The lowest values occurred upstream of the interaction and the highest near reattachment. For the present computations, maximum and minimum limits of 2.4 and 1.2 were used for C_r. With these limits imposed, the values of eddy viscosity are no longer matched between the inner and outer models for large regions of the flow field. A few solutions were obtained using $C_r = 2.4$ which is equivalent to using the Prandtl length scale. (Rodi used a constant value of 2.45 in his incompressible computations). Solutions were also obtained for several interaction flows varying the match point from $R_y = 100$ to 200. These results differed from each other by less than 3 percent.

substantial decrease at Mach numbers above unity (e.g., a factor of 4 decrease at Mach 5). Attempts to remedy this deficiency has focussed on free shear flows (jets/plumes/wakes) since the performance of the k-ε model for basic boundary layer flows was found to be adequate to Mach 5 and beyond (depending on wall conditions).

Over the years, a variety of compressibility-corrections have been formulated to address the issue of reduced mixing at higher Mach numbers. Explanations of the phenomenology causing this behavior have been varied and based on stability considerations, eddy-shocklet concepts, etc. The most widely-used correction for jets/plumes has been that of Dash et al. (8-75) to the k-ε model. The k-ε cc model (i.e. k-ε with compressible corrections) uses a correction to the turbulent viscosity, eq. (11), of the form:

$$\mu_{ti} = C_{\mu i}\, K\,(M_\tau)\rho\, \frac{k^2}{\varepsilon} \qquad (31)$$

where $C_{\mu i}$ is the incompressible coefficient (=.09) and $K(M_\tau) = C_\mu/C_{\mu i}$ is a curve fit which enforces agreement with the isoenergetic single stream shear layer data. In equation (31), M_τ is the turbulent fluctuation Mach number

$$M_\tau = q/a \qquad (32)$$

where $q = (u_i u_i)^{1/2}$ and the peak value of M_τ is used at each axial position of the shear layer. A number of compressibility corrections to the k-ε and higher order models have been proposed, some of which are summarized in Table V. The recent compressible dissipation corrections of Sarkar et al. (6-90) and Zeman (2-90) appear to have generated the most enthusiasm as evidenced by recent papers at the AIAA Fluids and Plasmadynamics Meeting in Hawaii (June 1991).

Papers by Dash (6-90), Viegas and Rubesin (6-91) , and Wilcox (6-91) all have explored the inclusion of these compressible-dissipation models into k-ε and k–ω turbulence model frameworks. In both the Sarkar and Zeman models, the turbulent dissipation rate, ε, is taken to be comprised of a solenoidal, incompressible component, ε_s, and dilatational, compressible component, ε_c, and thus:

$$\overline{\rho}\,\varepsilon = \overline{\rho}\,(\varepsilon_s + \varepsilon_c) \qquad (33)$$

which replaces $\overline{\rho}\,\varepsilon$ in the standard k-ε equations (See Table III).

Both Sarkar and Zeman integrate the incompressible form of the dissipation equation to obtain ε_s and model ε_c as follows:

Table V. TURBULENCE MODELS WITH COMPRESSIBILITY-CORRECTION

Dash et al. — kεCC/1: (1975, AFOSR-TR-75-1436)	$\mu_t = C_\mu (M_{T_{max}})\ \rho k^2/\epsilon$	Calibrated with Birch/Eggers Isoenergetic/One-Stream Shear Layer Data; Only Works for Simple Free Shear Flows
Childs and Caruso — kεCC/2: (1987, AIAA Paper 87-1439)	$\mu_t = C_\mu (M_T)\ \rho k^2/\epsilon$	Generalization of Above Model, Same Data Base for Calibrations
Nichols — kεCC/3: (1990, AIAA Paper 90-0494)	Additional Dissipation Terms in Turbulent Kinetic Energy Equation Plus Other Fixes	Calibrated by Spread Data; Works with Chien Near-Wall Model, M Dependency Criticized
Rubesin — kεCC/4: (1990, NASA CR 177556)	Models Extra Compressibility Terms in Favre-Averaged Formulation	Found to be Problematic Numerically by Viegas and Rubesin, 1991 Paper
Taulbee and Van Osdol (1991, AIAA Paper 91-0524)	Pressure Dilatation and Dilatation Dissipation Terms in k Modeled; Extra Equation for $\overline{\rho' \rho'}$ and $\overline{u_i''}$	Model Parameters Established from High-Speed BL Data
Sarkar et al. (1989, NASA CR 181959)	Compressible Dissipation, $\epsilon = \epsilon_s(1 + \alpha M_t^2)$; RS Model	$\alpha = 1$ from Isotropic Decay of Compressible Turbulence
Zeman et al. (1990, Phys. Fluids, Feb. 1990)	Compressible Dissipation, $\epsilon = \epsilon_s + \epsilon_d(M_t, \text{Kurtosis})$; RS Model	Fundamental Calibration as Above
Burr and Dutton (1990, AIAA Paper 90-1463)	ARS Extension of kε	
Wilcox (1991, AIAA Paper 91-1785)	kW with Multi-Scale Extensions and Sarkar/Zeman Blend	

Sarkar et al:

$$\varepsilon_c = \alpha_1 \varepsilon_s M_\tau^2 \tag{34}$$

Zeman:

$$\varepsilon_c = C_d F(M_\tau) \varepsilon_s \tag{35}$$

where

$$F(M_\tau) = 1 - \exp[(-M_\tau - 0.1]/0.6)^2] \tag{36}$$

for $M_\tau > 0.1$, and,

$$F(M_\tau) = 0 \tag{37}$$

for $M_\tau \leq 0.1$. In their calibrations of these compressible-dissipation models, Sarkar found $\alpha_1 = 1.0$ to provide the best agreement and Zeman found $C_d = .75$ to work best.

Sarkar and Zeman have incorporated their compressible-dissipation models into a Reynolds-Stress model framework where they solve the field equations for the varied stress components (i.e. for $\overline{u'u'}$, $\overline{v'v'}$, $\overline{u'v'}$, ----). Simplifying their models to work in a k-ε two-equation model framework leaves open some ambiguities with regard to the value of the turbulent viscosity μ_τ to be utilized. The initial interpretations of Dash (6-91) and Viegas/Rubesin(6-91) differed substantially and thus produced different results. This descrepency was addressed by Dash et al (9-91) and was associated with the interpretation of the turbulent viscosity, μ_τ, appearing in the diffusion terms of the mean flow equations, in the diffusion terms of the k and ε_s equations, and in the turbulent production term, $\wp$. Compressible and incompressible values of μ_τ ($\mu_{\tau c}$ and $\mu_{\tau s}$, respectively) are defined as follows:

$$\mu_{tc} = C_{\mu o} \bar{\rho} k^2/(\varepsilon_s + \varepsilon_c) \tag{38}$$

$$\mu_{ts} = C_{\mu o} \bar{\rho} k^2/\varepsilon_s \tag{39}$$

Dash used the compressible μ_τ for all diffusion terms (mean flow, k and ε), the compressible μ_τ for $\wp$ in the k equation and the incompressible μ_τ for $\wp$ in the ε equation. Viegas/Rubesin used the incompressible μ_τ for <u>all</u> terms. After reviewing

these two initial attempts, Dash explored this matter in greater detail to ascertain which interpretation was most consistent with the Reynolds-Stress formulation of Sarkar et al. A matrix of plausible interpretations is summarized in Table VI.

In Table VI D_f, D_k, and D_ε refer to the diffusive terms in the mean flow, k and ε equations respectively. $\wp_\kappa$ and $\wp_\varepsilon$ refer to the turbulent production term in the k and ε equations.

In reviewing the Sarker Reynolds-Stress equations, method A (Dash 6-91) appeared inconsistent since different values of production were employed in the k and ε equations. Method B (Viegas/Rubesin, 6-91) also appeared inconsistent since wherever a gradient transport hypothesis was employed by Sarkar et al., a compressible value of μ_τ was utilized whereas Viegas/Rubesin used incompressible values throughout. The different methods for including compressible-dissipation into k- ε listed in Table VI were assessed by Dash via comparisons with the spread rate data correlation of Birch and Eggers (NASA, 1972) LaRC correlation, for asymptotic isoenergetic/single-stream shear layers. The Sarkar formulation was used with α_1 = 1.0. Figure 1 exhibits the predictions for variants A - E vs the Mach number LaRC correlation. The spread rate parameter, σ (=1.855 $\Delta x/\Delta y$) is plotted vs the Mach number of the moving stream. As the Mach number increases above sonic, the spread parameter increased from the incompressible value (σ_0 ~ 11) indicating a marked decrease in spread rate with increasing Mach number. Variants A and E underpredict the rate of mixing throughout (σ's are too large) whereas variants B, C and D underpredict the rate of spread of $M_1 < 1.5$ and overpredict the rate of spread for $M_1 > 1.5$. Variants C and D have identical behavior whereas variant B shows somewhat smaller spread. Comparing with Sarkar's Reynolds-Stress (RS) predictions, variants A and E can be ruled out whereas variants B, C and D all produce spread behavior which appears quite comparable. Version D has been selected for reasons discusses by Dash (9-91).

As shown in Figure 1, Variant D overpredicts spread below M = 1.5 and underpredicts above M = 1.5 (this is true for both the Sarkar and Zeman formulations). In view of its simplicity, Dash (9-91) chose to work with the Sarkar formulation in the confines of Variant D, and, to revise it to better match the spread data. The revised version is described below. The compressible-dissipation, ε_c, is redefined as:

$$\varepsilon_c = \varepsilon_s \left[\alpha \tilde{M}_t^2 + \beta \tilde{M}_t^4 \right] \qquad (40)$$

where a Zeman lag is inserted ($\tilde{M}_t = M_t - \lambda$) and a fourth-order term is added.

The coefficients utilized are:

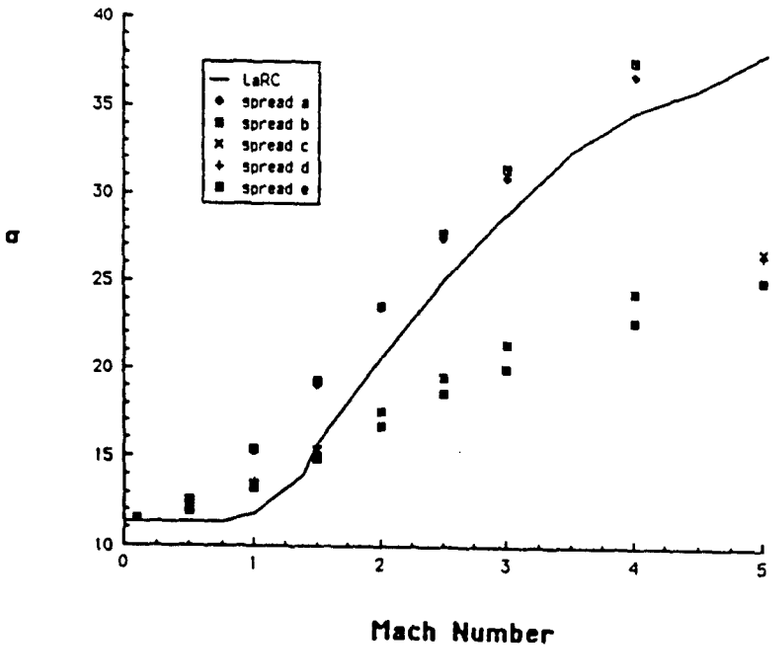

Figure 1. Comparison of Variants A-E of Table VI in Producing LaRC Isoenergetic/Single-Stream Spread Sheet

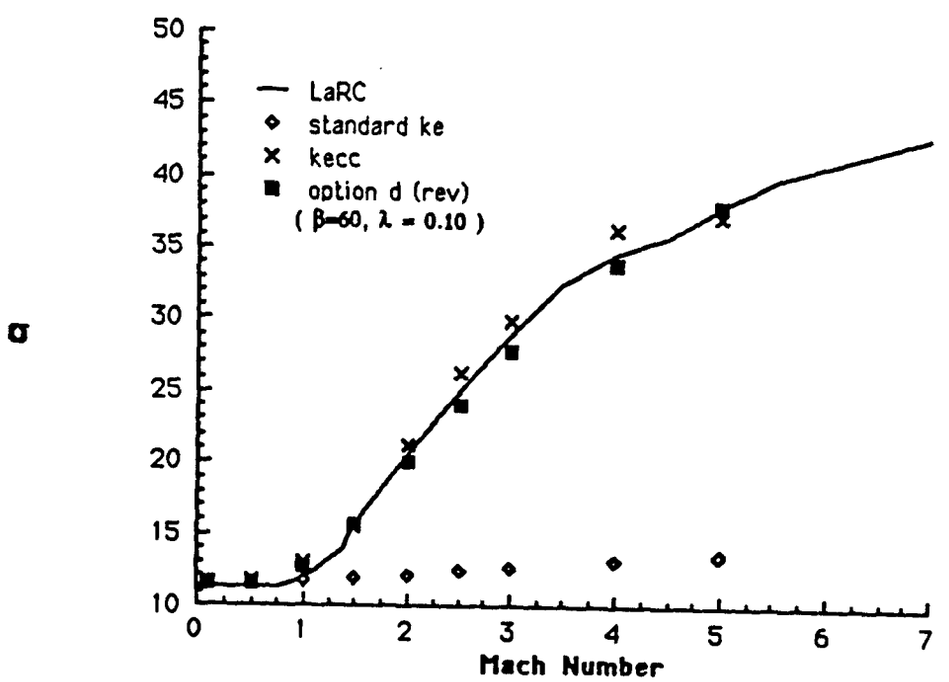

Figure 2. Comparison of kε CD (variant D of Sarkar) and kεCC Models versus LaRC Spread Sheet

TABLE VI. TURBULENT VISCOSITY USED IN INCORPORATING COMPRESSIBLE-DISSIPATION MODEL INTO k-ϵ (S-INC, C-COMP)

	D_F	D_k	D_ε	$\wp_k$	$\wp_\varepsilon$
A. DASH (6-91)	C	C	C	C	S
B. VIEGAS/RUBESIN (6-91)	S	S	S	S	S
C. 1st Revision	C	C	C	C	C
D. 2nd Revision	C	C	S	C	C
E. 3rd Revision	C	C	S	S	S

$\alpha = 1$ (same as Sarkar et al.)
$\lambda = 0.1$ (same as Zeman)
$\beta = 60$ (fits LaRC data the best)

Figure 2 shows performance of the revised model with the LaRC spread data and with the kεCC model (Dash et al., 8-75), also calibrated to fit this same area.

Two turbulence models have been calibrated to reproduce the isoenergetic/single-stream shear layer data. We can designate the revised Sarkar model in k-ε using Variant D is designated as the kεCD model. A preliminary attempt was made by Dash (9-91) to distinguish between their performance first using other data sets, and then profile comparisons including the behavior of turbulent quantities. In analyzing the isoenergetic/two-stream data of Chinzei et al. (1986) and the non-isoenergetic/two-stream data of Goebel and Dutton (4-91), the spread behavior is nearly identical and no distinguishing characteristics are observed. In comparing profiles, however, differences are significant . From a cursory look at the available data, the performance of the kεCD model appears to provide a more consistent behavior. In particular, turbulence stress and kinetic energy decrease with increasing convective Mach number as predicted by the kεCD but not by kεCC.

Relative to compressible modeling, a recent paper by Situ and Schetz (6-91) considered the addition of the fluctuating term $-\overline{\mu}\ \overline{\rho' v'}$ to the shear stress where a favorable comparison to a variety of shear layer and boundary layer flows was demonstrated. Appendix I provides details of this turbulence model concept.

3.4 Vortical/Curative Modifications

The basic k-ε model was developed for simple shear flows (planar shear layers and boundary layers). The turbulence field is assumed to be isotropic and the relating Boussinesq eddy viscosity assumption turbulent stress to mean strain is employed. For flows with any type of geometric complexity, corrections are required to enforce the desired behavior. Corrections are required for:

(1) axisymmetric behavior
(2) streamwise curvature
(3) swirl
(4) streamwise vorticity

and various other geometric distortions for simple planar flow, which are often very specialized and problem dependent. The corrections range from those being entirely heuristic to those attempting to be generalized and thus modeling the turbulent behavior. All the latter models achieve improved behavior via modifications to the ε

equations and thus they directly focus on the length scale issue. There are far too many corrections in usage to describe in this report. Rather, several will be briefly described to provide an understanding of how such corrections are made and how they improve the performance of the basic k-ε model.

The first corrections to the k-ε model were made in the early '70's to deal with the axisymmetric problem, namely, the inability of the basic model to analyze both planar and axisymmetric jets with the same constants. To have the k-ε turbulence model agree with basic low-speed, axisymmetric jet data, the constants must be revised or made to vary with jet parameters, or, additional terms must be added to the equations. The simplest modification entails changing C_1, from a value 1.43 for planar to 1.60 for axisymmetric jets. This forms the basic for some of the earlier work with k-ε in Great Britain in analyzing axisymmetric rocket plumes.

The next group of corrections make the coefficients dependent on the jet centerline velocity decay, dU_{CL}/dx, and are summarized below.

Launder, et al. (1972) kε1/kε2 models provide for

$$C_2 = 1.92 - aF, \quad a = 0.067 \ (=0.053 \text{ for } k\varepsilon 2)$$
$$C_\mu = .09 - bF, \quad b \equiv 0.1$$

where

$$F = \left\{ \frac{r^{1/2}}{2 \cdot U_{CL}} \left(\left| \frac{dU_{CL}}{dx} \right| - \frac{dU_{CL}}{dx} \right) \right\}^{0.2} \tag{41}$$

McGuirk and Rodi (1977) chose the coefficient C_1 to be

$$C_1 = 1.14 - 5.31 \frac{r^{1/2}}{U_{CL}} \frac{dU_{CL}}{dx} \tag{42}$$

while Morse (1977) selected

$$C_1 = 1.4 - 3.4 \left(\frac{k}{\varepsilon} \frac{dU}{dx} \right)^3_{CL} \tag{43}$$

In the above axisymmetric corrections, U_{CL}, is the jet centerline velocity and $r^{1/2}$, is the distance from the centerline to the half-velocity position.

All the above corrections are heuristic, use centerline values to change the turbulence away from the centerline, and are not extendible to more generalized flows. Pope (3-78), noting these issues, introduced a more generalized extension based on vortex stretching arguments which modifies the dissipation equation by adding an extra term, namely:

$$C_3 \chi \varepsilon^2/k \tag{44}$$

where

$$\chi = \omega_{ij}\, \omega_{jk}\, s_{ij} \tag{45}$$

with

$$S_{ij} = \frac{1}{2}\frac{k}{\varepsilon}\left(\frac{\partial u_i}{\partial x_j} + \frac{\partial u_j}{\partial x_i}\right) \tag{46}$$

and

$$\omega_{ij} = \frac{1}{2}\frac{k}{\varepsilon}\left(\frac{\partial u_i}{\partial x_j} + \frac{\partial u_j}{\partial x_i}\right) \tag{47}$$

For an axisymmetric jet (with no swirl), χ becomes:

$$\chi = \frac{1}{4}\left(\frac{k}{\varepsilon}\right)^3 \left(\frac{\partial u}{\partial r} - \frac{\partial v}{\partial x}\right)^2 \frac{v}{r} \tag{48}$$

and the constant $C_3 = .79$ was found to match jet data (axisymmetric jet into still air). This vortex stretching correction has potential generality and does go to zero for planar flows. However, in a review article by Launder (1985) the universality of the C_3 coefficient is questioned based on calculations of coaxial jets. Hanjalic and Launder (1980) suggest that a correction term of the form:

$$- C_3\, k \frac{\partial u_i}{\partial x_j}\frac{\partial u_\iota}{\partial x_m}\varepsilon_{ijk}\,\varepsilon_{\iota mk} \tag{49}$$

be added which is similar to Pope's in appearance but acts differently. The sign is different and this term is also operative for planar shear flows.

To illustrate the importance of these axisymmetric correction terms, consider a simple low speed, axisymmetric jet with a 10:1 velocity ratio. Figure 3 shows the predicted centerline velocity decay and jet boundaries obtained using the basic k-ε model and the k-ε model with the Launder CL (centerline) and Pope vortex stretching corrections (see Dash, 6-91 and Dash et al., 9-91 for details and discussions regarding the use of these corrections with the previous compressibility corrections provided in this section). As exhibited, inclusion of the axisymmetric correction slows down the mixing and produces a significantly larger jet size. For low speed jets such as this, the correction produces good agreement with data.

The next corrections discussed are those for streamline curvature. While both the mean flow and turbulence model equations contain a number of curvature terms arising from the transformation to curvilinear, surface-oriented coordinates, numerous investigators have demonstrated that additional, curvature corrections terms are required to account for the strong effects of curvature on turbulence structure. The analogy drawn by Bradshaw (1969) between curvature and buoyancy has been

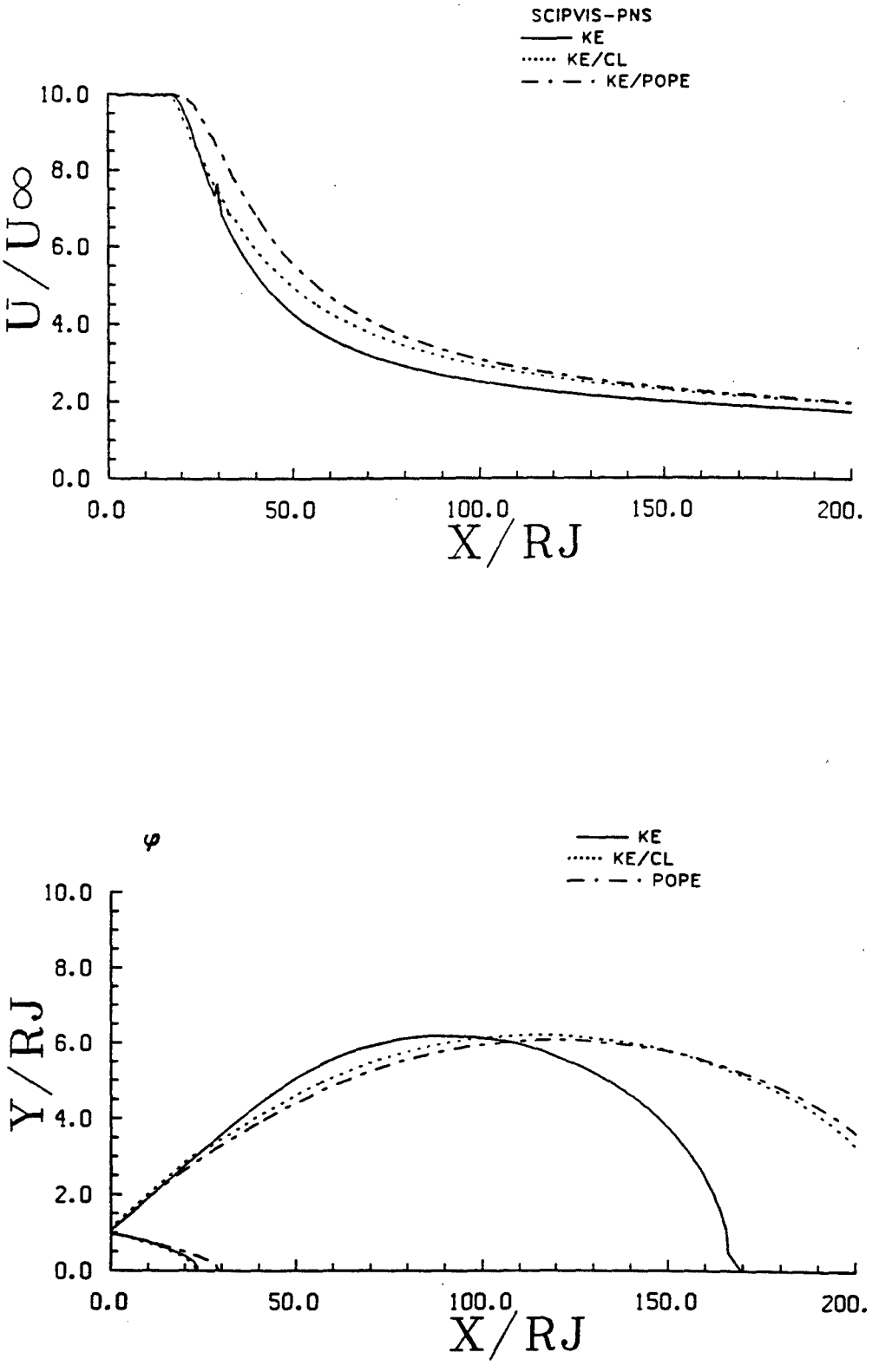

Figure 3. Comparisons of Launder and Pope Axisymmetric Correction for 10:1 Velocity Ratio Low Speed Jet

utilized by most investigators as the basis for heuristic corrections to algebraic or two-equation turbulence models. Defining the curvature parameters, $s = -KU/\partial U/\partial n)$, a curvature correction to the ML formulation (Bradshaw, 1973) is given by:

$$L = \frac{L_0 (1 - \alpha s)}{(1 - s)} \tag{50}$$

where L_0 is the planar value while α is a constant ($5 < \alpha < 10$). The treatment has been implemented for wall jets by Foloyan and Whitelaw (1976) who utilized a complete (inner/outer) mixing length formulation. For the present near-wall use of the mixing length formulation, this correction will only be required in situations with very large curvature since the near-wall correction to L_0 is negligible.

Launder and coworkers (3-77) have developed a curvature correction for the k-ε model which utilized a single empirical coefficient, C_c. The curvature correction is proportional to a Richardson number, Ri, based on the turbulence time scale. In their formulation, the local Richardson number is given by:

$$Ri = - KU \left(\frac{k}{\varepsilon}\right)^2 \frac{\partial U}{\partial n} \tag{51}$$

and the C_2 coefficient of the ε equation is modified as follows:

$$C_2 = 1.92 (1 - C_c Ri) \tag{52}$$

Values of C_c of about 0.2 have yielded optimal predictions for a variety of curved boundary layer flows as described by Launder et al., (3-77). An analogous type of curvature correction for the k-ε model has developed by Hah and Lakshminarayana (10-80). They have modified the C_1 coefficient of the ε equation as follows:

$$C_1 = 1.43 (1 + C_c Ri) \tag{53}$$

To illustrate the marked influence of these streamwise curvature corrections, we refer to the work of Dash et al., (10-85 and NASA CP 2432, 1986) for wall jets on curved surfaces. The case simulated the experiment of Wilson and Goldstein (9-76) (Re_s = 13,200) for a wall jet issuing from a .615 cm slot flowing over a circular cylinder with a diameter of 20.32 cm. The data for the jet half-radius variation is compared with a series of predictions in Figure 4. The following predictions were performed:

(a) Basic k-ε (inner Van Driest)

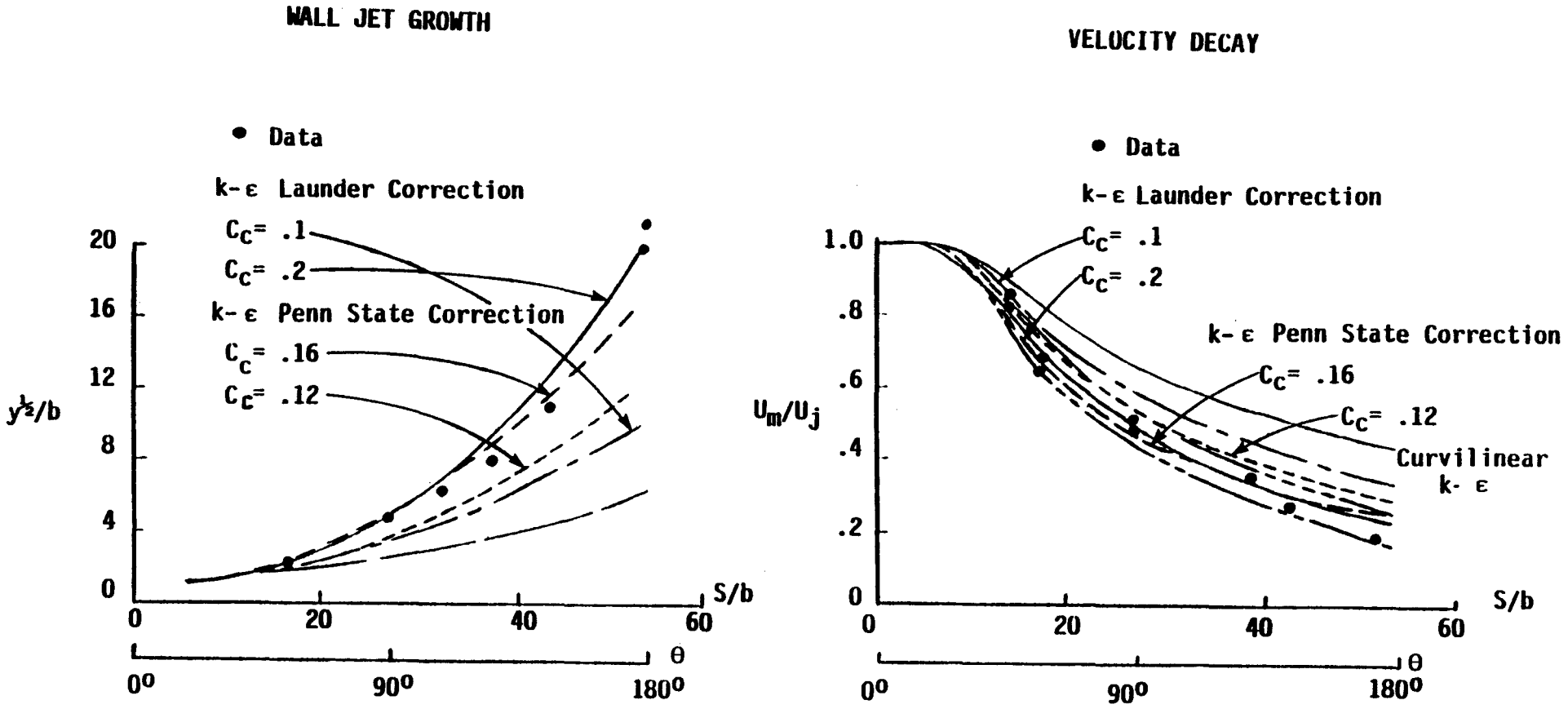

Figure 4. Assessment of Boundary Layer Curvature Correction With Mean Flow Properties.

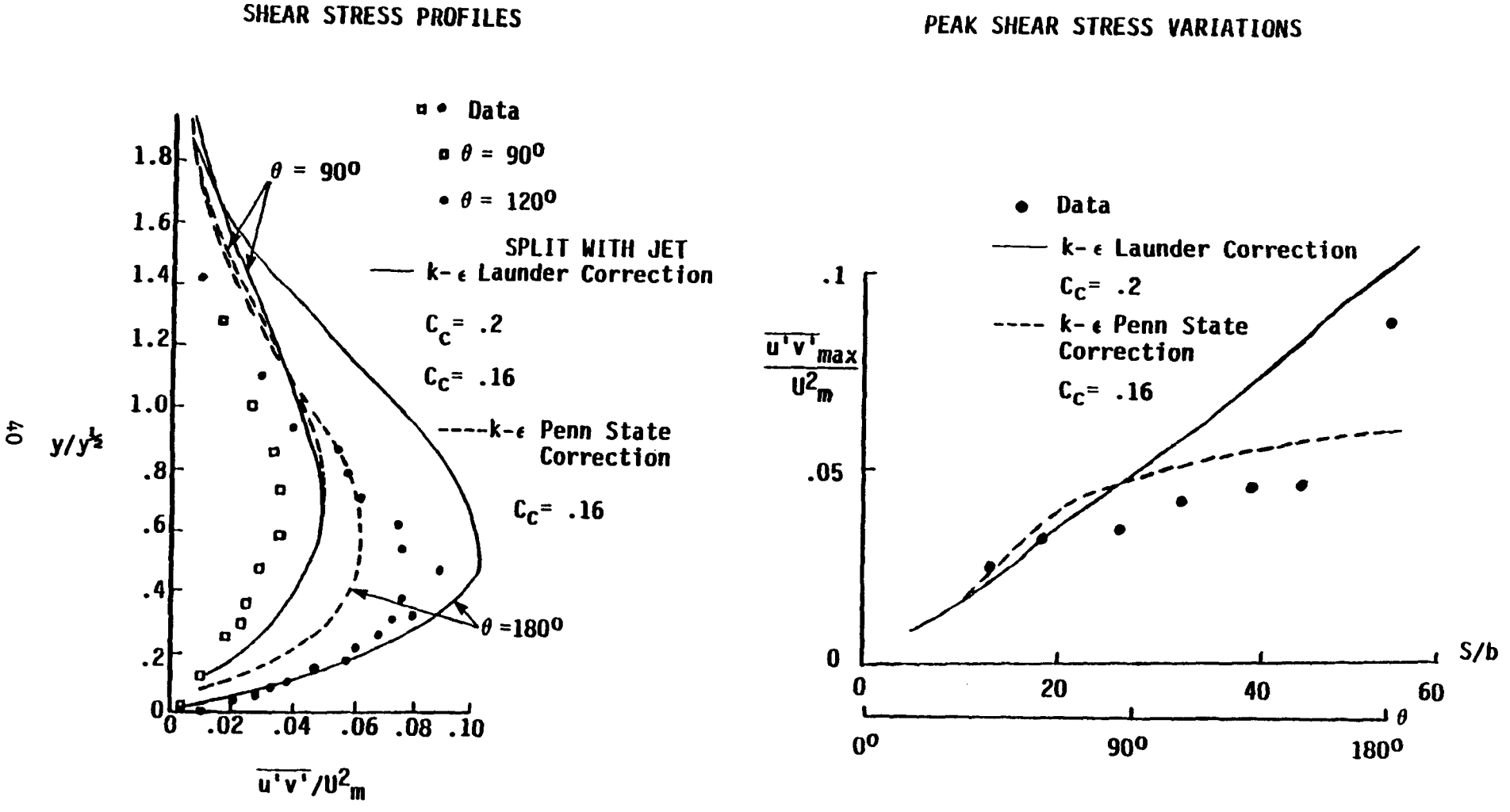

Figure 5. Assessment of Fluctuating Boundary Layer Properties for Curvature Correction on Curved Wall Jets.

(b) k-ε, Launder Correction

As above the k-ε curvature correction of Launder using C_c = .10 and .20.

(c) As above with k-ε curvature correction, eq. (53), using C_c = .12 and .16, Hah and Lakshminarayana (10-80)

Comparing the data for this case with that for the planar jet, we observe a pronounced effect of curvature on the jet growth rate (i.e., at x/b = 50, the planar jet half-radius is about 4 times larger). Applications of the basic curvilinear k-ε model grossly underestimates the growth rate yielding a variation comparable to that of the planar case. Launder et al., (3-77) recommend a value of C_c = .20 for their k-ε curvature correction but state that Priddini (1975) had found a value of C_c = .10 to work best for wall jets. We have implemented both these values and find the value of .20 to yield best agreement. For the C_1 curvature correction of eq. (53) (using the Launder Ri definition), the value of C_c = .16 is seen to yield good agreement with the data while the value of C_c = .12 underestimated the measured growth rate.

Comparable conclusions can be drawn from the comparison of predictions for maximum velocity decay also depicted in Figure 4. The predictions with the Launder correction with C_c = .20 and the C_1 correction with C_c = .16 are quite comparable and fit within the data band based on the experiments of Wilson and Goldstein, and other investigators. The other k-ε predictions underestimate the velocity decay rate.

Predicted profiles of the streamwise velocity at $\theta = 90^0$ (with C_c = .20, Launder and C_c = .16 Eq. (53) are indistinguishable and agree favorable with the data of Wilson and Goldstein which is invariant in similarity coordinates for $\theta = 45^0$. The case itself is, however, nonsimilar as seen by the comparisons with turbulent shear stress data depicted in Figure 5. The data exhibits a significantly greater peak shear stress level at 180^0 than at 90^0 as do the predictions. The predictions at 90^0 (C_c = .20, Launder and C_c = .16 with eq. (53) are in close agreement with each other and somewhat overestimate the shear stress. Those at 180^0 differ substantially with the Launder model overestimating and the Hah and Lakshminarayana model underestimating peak shear stress levels. Figure 5 also compares the predicted streamwise variation of peak turbulent shear stress with data. The two predictions are quite comparable up to 70^0 with the eq. (53) model yielding a decreased rate beyond 70^0 while the Launder model continues in an essentially linear fashion. Discounting the data point at 180^0, the trend provided by eq. (53) appears to be more consistent; moreover, the model yields values of peak turbulent shear stress which agree quite closely with the data of $0 < \theta < 150^0$.

4.0 MULTI-ZONE NAVIER-STOKES CODE

The code selected for turbulence model assessment studies is the PARCH Navier-Stokes (NS) code. PARCH is an outgrowth of the Ames Research Code (ARC) of Pulliam (3-84 and 1-85) and the propulsive extension, PARC, that Cooper (6-90) developed at AEDC. Like the AFWAL PNS code, PARCH embodies over ten years of continuous development, upgrade, and support by the government. ARC/PARC/PARCH represent the most popular and widely used NS codes in the United States. The PARCH version has unified the features of ARC and PARC and includes unique "patched grid" capabilities developed at AEDC to treat complex geometries using simple gridding procedures. With patched gridding, boundary conditions can be applied along any mapped grid lines of the computational domain, not just the bounding domain. This facilitates dealing with fins, struts, cavities, etc.

PARCH is an implicit code which is requisite for the efficient treatment of turbulent flows near walls where grid spacing is small and would severely limit time-steps if explicit methods were utilized. Separate 2D/AXISYMMETRIC and 3D versions are operational which have been specialized to various flow problems shown in Table VII. Versions of PARCH are operational with finite-rate chemistry and multi-phase flow. Multi-zone versions are available where each zone has internal patching capabilities as well. PARCH has been applied to aerodynamic flows (hypersonic vehicles, tactical missiles, circulation-control airfoils), to propulsive flows (rocket nozzles, gas turbines, scramjet inlets/combustions/nozzles), jets/plumes/wakes (aircraft jets, rocket plumes, RV wakes), and laser flows. Moreover, it is presently being used as a research tool under NASA/LaRC support to study advanced turbulence models for jets (in support of the high speed civilian transport program).

Turbulence models have been incorporated into PARCH in both a loosely-coupled manner and a strongly-coupled fashion. The PARCH/Gas Turbine version presently contains the following turbulence models:

(1) k-ε model, high Re version

(2) compressibility-corrected variants of the above with the corrections of Dash (8-75), Sarkar et. al (12-89), and Zeman (2-90)

(3) near-wall extensions including van-Driest two-layer coupling, the Chien (1982) low Re version, and the Rodi (1-91) one-equation hybrid approach

(4) geometric corrections for axisymmetric effects (Launder, 1985 and Pope (3-78) corrections), for swirl and streamwise curvature corrections (Penn State/Lakshminarayana, 12-86 and Imperial College)

(5) k-w model, high Re version

Table VII. WORKING VERSIONS OF PARCH CODE

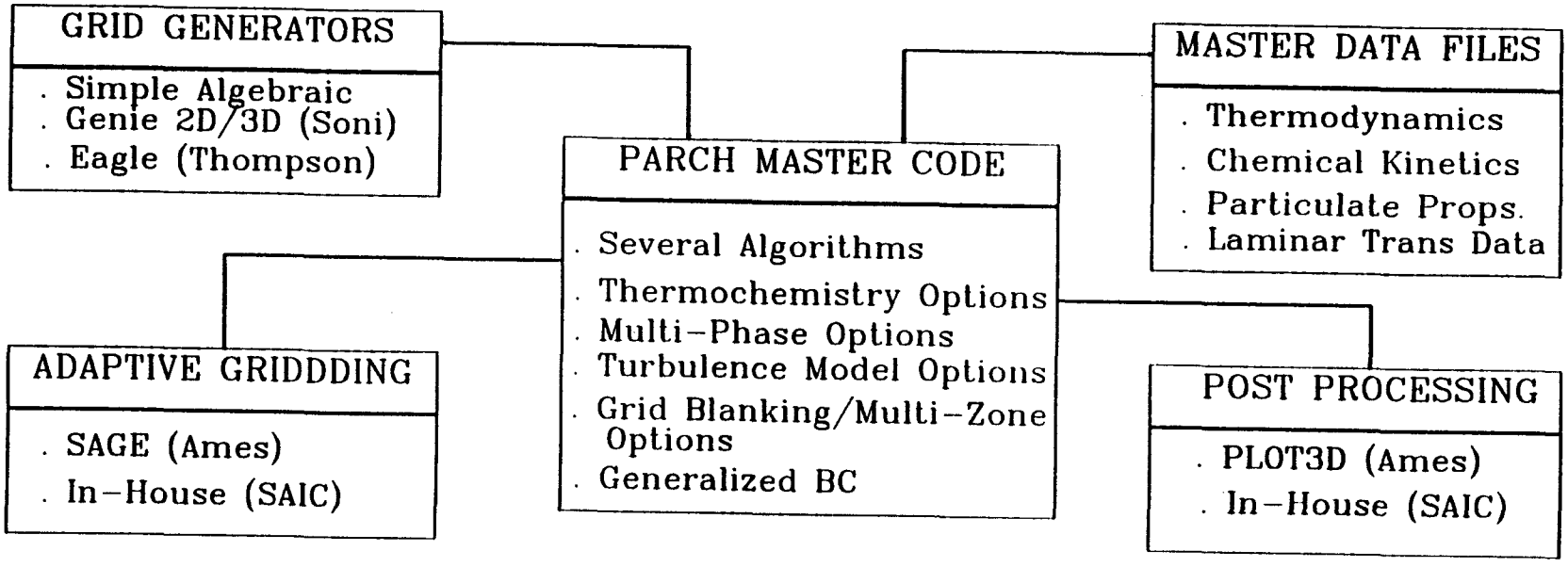

Table VII (cont.). SPECIALIZED VERSIONS OF PARCH CODE

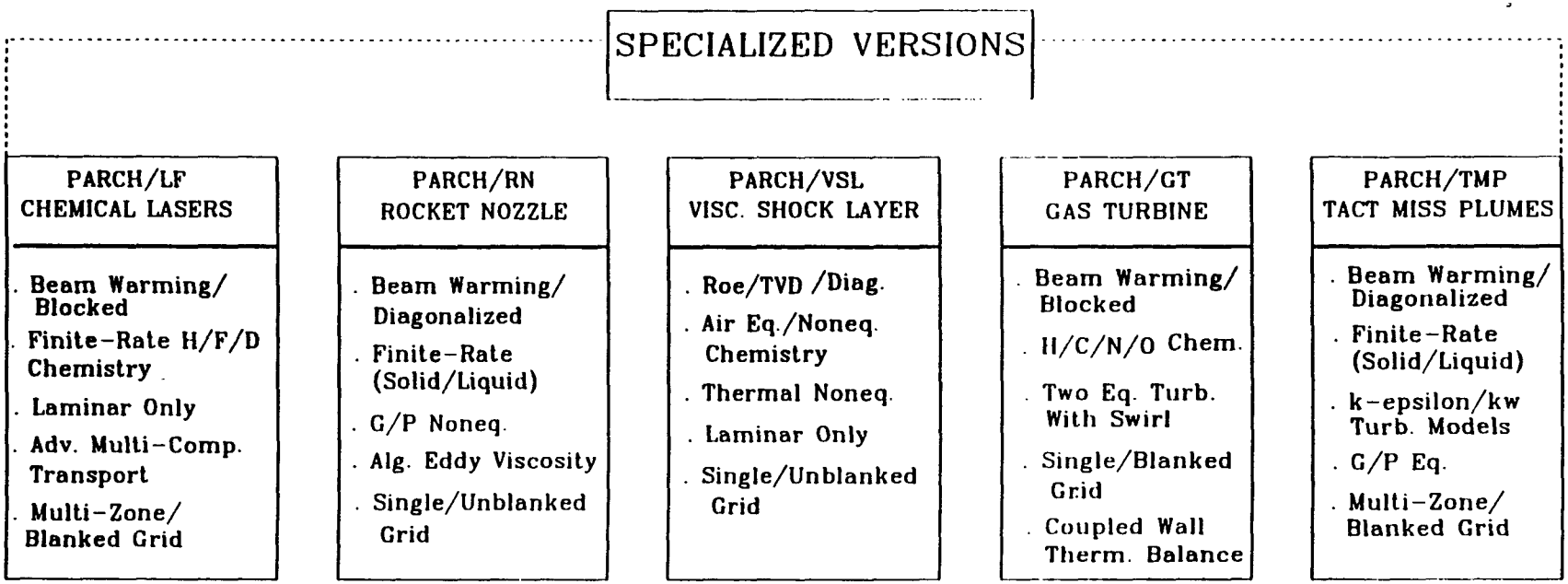

PARCH has been applied to a very large data base of fundamental flows as well as to many complex, three-dimensional flows as demonstrated by Dash et. al (6-91, 1-91, and 10-89), York et. al (6-89 and 11-89), and Sinha et. al (7-88 and 7-89).

The selection of PARCH as a generalized tool to study the behavior of turbulence medels in high speed flows is motivated by many new practical factors. With current generation missiles and spacecraft having highly integrated propulsive systems, one cannot separately study aerodynamic and propulsive flows.

The exhaust flow from integrated propulsive systems can wet large protions of the aerodynamic surfaces. This flow can be chemically-reacting and for missiles with solid-propellant rockets, will be multi-phase. With lateral control jets replacing conventional aerodynamic control surfaces on many missiles, the ability to analyze such flowfields is felt to be requisite. PARCH which has chemical and multi-phase capabilities, is the only 3D Navier-Stokes Code now being used in a design environment to support the development of varied-missile systems with integrated propulsive systems and missiles with lateral control jets.

Another selection criterion for PARCH is the validation of the code with its included turbulence models. This has occured over a five year period starting with the inclusion of the basic high Re version of k-ε and checkout for varied high speed free shear flows, and versions of k-ε coupled to various near-wall models. It takes many man-years of effort to incorporate an advanced turbulence model into a Navier-Stokes code and get it to work properly in a broad spectrum of flow problems. No other Navier-Stokes code has the experience base of PARCH with advanced turbulence models.

Finally PARCH is now used as a "standard" tool by many different communities dealing with aerodynamic, propulsive, signature and acoustic problems. PARCH is a standard component of the SDIO system of codes for missile detection, the SPIRITS system of codes for aircraft/helicopter detection, the HSCT system of codes (MICOM) NSWC, etc) for missile design, etc., etc. All these communities are dealing with the turbulence problem in a practical manner and their experience with PARCH will provide significant contributed value to envisioned work by Wright-Labs with this code.

5.0 TURBULENCE MODELING ROADMAP

In order to accommodate a wide range of practical engineering problems using a generic turbulence closure model, a "building block" approach will be required. This approach consists of evaluating a variety of turbulent boundary layer flows relative to corresponding validation cases which can be used to calibrate closure constants (or functional coefficients) together with appropriate damping terms. The methodology would commence with simple unit level problems and progress to more complex flows with combined effort as the experience based is enhanced. Table VIII shows the descending order of flow status that should be considered. The end product of the methodology will provide a matrix (table) of closure coefficients and damping functions that can be used in the proposed hybrid turbulence model that will allow the user to "dial-a-model" as required to solve the problem at hand. Several techniques that can be used to develop the building block methodology will be addressed in this section as well as the identification of a fundamental database for validation.

The building-block matrix shown in Table VIII will consist of compressible boundary layer and jet flowfields that are 2D or axisymmetric. While several successes have been demonstrated for unit problems, coupling of unit level problems with compressibility has not been established. For a generic turbulence model to analyze fundamental wall bounded and jet flowfields, the turbulence modeling in each flow state must be validated in a reliable manner. Consequently, a systematic development from the simplest flow to the more complex flows will be required. The emphasis of our approach will be on boundary layer type flows. A similar approach for jet flowfields has been proposed to NASA (Dash et al, 10-91) that would complement proposed work for a Phase II program.

5.1 Wall Roughness

Appendix A addressed issues of wall roughness in boundary layer flow. The modification to the C-S model to incorporate the van-Driest local vortex generating factor was shown to be inadequate since the factor did not allow for roughness elements greater than the sublayer thickness. Since the near wall velocity distribution can be dependent upon many geometric variables that define surface texture, the concept of Rotta (1962) will be adapted. Here, the influence of surface roughness is felt only close to the wall such that the law of the wall relations could be used by shifting the reference plane by some distance ($-\Delta y^+$) with respect to mean roughness level. To accommodate the no-slip condition at the new surface, the reference plane would be required to move in the direction opposite to the mean flow at a rate that depends upon the shift.

Cebeci and Chang (7-78) used the Rotta criteria in an algebraic mixing length model but allowed for the no-slip condition to be maintained at $y^+ = 0$. Chang (5-71) used reference plane slip velocity but did not allow for a shift in the reference plane

Table VIII. Building-Block Turbulence Modeling

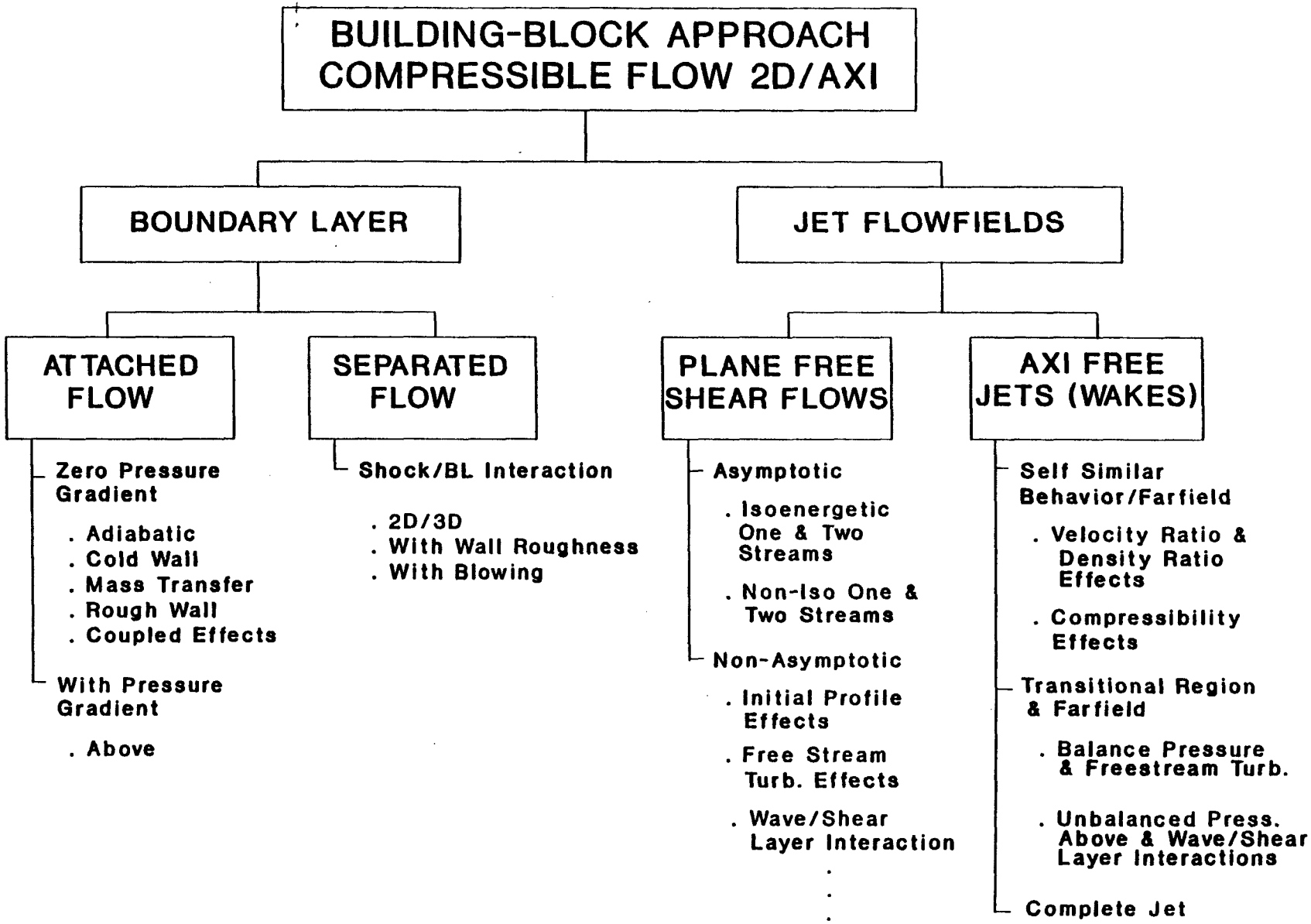

position. Laganelli (1-75) as well as Krogstad (6-91) considered both aspects of the Rotta concept. The latter paper provided a thorough examination of the damping requirements and showed excellent comparisons to incompressible data. In both cases, the authors chose to characterize the reference surface by a single roughness length scale, namely, the equivalent sandgrain roughness height which is easily obtained. In a recent investigation, Laganelli and Scaggs (6-90) reviewed the single sandgrain roughness length scale criteria of Dirling (6-73), which was developed from incompressible data, and demonstrated that the criteria could be used for compressible flow conditions. The authors (Laganelli and Scaggs, 1-86) determined that a unit Reynolds number (velocity scale) was required in the equivalent sandgrain roughness parameter. The authors also reviewed the reference plane shifting criteria using a boundary layer code and recommended a technique to define the reference plane position. A comparison to compressible data showed good agreement.

When the roughness elements just protrude through the viscous sublayer, turbulence production can be generated by the individual roughness elements where the eddy length is on the order of the element size. In regions away from the wall, the impact of the vortex generating roughness elements could have an effect on local equilibrium (i.e. production is approximately equal to dissipation).. However, with the use of two-equation models, the field equations should provide insight into near-wall modeling requirements especially since the kinetic energy is carried to the wall.

Finally, it should be noted that Arora et. al (11-82) used the technique of Cebeci and Chang in a two-equation k-ε model (using the wall function method) and the assumption of equilibrium away from the wall. Comparison of the method to incompressible and compressible data showed good agreement which could render the no-slip condition $y^+ = 0$ as opposed to the reference plane as not important.

The velocity distribution in the wall region given by Krogstad (6-91) is

$$u^+ = \int_0^{y^+} \frac{2dy^+}{1+\sqrt{1^+(2\ell^+D_R)^2}} \qquad (54)$$

where ℓ^+ is the dimensionless mixing length and D_R is a roughness damping function (given in the bracket of Eq. A-12). Since D_R is limited to $D_R \leq 1$ (as given in Eq. A-12), Krogstad proposed a shift such that

$$D_R = 1 - e^{-y^+/A^+} + exp\left[-\frac{y^+}{A^+}\left(\frac{70}{k_T^+}\right)^{3/2}\right]\left[1+exp\left(-\frac{70}{k_T^+}\right)\right]^{1/2} \qquad (55)$$

An examination of the above shows the damping term to be similar to that given by Eqs. (A-13) and (A-14). However, Eq. (55) appears to have correct asymptotic behavior in both the linear region of the sublayer as well as the log-law (slope) region

that correctly accounts for the velocity shift. The form given by Eqs (A-13) and (A-14) used an average value in the sublayer region and does not have the asymptotic characteristics of Eq. (55).

This work should provide excellent near wall modeling techniques to incorporate into the proposed hybrid k-ε turbulence model.

5.2 Mass Transfer

Appendix A also describes the basic methodology that has been used by the modelers to treat mass transfer effects. Essentially, corrections have been made to the damping coefficient such that $A^+ = A^+ (v_w)$. These corrections have been adapted into algebraic eddy viscosity models as well as two-equation models. For the k-ε type, modifications are usually made to damping coefficients in the expontial term in wall functions, van Driest bridging techniques, and low Reynolds number near-wall techniques. The k-ω type have also featured mass transfer modeling using law of wall relations coupled to boundary conditions using a perturbation solution in the near wall region. However, all of the above methods have shown success for incompressible flow conditions only. To the authors best knowledge, no-one has demonstrated the ability to predict mass transfer effects subject to compressible flow.

Rajendran and Laganelli (12-89) considered the arguments of van-Driest that the presence of the wall can modify the universal constant (Karman constant) such that

$$\kappa = \kappa \ [1\text{-}\exp\ (\text{-}y/A)]$$

or that the mixing length must be charged to

$$\iota = \kappa\, y\ [1\text{-}\exp\ (\text{-}y/A)]$$

An examination of compressible mass transfer data of Martellucci et al (4-74) and Danberg (1-67) shows that the slope in law of the wall coordinates deviates from the non-blowing value and changes with increasing blowing. Accordingly, Rajendran and Laganelli suggest that the damping term he modified in the same spirit as wall roughness in as much as wall blowing has the opposite effect as roughness in law of the wall coordinates. For this condition, the damping can be expressed as

$$[1-exp(-y^+/A^+)] + \beta (y^+/A^+)^n \ exp\ [B_u/B_{u_{cr}}] \qquad (56)$$

where

$$\beta = \beta\ (\lambda) = (\rho v)_w / (\rho u)_e \qquad (57)$$

$$Bu = (\lambda/St) \tag{58}$$

$$Bu_{cr} = \exp\ [2.7726(W-0.5)] \tag{59}$$

$$W = (Tw/Te)^{-.125} + 0.125M_e \tag{60}$$

In the above, the critical blow-away parameter Bu_{cr} was determined by Laganelli et. al. (4-75) to vary between a value of 4 (incompressible) to 64 (compressible) using data from a several facilities over a range of Mach number and wall temperature ratio. The technique was used in the Baldwin-Lomax algebraic eddy viscosity model and the constants β and n were determined from the data of Martellucci et al (4-74). This initial result showed promise and will allow for a technique to be further evaluated in a Phase II program.

With the ability to provide more physics to the damping coefficient A^+ using the kinetic energy equation, together with the heuristic arguments developed for near wall functions, we believe that the ability to characterize mass transfer can be accomplished. This can be demonstrated by comparing the exponent terms from the damping functions of van Driest and Norris-Reynolds i.e.

$$Y^+/A^+ = C_3\ \sqrt{k}\ y/\upsilon$$

which leads to the definition of the damping coefficient to be $A^+ = U_\tau / C_3\ k^{1/2}$. Here, one has the added advantage of the kinetic energy which is provided by the field equation and should provide better physics for determining characteristics of $A^+ = A^+ (v_w)$ as opposed to data correlations.

5.3 Compressibility

Section 3.3 addressed issues concerning compressible modifications to the standard k-ε incompressible field equations. Specifically, investigations were made by Dash et al (6-91 and 9-91), Viegas-Rubesin (6-91), and Wilcox (6-91) that considered adaption of the Sarkar et al (12-89 and 6-90) and Zeman (2-90) compressible-dissipation models to the k-ε and k-ω two-equation turbulence models, respectively. While Dash et al and Viegas-Rubesin focussed on mixing layers, Wilcox considered both mixing layers and wall bounded flows. The authors noted some variation in the compressible models.

Several observations can be drawn from the work of the above investigators which, when supplemented by the work of Horstman (6-91) provide a practical path that can be followed to enhance the prediction of compressible shear flows. Since section 3.3 focussed on free mixing layers, the immediate near path should consider the impact of these compressible modifications to the turbulence two-equation models in analyzing wall bounded flows.

When the Sarkar et al and Zeman compressible terms were added to the k-ε and k-ω models, a comparison with free shear layer data showed that the compressibility effects on spreading rate was reasonably predicted. However when applied to adiabatic, flat plate compressible boundary layer flow data ($M \leq 5$), the compressible corrections tended to underpredict skin-friction data while the unmodified turbulence two-equation model predicted this data quite well. Wilcox modified the coefficients in the Sarkar model to force agreement with the skin-friction data and subsequently used the modified version to analyze the free shear data base. Wilcox's experiences indicated that the compressibility modifications can not be arbitrarily extended to the near wall region, even for simple parallel shear flows. Initial application of the Sarkar compressible modifications to separated flow conditions ($M<3$) provided a larger separation length than the unmodified models with significantly better agreement with data (Dash, 9-91).

Wilcox (6-91), demonstrated that the Sarkar and Zeman models were inaccurate in the near wall region and developed an improved model that combines the Zeman extended lag effect with the Sarkar dilatational dissipation effects on the turbulent Mach number. When the hybrid model was applied to the limited data base of mixing layers ($M_c<2$), adiabatic flat-plate boundary layers ($M<5$), and separated flows ($M<3$), data trends were correctly predicted. The k-ω equations were used for this examination.

Horstman (6-91) used the standard k-ε model and two modifications of this model and compared the results to a range of supersonic/hypersonic separated flows. The modified k-ε models consisted of the standard k-ε equations and a one-equation model (hybrid, Rodi, 1-91) for length scale in the near wall region and the standard k-ε model with additional compressible terms (as provided from Farve averaging by Rubesin, 6-90). The standard k-ε tended to underpredict the separation length and overpredict skin-friction and heat transfer. The Rodi hybrid model tended to increase the separation zone while underpredicting skin-friction and heat transfer in the reattachment region. The k-ε model with additional compressible terms tended to provide the same trends as the hybrid model but was difficult to implement readily. An examination was made to determine the impact of individual effects of compressible modifications and length scale (Rodi) modifications. It was shown that both compressible and length scale modifications increased the separation zone length while length scale alone changed skin-friction and heat transfer in the reattachment region.

Based on such assessments, our building block approach will consist of "carefully" combining improvements for free shear layer flows and boundary layer flows using the standard k-ε model with compressible modifications of Dash (9-91) as the baseline model. Near-wall behavior will be explored using low Reynolds number modifications (with compressible correction) and the Rodi hybrid length scale modifications (also with appropriate compressible modifications).

5.4 Pressure Gradient (Curvature)

Section 3.4 addressed issues concerning vortical-curvature modifications. These modifications include corrections for axisymmetric behavior, streamwise curvature, swirl, and streamwise vorticity. As noted, these modifications have been made to the constants in the ε equation of the k-ε two-equation model.

Consistent with our building block approach, a systemetric evaluation of varied geometric corrections will be required. It is imperative to couple the assessment of the varied geometric corrections with the assessment of the compressibility-correction (both influence the length scale), and, with the near-wall formulation. The geometric corrections are generally formulated for low speed flows and they may not work without recalibration for higher speed flows even with the compressibility-correction implemented.

5.5 Compressible Flow Database

The previous sub-sections considered issues and methodologies that have been used to predict attached/separated boundary layer and jet flow fields. Moreover, several of the methodologies have been shown to predict favorable and adverse pressure gradient flows subject to compressible flow conditions. Our objective has been the development of a generic turbulence closure model capable of providing near term solutions to a wide range of engineering problems. Accordingly, we have identified the k-ε two-equation model with variations to meet these near term goals. Inparticular, this will involve the hybrid concept that consists of the standard k-ε model and a one-equation model for length scale. Variations will require a systematic investigation to provide compressible corrections, curvature corrections, roughness and blowing corrections.

A database will be required to provide this systematic investigation. The Stanford conferences, NASP symposiums, and recent AIAA meetings/workshops have established a formidable list of test results which can be used to develop validation cases. Table IX lists a database of compressible flow experiments for boundary layer and jet flowfields. This preliminary database is consistent with the building block approach described in Table VIII. While several of these references provide data for unit flow problems (mass transfer, for example), other define experiments for several unit level problems. The database allows development for simple flat plate, adiabatic parallel shear flows to complex shock/boundary layer interactions and subsequent

Table IX. SOURCES OF COMPRESSIBLE FLOW DATABASE

BOUNDARY LAYER	SOURCE	FREE SHEAR LAYER/MIXING	SOURCE
dP/dX = 0			
• Adiabatic	Bradshaw (1-91), Marvin-Coakley (11-89), NASP	• Balanced	Eggers (9-66) Padova (9-85) NASA SP-321
• Cold Wall	Bradshaw (1-91), Marvin-Coakley (11-89), NASP		
• Mass Trans. - cold wall - hot wall	 Danberg (1-67), Martellucci et al. (4-74) Danberg (1-67), Martellucci et al. (4-74)	• Unbalanced • One-Stream	Seiner et al. (5-85) Seiner et al. (3-91), non-iso
• Roughness	Christoph et al. (2-87), Dissimilli-Scaggs (6-91) Goddard (1-59), Berg (7-78), Holden (1-84)	• Two-Stream	Chinzei et al. (5-86), iso Goebel-Dutton (1-90), non-iso Sullins (4-89), @ boundary walls Papamoschou-Roshko (1989) Samimy-Elliot (3-90)
• Roughness/ Blowing	Voisenett (6-79)		
dP/dX ≠ 0		• Wall Jet	Kraemer-Tiwari (12-83) Situ-Shetz (6-91)
• Curvature	Marvin-Coakley (11-89), Rubesin (1-89), NASP		
• Shock/B.L. Interaction	Settles-Dodson (6-91), Marvin-Coakley (11-89), NASP		
• Favorable/ Roughness	Laganelli-Scaggs (11-87)		
• Separation/ Roughness	Dissimilli-Scaggs (6-91)		

Other Sources: STANFORD II (Kline et al., 1982)
Martellucci et al. (PTP-S, 3-81)
Bushnell (1-91)

coupling of flow states. Most of these test cases (sans mass transfer and rough wall data) have been used by previous modelers using conventional techniques and in some cases with modifications to standard techniques. The quality of this database has essentially been judged and its limitations defined.

Finally, Table X shows how the building block approach can be used to develop a matrix for a turbulence "dial-a-model" to suit specific classes of engineering problems. It is our position to use the hybrid versions of the k-ε turbulence model with appropriate compressible corrections as the baseline model. Essentially this table would be structured having established the ability to predict compressible zero-pressure gradient, adiabatic and cold wall conditions for two-dimensional/axisymmetric flow fields.

As shown in Table X and described in the text, near-wall length scales will require modifications to include mass transfer, roughness, and curvature. These modifications will require adjustments to constants (which can become functional coefficients) and/or adjustments to a reference plane which requires the no-slip conditions at this plane. As noted by Rotta, this requires a shift ($-\Delta y^+$) relative to near roughness level and $+\Delta y^+$ (Rajendran and Laganelli) for mass transfer. For curvature these adjustments can be made to either length scales or the constants in the k-ε transport equations.

A potential variation to the above would be to provide a functional form for the constants, C_1, C_2, σ_k, and σ_ε to include wall effects. We have seen that low Reynolds number forms to the k-ε equations modify the constants C_1 and C_2 to include damping terms (mass transfer and roughness) or velocity gradients of mean flow for curvature.

We believe that the baseline compressible model together with the extensive experience base of k-ε modelers to predict a wide range of incompressible/compressible flow engineering problems, will provide the insight to complete the matrix of Table X. However, this will require the systematic building block approach and database described above.

Table X. Building-Block: Dial-A-Model Matrix for Turbulence Closure Near-Wall Requirements

k-ε TWO-LAYER MODEL (Standard with Compressible Corrections)	MASS TRANSFER	ROUGH WALLS	CURVATURE (dP/dX)
$\mu_t = C_\mu \rho k^{1/2} \ell_\mu$ $\ell_\mu = C_\ell y[1 - \exp(-26 R_T/A_\mu A^+)]$	$\frac{R_T}{A^+} = f\left[\frac{(\rho v)_w}{(\rho u)_e}, \frac{T_w}{T_e}, M_e\right]$	$A^+ = f(R_T, k_\tau^+)$	$A^+ = f(P^+)$
$\epsilon = k^{3/2} \ell_\epsilon$ $\ell_\epsilon = C_\ell y(1 + C_4/R_T)^{-1}$	C_ℓ fixed $C_\ell = f(\kappa, v_w^+)$	C_ℓ fixed $C_\ell = f(\kappa, k_\tau^+)$	C_ℓ fixed $C_\ell = C_\ell(\kappa, P^+)$
$C_\ell = \kappa C_\mu^{-3/4}$	fixed $\kappa = \kappa(v_w^+)$	fixed $\kappa = \kappa(k_\tau^+)$	fixed
$R_T = C_\ell \sqrt{k}\, y/\nu$			
$C_4 = 13.2$	$C_4 = C_4\ (v_w^+)$	$C_4 = C_4(k_\tau^+)$	$C_4 = C_4(P^+)$
$50.5 \le A_\mu \le 70$	TBD	TBD	TBD
$A^+ = 26$ $A^+ \sim u_\tau/C_3\sqrt{k}$	$u_\tau/C_3 k^{1/2}$ $C_3 = C_3(v_w^+)$	$A^+ = A^+(k_\tau^+)$	$A^+ = A^+(P^+)$
C_μ (=0.09), C_1, C_2	fixed functional	fixed functional	fixed functional
Parameters	$v_w^+ = v_w/u_\tau$, $= v_w/k^{1/2}$	$k_\tau^+ = u_\tau k_\tau/\nu$, $= k^{1/2} k_\tau/\nu$	$P^+ = \frac{\nu}{\rho u_\tau^3}\frac{dP}{dX}$, $= \frac{\nu}{\rho k^{3/2}}\frac{dP}{dX}$

6.0 ASSESSMENT OF PHASE I PROGRAM AND RECOMMENDATIONS FOR PHASE II EFFORT

6.1 Assessment of Phase I Program

A through review has been made to idenitfy a turbulence closure model capable of treating a wide range of practical engineering problems. The review has focussed on high Mach number compressibility effects for simple turbulent flows-boundary layers as well as free hear layers. Consideration was also given to wall effects such as roughness, blowing, and curvarture as well as flows experiencing separation and interactions. The process of selecting a turbulence model also considered adaptability to a multizonial Navier-Stokes solver with a long history in the industrial community.

It was determined that a hybrid k-ε model had the potential to meet the above objections for near term resolution to engineering problems. Specifically, the hybrid model consists of the standard two-equation high Reynolds number k-ε turbulence model for treating the outer layer and a one-equation model (with correct length prescription and the ε of the k-ε two-equation model) to treat the inner viscous layer. The hybrid model which was introduced by Rodi for incompressible flows has been successfully applied to analyze compressible flows including complex shock/boundary layer interactions. The hybrid model was chosen for a number of reasons, namely:

- k-ε two-equation model is the most widely used turbulence model in the scientific community
- it has an extensive experience base to treat a wide range of engineering problems
- use of the one-equation model to treat the length scale in the near-wall region eliminates numerical problems associated with the ε equation in the k-ε two-equation model
- one-equation models have demonstrated success to provide engineering solutions for flows subject to serve adverse pressure gardients and has demonstrated success to provide engineering solutions for hypersonic flows subject to complex shock/boundary layer interactions
- provides details of the turbulence structure as well as wall conditions
- k-ε transport equations have demonstrated success in adapability to industrial codes

Several turbulence models were reviewed that included zero-equation type where both length and velocity scales are algebraically prescribed, one-equation models where the length scale is prescribed and the velocity scale is determined by a kinetic energy transport equation, and the two-equation models where both length and velocity scales are determined by field equations; the hybrid k-ε being in the latter class. Variation in these models that have shown success include the one-half equation model of Johnson and King, the one-equation models of Goldberg and Baldwin and Barth, and a number of variations to the standard high Reynolds number k-ε model. Recent success has also been reported by Situ and Schetz who included extra terms in the basic shear stress equation to treat compressibility effects.

Finally, Dash et al, Wilcox, Horstman, and Viegas and-Rubesin considered the impact of compressibility with modifications to the two-equations turbulence models. Horstman considered the extra compressible terms suggested by Rubesin (cascadsed from Favre averaging) and compared this result to the standard k-ε and the hybrid k-ε noted above. It was determined that both the hybrid k-ε and the extra compressible terms k-ε model provided better resolution to interacting flows where the former gave better control on separation zone length and magnitude of wall heat transfer. The work by Dash, Wilcox, and Viegas-Rubesin considered adaption of the Sarkar et al and Zeman compressible terms to the two-equation models. It was determined that the compressible terms provided the reduction in the spread rate of mixing layers; but when applied to boundary layer flows (Wilcox) underpredicted results compared to unmodified turbulence models. However, the Wilcox model is not hybrid and our use of k-ε with the Rodi near wall formulation may remedy this deficiency.

Recognizing the potential of the hybrid k-ε turbulence model and the issues concerning compressibility, a building block approach has been identified that can provide a matrix of turbulence closure parameters that can be used with the hybrid k-ε model to solve a wide range of practical engineering problems. This matrix will provide the user with a "dial-a-model" menu capable of analyzing boundary layer and free shear layer flows. In order to develop this matrix through a building block approach, a database and a multizone Navier-Stokes solver were identified. The database consists of attached/separated boundary layer flows as well as plane free shear axisymetric free jet flows. This compressible flow database has been used by the scientific community and has been judged for quality and limitations for validating models.

The multizone Navier-Stokes solver identified for the building-block investigation is the PARCH code which is an outgrowth of the Ames Research Code (ARC) and the propulsive extension, PARC, developed at AEDC. PARCH embodies over ten years of continuous development, upgrade, and support by various DoD agencies. ARC/PARC/PARCH represent the most popular and widely used NS codes in the United States. A simplified version of the PARCH code that does not include chemistry is recommended for the development of the turbulence closure matrix.

6.2 Recommendations for Phase II Effort

A Phase II program is recommended that will focus on boundary layer type flows. Similar efforts are currently being proposed to NASA (by Sciences Application International Corporateion) to investigate free shear and axisymmetric jet flows. Both of these programs would compliment each other and could be developed in a concurrent fashion for technical interchange and cost effectiveness.

Prior to excersing the building block methodology, it will be necessary to resolve the compressibility issues identified in the Phase I investigation. The database will be used together the concepts proposed in this investigation; namely to include the Sarkar and Zeman compressible-dilatation terms, or some modification of the two, into the hybrid k-ε model. It is also recommended that a low Reynolds number version of the k-ε model, such as Chien, be modified in the same fashion for comparison. Having established a baseline compressible turbulence model, the building block methodology can proceed from simple to more complex flows to treat attached/separated flows including roughness, blowing, and curvature. Unit level problems will be investigated to develop the "dial-a-model" turbulence matrix. Coupling of individual effects will be required to ensure the extent of modeling capability as well as the ability to reduce to unit level problems.

A by-product of this Phase II effort will be the development of a "Turbulence Tutorial". This tutorial will consist of a two-dimensional boundary layer solver with several turbulence closure models ranging for zero-equation to two-equation levels. Also included in the turbulence turorial package will be a database and user-manual that will provide directions on use of the tutorial to be adapted to a PC that can include a post-processor, graphics, and windows to allow students, researchers, and teachers the opportunity to learn/explore/teach turbulence issues. While such a product could be an invaluable eductaional tool (university), it also provides a mechanism for researchers to test turbulence models and variations of prior to insertion into complex NS solvers (industry and government).

REFERENCES

Abdol-Hamid, K. S. and Wilmoth, R.G., "Multiscale Turbulence Effects in Underexpanded Supersonic Turbulence Effects in Underexpanded Supersonic Jets", AIAA Paper 90-2002, June 1990.

Andersen, P.S., Kays, W.M., and Moffat, R.J., "The Turbulent Boundary Layer on a Porous Plate: An Experimental Study of the Fluid Mechanics for Adverse Free-Stream Pressure Gradients", Dept. of Mechanical Engineering, Stanford Univ., Report HMT-15, May 1972.

Arina, R., Iuso, G. and Onorato, M., "Experimental and Numerical Analysis of Low-Reynolds Number Turbulent Channel Flows", AIAA Paper 91-1788, Honolulu, June 1991.

Arman, B. and Rabas, T. "Prediction of the Pressure Drop in Transverse, Repeated-Rib Tubes with Numerical Modeling", ASME/AICHE, Nat'l Ht. Trans. Conf., Minneapolis, MN, July 1991.

Arora, R., Kuo, K.K., Razdan, M.K., "Near Wall Treatment for Turbulent Boundary-Layer Computations", AIAA J. Vol. 20, No. 11, Nov. 1982.

Baker, R.J. and Launder, B.E., "The Turbulent Boundary With Foreign Gas Injection-II. Predictions and Measurements in Severe Streamwise Gradients", Int. J. of Ht. and Mass Transf., Vol. 17, 1974, pp. 293-306.

Baldwin, B.S., and Barth, T.J., "A One-Equation Turbulence Transport Model for High Reynolds Number Wall-Bounded Flows", AIAA Paper 91-0610, Jan. 1991 (also NASA TM-102847, Aug. 1990).

Baldwin, B.S. and Lomax, H. "Thin Layer Approximation and Algebraic Model for Separated Turbulent Flows", AIAA Paper 78-257, Huntsville, AL 1978.

Berg, D.E., "Surface Roughness Effects on the Hypersonic Turbulent Boundary Layer", Ph.D. Dissertation, CAL. Tech. 1977, also AIAA Paper 78-1159, Seattle, WA, July 1978.

Birch, S.F. and Eggers, J.M., "A Critical Review of the Experimental Data for Development Free Turbulent Shear Layers", NASA SP-321; 1973, pp. 11-40.

Bradshaw, P. and Launder, B.E. "Collaborative Testing of Turbulence Models", AIAA Paper 91-0215, Reno, NV, Jan. 1991.

Bradshaw, P., "Effect of Streamwise Curvature on Turbulent Flow", AGARDograph No. 169, 1973.

Bradshaw, P., "The Analogy Between Streamline Curvature and Buoyancy in Turbulent Shear Flow", J. Fluid Mec., Vol. 36, pp. 177-191, 1969.

Brankovic, A. and Syed, S. "Validation of Reynolds Stress Turbulence Model in Generalized Coordinates", AIAA Paper 91-1782, Honolulu, June, 1991.

Burr, R.F. and Dutton, J.C., "Numerical Modeling of Compressible Reacting Turbulent Shear Layers", AIAA Paper 90-1463, June 1990.

Bushnell, D.M. "Turbulence Modeling in Aerodynamic Shear Flow - Status and Problems", AIAA Paper 91-0214, Reno, NV, Jan. 1991.

Cebeci, T. and Chang, K.C., "Calculations of Incompressible Rough Wall Boundary Layer Flows", AIAA J. Vol. 16, July 1978, pp. 730-735.

Cebeci, T. and Smith, A.M.O., Analysis of Turbulent Boundary Layers Academic Press, N.Y. 1974.

Cebeci, T. and Smith, A.M.O., "Analysis of Turbulent Boundary Layers", Series in Applied Mathematics and Mechanics, Vol. XV, Academic Press, Orlando, FL. 1974.

Chang, Y.Y., "Computations of Incompressible Turbulent Boundary Layers on Rough Surfaces", Nat'l Research Council of Canada, Ottawa, Aero. Rpt. LR-546, May 1971.

Chen, H.C. and Patel, V.C., "Evaluation of Axisymmetric Wakes from Attached and Separated Flows", Turbulent Shear Flows, 6, Springer-Verlag, Berlin Heidelberg, 1989, pp. 215-231.

Chen, H.C. and Patel, V.C. "Near-Wall Turbulence Models for Complex Flows Including Separation", AIAA J., Vol. 26, pp. 641-648, 1988.

Chen, P. and Kim, S.W., "A Multiple-Time-Scale Turbulence Model Based on Variable Partitioning of Turbulent Kinetic Energy Spectrum", AIAA-88-0221, Reno, NV, Jan. 1988.

Chen, Y.S. "Applications of a New Wall Function to Turbulent Flow Computations", AIAA Paper 86-0438, Reno, NV., Jan. 1986.

Chien, K.Y. "Predictions of Channel and Boundary Layer Flows with a Low Reynolds Number Turbulence Model", AIAA J. Vol. 20; No.1 pp. 33-38, 1982.

Chinzei, N.G., et al. , "Spreading of Two-Stream Supersonic Turbulent Mixing Layers", Physics of Fluids, Vol. 29, No. 5, 1986, pp. 1345-1347.

Chinzie, N., et al., "Spreading of Two-Stream Supersonic Mixing Layers", Phys. Fluids, V. 29, No. 5, May 1986.

Christoph, G.H., Laganelli, A.L., and Scaggs, N.E., "Numerical Simulation of Flow Over Rough Surfaces, Including Effects of Surface Blowing and Pressure Gradients", AFWAL/TR-87-TBD, also SAIC Report # 87/1009, Feb. 1987.

Cooper, G. and Sirbaugh, J. "The PARC Distinction: A Practical Flow Simulator", AIAA Paper 90-2002, June 1990.

Cousteix, J., Arnal, D., Aupoix, B., and Gleyzes, C., "Recent Studies on Transition and Turbulence at ONERA-CERT", AIAA Paper 91-0332, Reno, NV., 1991.

Danberg, J.E., Van Gulick, P. and Kim, J. "Turbulence Modeling for Steady Three-Dimensional Supersonic Flows", AD-A170-042, June 1986.

Danberg, J.E., "Characteristics of the Turbulent Boundary Layer With Heat and Mass Transfer: Data Tabulation", NOLTR-67-6, (Naval Ordnance Lab Research Report 280), Jan. 1967.

Danberg, J.E., "Characteristics of the Turbulent Boundary Layer With Heat and Mass Transfer: Data Tabulation", NOLTR 647-6, (Naval Ordnance Lab Research Rpt. 280), Jan. 1964.

Dash, S.M., et. al., "Computer Code for HSCT Exhaust Flowfield Simulation and Observations on Turbulence Modeling", AIAA Paper 91-3297, Baltimore, MD, Sept. 1991.

Dash, S.M., Sinha, N., York, B.J., Kenzakowski, D.C., and Lee, R.A., "Computer Codes for HSCT Exhaust Flowfield Simulation and Observations on Turbulence Modeling", 9th AIAA Applied Aerodynamics Conference, AIAA Paper 91-3297, Baltimore, MD, September 23-26, 1991.

Dash, S.M., Walker, B.J., and Seiner, J.M., "A Building-Block Approach for Turbulence Model Validation/Upgrade Focussed on High-Speed Jet Flows", 1992 JANNAF Propulsion Meeting, February 24-28, 1992. (SAIC/FW TA-37)

Dash, S.M. "Observations on CFD and Turbulence Model Validation/Calibration for the Simulation of High-Speed Propulsive Flowfields", Invited Paper for CFD code Validation/Calibration Workshop - JANNAF/AIAA Airframe Integration Panel, Reno, NV. Jan. 1991.

Dash, S.M., "Observations on Practical Turbulence Modeling for High-Speed Jet/Plume Flowfields", AIAA Paper 91-1789, Honolulu, June 1991.

Dash, S.M., "PARCH Propulsive/Plume Flowfield Codes", EO Aerial Targeting Models User's Meeting, Wright-Patterson AFB, Oct. 24-25, 1989, pp. 421-446.

Dash, S.M., "Turbulence Modeling for Computations of High Speed Flows - State-of-the-Art", Fifth NASP Technology Symposium, NASP CP 5029, pp. 287-320, Oct. 1988.

Dash, S.M., York, B.J., Sinha, N. and Dvorak, F.A., "Wall Jet Analysis for Circulation-Control Aerodynamics: Part I: Fundamental CFD and Turbulence Modeling Concepts", Proceedings of the Circulation-Control Workshop, NASA CP 2432, 1986, p. 23-70.

Dash, S.M., Beddini, R.A., Wolf, D.E. and Sinha, N., "Viscous/Inviscid Analysis of Curved Sub-or Supersonic Wall Jets", AIAA Paper 83-1679, Danvers, MA, July 1983.

Dash, S.M., Wilerstein, G. and Vaglio-Laurin, R., "Compressible Effects in Free Turbulent Shear Flows", AFOSR, TR-75-1436, Aug. 1975.

Dismile, P.J. and Scaggs, N., "Mach 6 Turbulent Boundary Layer Characteristics on Smooth and Rough Surfaces", AIAA Paper 91-1762, Honolulu, HI, June 1991.

Donaldson, C. and Gray, K.E., "Theoretical and Experimental Investigation of the Compressible Free Mixing of Two Dissimilar Gases", AIAA Journal, Vol. 4, 1966, pp. 2017-2025.

Eggers, J.M., "Velocity Profiles and Eddy Viscosity Distribution Downstream of a Mach 2.2 Nozzle Exhausting into Quiescent Air", NASA TN-D-3601, 1966.

Foloyan, C.O. and Whitelaw, J.H., "The Effectiveness of Two-Dimensional Film-cooling Over Curved Surfaces", ASME Paper 76-HT-31, 1976.

Fujisawa, N., Rodi, W. and Schonung, B., "Calculations of Transitional Boundary with a Two-Layer Model of Turbulence", Proc. 3rd Int. Symp. on Transport Phenomena and Dyn. of Rotating Machinery, Honolulu, Apr. 1990.

Gatski, T.B., "Turbulence Modeling of Compressible Flows", 7th NASP Symp. Paper No. 28, Oct. 1989.

Goddard, F.E., "Effect of Uniformly Distributed Roughness on Turbulent Skin-Friction Drag at Supersonic Speeds", JAS, 26, pp. 1-15, Jan. 1959.

Goebel, S.G. and Dutton, J.C., "Experimental Study of Compressible Turbulent Mixing Layers", AIAA J. Apr. 1991, pp. 538-546.

Goebel, S.G. and Dutton, J.C., "Velocity Measurements of Compressible, Turbulent Mixing Layers", AIAA Paper 90-0709, January 1990.

Goldberg, U.C., "Turbulent Flow Computations with a Two-Time Scale One-Equation Model", AIAA Paper 91-1790, Honolulu, June 1991.

Gorski, J.J., "A New Near-Wall Formulation for the k – ε Equations of Turbulence", AIAA Paper 86-0556, Reno, NV, Jan. 1986.

Gupta, R.N., Moss, J.N., Zoby, E.V., and Simmonds, A.L., "An Evaluation of Turbulence Models for Massively Blown Surfaces", Prog. Astro. and Aero. Vol. 85, Ed. P.E. Bauer and H.F. Collicott, AIAA Series pp. 446-471.

Hah, C and Lakshminarayana, B., "Prediction of Two and Three-Dimensional Axisymmetrical Turbulent Wakes, Including Curvature and Rotation Effects," AIAA J., pp. 1196-1204, October 1980.

Hanjalic, K. and Launder, B.E., ASME J. of Fluids. Eng.,102, 1980.

Hanjolic, K. and Launder, B.E. "Contribution Towards a Reynolds Stress Closure for Low-Reynolds-Number Turbulence", J. Fluid Mech., Vol. 74, pp. 593-610, 1976.

Holden, M.S., "Experimental Studies of Surface Roughness Shape and Spacing Effects on Heat Transfer and Skin-Friction in Supersonic and Hypersonic Flows", AIAA Paper 89-0016, Jan. 1984.

Hortsman, C.C., "Hypersonic Shock-Wave Turbulent - Boundary - Layer Interaction Flows - Experiment and Computation", AIAA Paper 91-1760, Honolulu, 1991.

Iacavides, H. and Launder, B.E., "The Numerical Simulation of Flow and Heat Transfer in Tubes in Orthogonal - Mode Rotation", Proc. 6th Symp. of Turb. Shear Flows, Toulouse, France, 1987.

Johnson, D.A. and Coakley, T.J., "Improvements to a Nonequilibrium Algebraic Turbulence Model", AIAA J. Vol. 28, No. 11, Nov. 1990.

Johnson, D.A. "Transonic Separated Flow Predictions with an Eddy-Viscosity/Reynolds-Stress Closure Model", AIAA J. Vol. 25, No. 2, Jan. 1987.

Johnson, D.A. and King, L.S., "A Mathematically Simple Turbulence Closure Model for Attached and Separated Turbulent Boundary Layers", AIAA J., Vol. 23, Nov. 1985, pp. 1684-1692.

Jones, W.P., and Launder, B.E., "The Prediction of Laminarization with a Two-Equation Model of Turbulence", International Journal of Heat and Mass Transfer, Vol. 15, February 1972, pp. 301-314.

Kim, S.W. and Chen, P., "A Multiple-Time-Scale Turbulence Model Based on Variable Partitioning of Turbulent Kinetic Energy Spectrum", AIAA Paper 88-0221, Reno, NV., Jan. 1988.

King, L.S. and Johnson, D.A., "Separated Transonic Airfoil Calculations with a Nonequilibrium Turbulence Model", NASA TM-86830, November 1985.

Kline, S.J., Cantwell, B.J. and Lilley, G.M., "Proceedings, 1980-81 AFSOC-HTTM-Stanford Conference on Complex Turbulent Flows - Comparison of Computation and Experiment", Vols 1-3, Stanford Univ., 1982.

Kolmogorov, A.N., "Equations of Turbulent Motion of an Incompressible Fluid", Izvestia Academy of Sciences, USSR; Phy., V-6, 1942.

Kraemer, G.O. and Tiwari, S.N., "Interaction of Two-Dimensional Transverse Jet with Supersonic Mainstream", NASA CR-175446, December 1983.

Krogstad, P.A., "Modification of the van Driest Damping Function to Include the Effects of Surface Roughness", AIAA J., Vol. 29, No. 6, June 1991.

Laganelli, A.L. and Scaggs, N.E., "Equivalent Sandgrain Methodology for Compressible Flows", AIAA Paper 90-1718, Seattle, WA, June 1990.

Laganelli, A.L. and Wolfe, H., "Prediction of Fluctuating Pressure in Attached and Separated Turbulent Boundary Layer Flow", AIAA Paper 89-1064, 12th Aeroacoustic Conference, April 1989.

Laganelli, A.L. and Scaggs, H.E., "Upstream Pressure Gradient Effects on Boundary Layer Characteristics Over Rough Surfaces", AFWAL-TR-87-TBD, Nov. 1987, also SAIC Rpt. # 87/1177, Nov. 1987.

Laganelli, A.L. and Scaggs, N.E., "Wall Shear Characteristics on Smooth and Rough Surfaces Based on Acoustic Measurements", AFWAL TR-85-3114, January 1986.

Laganelli, A.L., "An Examination of the Coupling Between Mass Transfer and Roughness in a Compressible, Pressure Gradient Region using an Eddy Viscosity Concept", GE TIS SDR-004, Jan. 1975.

Lakshminarayana, B., "Turbulence Modeling for Complex Shear Flows", AIAA Journal, Vol. 24, No. 12, Dec. 1986, pp. 1900-1917.

Lam, C.K.G. and Bremhorst, K. "A Modified Form of the k-ε Model for Predicting Wall Turbulence", J. of Fluid Engr., Vol. 103, 1981, pp. 456-460.

Launder, B.E., "Low-Reynolds Number Turbulence Near Walls", Univ. of Manchester Inst. of Sci. and Tech., Thermo-Fluids, Div. Rpt. TFD/86/4, 1986.

Launder, B.E., "Progress and Prospects in Phenomenological Turbulent Models" Theoretical Approaches To Turbulence, V. 58, Springer-Verlag, 1985, Chapter 7.

Launder, B.E., Reynolds, W.C. and Rodi, W., Turbulence Models and Their Applications, Editions Eyrolles, France, 1984.

Launder, B.E., "Stress Transport Closures - Into the Third Generation", Symp. Turbulent Shear Flows III, pp. 259-266, Springer Verlag, 1982.

Launder, B.E. and Spalding, D.B., Lectures in Mathematical Models of Turbulence, Academic Press, N.Y. 1979.

Launder, B.E., Priddin, C.H. and Sharma, B.I., "The Calculation of Turbulent Boundary Layers on Spinning and Curved Surfaces", ASME J. Fluids Eng., pp. 231-139, March 1977.

Launder, B.E., and Spalding, D.B., "The Numerical Computation of Turbulent Flows", Appld Mech. and Eng. (1974) pp. 269-289.

Launder, B.E., and Sharma, B.I., "Application of the Energy-Dissipation Model of Turbulence to the Calculation of Flow Near a Spinning Disc", Letters in Heat and Mass Transfer, Vol. 1, 1974, pp. 131-138.

Launder, B.E., Morse, A., Rodi, W., and Spalding, D.B., "Prediction of Free Shear Flows - A Comparison of the Performance of Six Turbulence Models", pp. 361-426, Free Turbulent Shear Flows, NASA SP-321, Conference Proceedings, NASA Langley Research Center, Hampton, VA., 1972.

Launder, B.E., "Progress and Prospects in Phenomenological Turbulence Models", CH VII, Theoretical Approaches to Turbulence., Vol. 58, Ed. Dwyer, D.L., et al, 1985 Springer-Verlag.

Lin, T.C. and Bywater, R.J., "The Evaluation of Selected Turbulence Models for High-Speed Rough-Wall Boundary Layer Calculations", AIAA Paper 80-0132, Pasadena, CA, Jan. 1980.

Lumley, J.L. (Ed.): Whither Turbulence - Turbulence at the Crossroads. Lecture Notes in Physics 357, Springer, 1990.

Lumley, J.L., "Turbulence Modeling", Journal of Applied Mechanics, Vol. 50, pp. 1097-1103, 1983.

Martellucci, A., Weinberg, S. and Page, A., "Maneuvering Aerothermal Technology (MAT) Program: Data Bibliograph", BMO-TR-82-15, March 1981.

Martellucci, A., Hahn, J., and Laganelli, A., "Effect of Mass Addition and Angle of Attack on the Turbulent Boundary Layer Characteristics of a Slender Cone", Vol's. I, II and III, SAMSO TR-73-147 and SAMSO TR-74-112, Part II, April 1974.

Marvin, J.G. and Coakley, T.J., "Turbulence Modeling for Hypersonic Flows", NASP TM 1087, Nov. 1989.

Marvin, J.G., "Turbulence Modeling for Computational Aerodynamics", AIAA Journal, Vol. 21, No. 7, pg. 941, 1983.

McDonald, H. and Fish, R.W., "Practical Calculations of Transitional Boundary Layers", Introd. Ht. and Mass Trans. Vol. 16, 1973, pp. 1729-1744.

McGuirk, J.J. and Rodi, W., "The Calculation of Three-Dimensional Jets", Symposium on Turbulent Shear Flows Penn State, 1977.

McGuirk, J.J. and Rodi, W., "The Calculation of Turbulent Boundary Layers on Spinning and Curved Surfaces", ASME J. Fluids

Menter, F.R., "Performance of Popular Turbulence Models for Attached and Separated Adverse Pressure Gradient Flows", AIAA Paper 91-1784, Honolulu, June 1991.

Mŏnsour, N.N., Kim, J. and Moin, P., "Reynolds Stress and Dissipation Rate Budgets in Turbulent Channel Flow", J. Fluid Mech. Vol. 194, pp. 15-44, 1988.

Morse, A.P., "Axisymmetric Turbulent Shear Flows With and Without Swirl", Ph.D. Thesis, London University, England, 1977.

NASA (1972): "Free Turbulent Shear Flows" NASA Langley Research Center, Conf. Proc., NASA SP-321, 1972.

(NASP, 1991) Tenth National Aero-Space Plane Technology Symposium Vol. II - Computational Fluid Dynamics" NASP CP-10059 Monterey, CA, April, 1991.

(NASP,1990a), Ninth National Aero-Space Plane Technology Symposium - Vol. II - Computational Fluid Dynamics, NASP-CP-905L, Orlando, FL. Nov. 1990.

(NASP,1990b), Eighth National Aero-Space Plane Technology Symposium, Vol. II - Computational Fluid Dynamics, NASP-CP-8046, Monterey, CA. March 1990.

(NASP, 1989a) Seventh National Aero-Space Plane Technology Symposium, Vol. I - Computational Fluid Dynamics, NASP-CP-7042, Cleveland, OH Oct. 1989.

(NASP, 1989b) Sixth National Aero-Space Plane Technology Symposium, Vol. II - Computational Fluid Dynamics, NASP-CP-6037, Monterey, CA April 1989.

Norris, L.H. and Reynolds, W.C., "Turbulent Channel Flow With a Moving Wavy Boundary", Rpt. No. FM-10, Stanford Univ. Dept. M.E., 1975.

Padova, C., "Non-Reacting Turbulent Mixing Experiment", AFRPL TR-85-066, September 1985.

Papamoschou, D. and Koshko, A., "The Compressible Turbulent Shear Layer - An Experimental Study", J. Fl. Mech. 197, 453, 1989.

Patel, V.C., Rodi, W. and Scheuerer, G., "Turbulence Models for Near-Wall and Low Reynolds Number Flows: A Review", AIAA J. Vol. 23, pp. 1308-1319, 1985.

Pope, S.B., "An Explanation of the Turbulent Round-Jet/Plane-Jet Anomaly", AIAA J. Mar. 1978, pp. 279-281.

Priddin, C.H., "The Behavior of the Turbulent Boundary Layer on Curved Porous Walls", Ph.D. Thesis, University of London, 1975.

Pulliam, T.H. and Steger, J.L., "Recent Improvements in Efficiency, Accuracy, and Convergence for Implicit Approximate Factorization Algorithms", AIAA Paper 85-0360, Reno, NV. Jan. 1985.

Pulliam, T.H., "Euler and Thin-Layer Navier-Stokes Codes: ARC2D, ARC3D", Notes for Computational Fl. Dyn. User's Workshop UTSI Pub. E02-4005-023-84, March 1984, pp. 14.1-15.85.

Rajendran, N., and Laganelli, A.L. "Eddy Viscosity Modeling for Compressible Flow with Transpiration Cooling," White Paper submitted to WRDC/FIM, Dec. 1989.

Richmond, M. and Patel, V.C., "Convex and Concave Surface Curvature Effects in Wall-Bounded Turbulent Flows", AIAA J. Vol. 29, No. 6, June 1991.

Rodi, W., "Experience with Two-Layer Models Combining the $k - \varepsilon$ Model with a One-Equation Model Near the Wall", AIAA Paper 91-0216, Reno, NV, 1991.

Rodi, W. and Schenerer, G., "Scrutinizing the $k - \varepsilon$ Model Under Adverse Pressure Gradient Conditions", J. Fluids Eng. 108, 1986, pp. 174-179.

Rodi, W., "Examples of Turbulence-Model Applications", in Turbulence Models and Their Applications, edition Eyrolles, Paris, 1984, pp. 295-401.

Rodi, W., "Examples of Turbulence Models for Incompressible Flow", AIAA Journal, Vol. 20, No. 7, pg. 872, July 1982.

Rotta, J.C., "Turbulent Boundary Layers in Incompressible Flow", Prog. in Aero Sciences, Pergamon, Oxford, England, V.2, 1962.

Rubesin, M.W., "Extra Compressibility Terms for Favre-Averaged Two-Equation Models of Inhomogeneous Turbulent Flows", NASA CR 177556, June 1990.

Rubesin, M.W., "Turbulence Modeling for Aerodynamic Flows", AIAA Paper 89-0606, Reno, NV Jan. 1989.

Rubesin, M.W., and Viegas, J.R., "A Critical Examination of the Use of Wall Functions as Boundary Conditions in Aerodynamic Calculations", Proc. 3rd Symposium on Numerical and Physical Aspects of Aerodynamic Flow, Long Beach, CA, Jan. 1985.

Saffman, P.G., "A Model for Inhomogeneous Turbulent Flow", Proc. Roy Soc, Lond, Vol. A317, pp 417-433, 1970.

Samimy, M. and Elliot, G.S. "Effects of Compressibility on the Characteristics of Free Shear Layers", AIAA J., V. 28, No. 3, Mar. 1990.

Sarkar, S. and Balakrishnan, L. "Application of a Reynolds Stress Turbulence Model to the Compressible Shear Layer", AIAA Paper 90-1465, Seattle, June 1990.

Sarkar, S., Erlebacher, G., Hussaini, M.Y., and Kreiss, H.O., "The Analysis and Modeling of Dilitational Terms in Compressible Turbulence", NASA CR 181959, CASE Report No. 89-79, Dec. 1989.

Seiner, J.M, "Experimental Research on Aero Acoustics of Supersonic Jets", SAIC High-Speed Jet/Plume Turbulence Modeling Workshop Proceedings, SAIC, Fort Washington, PA, March 1991.

Seiner, J.M., Dash, S.M. and Wolf, E.E., "Analysis of Turbulent Under-Expanded Jets - Part II: Shock Noise Features Using SCIPVIS", AIAA Journal, Vol. 23, May 1985, pp. 669-677.

Settles, G.S. and Dodson, L.J., "Hypersonic Shock/Boundary Layer Interaction Database", AIAA Paper 91-1763, Honolulu, HI, June 1991.

Shang, J.S., Hankey, W.L. and Law, C.H., "Numerical Simulation of Shock Wave-Turbulent Boundary Layer Interaction", AIAA Journal Vol. 14, No. 10, Oct. 1976.

Shang, J.S., "Computation of Hypersonic Turbulent Boundary Layers with Heat Transfer", AIAA Paper 73-699, July 1973.

Shih, T.H., "An Improved $k - \varepsilon$ Model for Near-Wall Turbulence and Comparison With Direct Numerical Simulation", NASA TM 103221, August 1990.

Shih, T.H. and Monsour, N.N., "Modeling of Near-Wall Turbulence", in Engineering Turbulence Modeling and Experiments els. W. Rodi, E.N. Ganic, Elsevier. 1990, pp. 13-22.

Shirazi, S.A. and Truman, C.R., "Comparison of Algebraic Turbulence Models for PNS Predictions of Supersonic Flow Past a Sphere-Cone", AIAA Paper 87-0544, Reno, NV, 1987.

Sinha, N., York, B.J., Ong, C.C., Stowell, G.M., and Dash, S.M., "Navier-Stokes Analysis of High-Speed Propulsive Flowfields Using the PARCH Code", AIAA Paper 89-2796, Monterey, CA, July 1989.

Sinha, N., York, B.J., and Dash, S.M., "Applications of a Generalized Implicit Navier-Stokes Code, PARCH, to Supersonic and Hypersonic Propulsive Flowfields", AIAA Paper 88-3278, Boston, MA, July 1988.

Sislian, J.P. "Equations of Motion and Two-Equation Turbulence Model for Plane or Axisymmetric Turbulent Flows in Body-Oriented Orthogonal Curvilinear Coordinates and Mass-Averaged Dependent Variables", NASA CR-3025, 1978.

Situ, M. and Schetz, J.A. "New Mixing-Length Model for Turbulent High-Speed Flows", AIAA J., Vol. 29, No. 6, June 1991.

Spalding, D.B., "The Vorticity-Fluctuations (k-ω) Model of Turbulence; Early Papers", CFD/82/17, Imperial College, London, Nov. 1982.

Speziale, C. and Abid, R., "On Compressible Corrections to Two-Equation Turbulence Models for Supersonic and Hypersonic Flows", AIAA Paper 91-1781, June 1991.

Speziale, C.G., Abid, R., and Anderson, E.C., "A Critical Evaluation of Two-Equation Models for Near Wall Turbulence", AIAA Paper 90-1481, Seattle, WA, 1990.

Sugavanan, A., "Evaluation of Low Reynolds Number Turbulence Models for Attached and Separated Flows", AIAA Paper 85-0375, Reno, NV, 1985.

Sullins, G., "Shear Layer Mixing Tests", APL/JHU, Apr. 1989.

Ting, L. and Libby, P.A., "Remarks on the Eddy Viscosity in Compressible Mixing Flows,", J. of Aero. Sci., October 1960, pp. 797-798.

Townsend, A.A., "The Structure of Turbulent Shear Flow", Cambridge Univ. Press, Cambridge, England, 1976.

van Driest, E.R., "On Turbulent Flow Near Wall", J. Aero. Sci., 23, 1956, p. 1007.

van Driest, E.R., "Turbulent Boundary Layer in Compressible Fluid", J. Aero. Sci., 18, No. 3, March 1951.

Viegas, J.R. and Rubesin, M.W., " A Comparative Study of Several Compressibility Corrections to Turbulence Models Applied to High-Speed Shear Layers", AIAA Paper 91-1783, Honolulu, June 1991.

Verong, S.T. and Coakley, T.J., "Modeling of Turbulence for Hypersonic Flow With and Without Separation", AIAA Paper 87-0286, Reno, NV, Jan. 1987.

Voisinet, R.L., "Influence of Roughness and Blowing on Compressible Turbulent Boundary Layer Flow", NWSC, Rpt. # NSWC-TR-79-153, June 1979.

Wilcox, D.C., "A Half Century Historical Review of the $k - \omega$ Model", AIAA Paper 91-0615, Reno, NV, 1991.

Wilcox, D.C., "Progress in Hypersonic Turbulence Modeling", AIAA Paper 91-1785, Honolulu, June 1991.

Wilcox, D.C., "Supersonic Compression - Corner Applications of a Multiscale Model for Turbulent Flows", AIAA Journal, Vol. 28, No. 7 July 1990.

Wilcox, D.C., "Reassessment of the Scale Determining Equation for Advanced Turbulence Models", AIAA Journal, Vol. 26, Nov. 1988.

Wilcox, D.C., "Multiscale Model for Turbulent Flows", AIAA Journal, Vol. 26, Nov. 1988, pp. 1311-1320.

Wilcox, D.C. and Rubesin, M.W. , "Progress in Turbulence Modeling for Complex Flow Fields Including The Effect of Compressibility", NASA TP 1517, 1980.

Wilson, D.J. and Goldstein, R.J., "Turbulent Wall Jets with Cylindrical Streamwise Surface Curvature", ASME J. Fluids Eng., pp. 550-557, Sept. 1976.

Wolfshtein, M., "The Velocity and Temperature Distribution in One-Dimensional Flow with Turbulence Augmentation and Pressure Gradient", Int. J. Heat and Mass Transfer, Vol. 12, 1969, pp. 301-318.

York, B.J., Sinha, N. and Dash, S.M., "PARCH Navier-Stokes Code Analysis of Rocket and Airbreathing Nozzle/Propulsive Flowfields", JANNAF 18th Plume Technology Meeting, Monterey, CA, Nov. 14-17, 1989.

York, B.J., Sinha, N., Ong, C.C., and Dash, S.M., "PARCH Navier-Stokes Reacting/Multi-Phase Analysis of Generalized Nozzle Flowfields", AIAA Paper 89-1765, Buffalo, NY, June 1989.

Zeierman, S. and Wolfshtein, M., "Turbulent Time Scale for Turbulent-Flow Calculations", AIAA J., Vol. 24, No. 10, Oct. 1986.

Zeman, O., "Dilitation Dissipation: The concept and application in modeling compressible mixing layers", Phys. Fluids A, Vol. 2, No. 2, February 1990.

APPENDIX A

MODIFICATION TO CEBECI-SMITH MODEL

A.1 C-S Model with Compressible Effects

For a one-dimensional non-steady flow, the momentum boundary layer equation can be expressed as

$$\partial u/\partial t = (\mu/\rho)\,(\partial^2 u/\partial y^2) \qquad \text{(A-1)}$$

with the boundary condition $u(o,t) = U_o \cos(ft)$. The solution to the above diffusion type equation is easily obtained. Cebeci extended Stokes flow to include compressible effects (non- isothermal) by consideration of the non-steady momentum equation in the form

$$\rho\,\partial u/\partial t = \partial/\partial y\,(\mu \partial u/\partial y) \qquad \text{(A-2)}$$

and introducing the transformation $dy = \mu dz$ with the product $\overline{\rho\mu}$ representing some average value over the sublayer region, Equation (A-2) becomes

$$\partial u/\partial t = 1/(\bar{\rho}\,\bar{\mu})\,(\partial^2 u/\partial z^2) \qquad \text{(A-3)}$$

The solution to Equation (A-3) subject to boundary conditions from the incompressible development, becomes

$$u/u_0 = \exp(-mz)\,[\cos ft - mz] \qquad \text{(A-4)}$$

where $m = [(f/2)\,\overline{\rho\mu}]^{1/2}$ = constant $u^+_s\,(\overline{\rho\mu}/\nu)^{1/2}$ for $u^+_s = (\tau_w/\bar{\rho})^{1/2}$. The damping function can then be expressed as

$$[1 - \exp(-y^+_w/A^+_s)] \qquad \text{(A-5)}$$

where

$$y^+_w = u^+_w\, y/\nu_w \text{ and } A^+_s = 26\left(\frac{\rho_w}{\bar{\rho}}\right)^{1/2}\left(\frac{\bar{\mu}}{\mu_w}\right) \qquad \text{(A-6)}$$

Here one notes the choice of the constant as the incompressible value of 26.

In the above formulation, one could potentially use a reference enthalpy (Eckert, for example) and a viscous power law relationship instead of the average properties of $\bar{\rho}$ and $\bar{\mu}$. In the former, the equation of state could be assumed such that $\rho \sim 1/T$ and the latter as $\mu = \mu(T)$. In this manner, direct use of the Mach number and wall temperature ratio (T_W/Ta_W) would be obtained to have an explicit compressible and non-isoenergetic function. Most investigators have chosen to use local values for ρ and μ.

A.2 C-S Model with Pressure Gradient and Mass Transfer

Cebeci recognized that the expression given by Equation (A-6) had to be modified to account for incompressible flows with pressure gradients and mass transfer. This was accomplished by redefining the parameter A in terms of a sublayer friction velocity rather than its wall value, such that

$$A = 26\, \nu_w\, (\tau_s/\rho_s)^{-1/2} = A^+\, \nu_w/(\tau_w/\rho_w)^{1/2}$$

By neglecting the convective component in the stream direction in the momentum equation, the friction velocity in the sublayer can be approximated as

$$d\tau_s/dy - (\nu_w/\nu)\,\tau_s = dp/dx \qquad \text{(A-7)}$$

and for a value of $y_s^+ = 11.8$, the solution of Equation (A-7) allows for the damping coefficient to become

$$A^+ = A^+(\nu_w, dp/dx)$$

The damping constant can be expressed as

$$A^+ = 26\,\frac{1}{N}\,(\rho_w/\bar{\rho})^{1/2}\,(\bar{\mu}/\mu_w) \qquad \text{(A-8)}$$

- $\frac{1}{N}$: pressure gradient & mass transfer contribution
- $(\rho_w/\bar{\rho})^{1/2}\,(\bar{\mu}/\mu_w)$: compressible contribution
- 26: incompressible value

where

$$N = \left\{\frac{\bar{\mu}}{\mu_w}\left(\frac{\rho_e}{\rho_w}\right)\frac{P^+}{v_w^+}\left[1 - \exp\left(-11.8\,\frac{\mu_w}{\mu}\,v_w^+\right)\right] + \exp\left(-11.8\,\frac{\mu_w}{\mu}\,v_w^+\right)\right\}^{1/2} \qquad \text{(A-9)}$$

for

$$P^+ = \frac{\nu_e \quad u_e \; du_e/d\chi}{(\tau_w/\rho_w)^{3/2}} = (\mu_e/\rho_e^2)\,(dp/d\chi)/(\tau_w/\rho_w)^{3/2} \qquad \text{(A-10)}$$

$$v_w^+ = v_w/u_\tau$$

A.3 C-S Model with Roughness Effects

In the classic van Driest paper that introduced the damping function for the near wall region, the concept was extended to include rough wall effects. An artificial mixer (vortex generator) was introduced at the wall to mitigate the damping function $(1\text{-}e^{-y/A})$. This implies that the wall roughness encompasses the viscous sublayer such that the stabilizing effect of viscosity is negated and the effect of turbulence is felt all the way to the wall. Observation of experimental data, in law of wall parameters, shows the velocity profile to decrease with increasing roughness height. van Driest noted that the damping effect of the wall extends approximately $y^+ = 60$. As a result, for roughness elements which extend to a value of $y^+ = 60$, the viscous influence of the wall should be nullified.

In order to accommodate the effects of roughness within the near wall viscous region (i.e., $k_r^+ < 60$ where $k_r^+ = u_\tau k_r/\nu_w$ for k_r some r.m.s average height), a local vortex generating factor is introduced. This is accomplished by adding a factor that is similarand on the same order of the damping factor, namely

$$e^{-y^+/26} - e^{-0\,(y^+/26)}$$

Since the vortex generating factor should be allowed to grow with the size of roughness, the factor was modified to a form

$$\exp\,(-60\; y^+/\,26\; k_r^+) \qquad \text{(A-11)}$$

such that at $y^+ = k_r^+ = 60$, the disturbance factor just offsets the damping factor. The mixing length is then expressed as

$$l_m^+ = \kappa y^+ \,[\, 1 - \exp\,(-y^+/26) + \exp\,(-60y^+/k_r^+)] \qquad \text{(A-12)}$$

An examination of the above shows that the van Driest formulation will not decrease any further once the sublayer has been eradicated by a sufficiently large roughness height ($k_r^+ > 60$) which is in conflict with experimental evidence (McDonald-Fish, 1973). In order to allow the damping factor to be in excess of unity, an incremental factor due to roughness is introduced, namely

$$D_{kr} = [\, 1 + k_r^+ / 30y^+] \exp(-2.3y^+/k_r^2) \qquad \text{(A-13)}$$

such that damping becomes

$$D = D_s + D_{kr} \qquad \text{(A-14)}$$

Here, D_S is the original smooth wall damping term and D_{kr} provides the sole means of introducing the effect of roughness into the prediction process. The mixing length is now written as

$$\iota_m^+ = k\, y^+ D \qquad \text{(A-15)}$$

Further comments concerning this development were addressed in the text. It should be noted that the form of Equation (A-15) is similar to that which was recently derived by Krogstad (6-91).

The turbulent viscosity coefficient is obtained from the inner to the outer layer about a switch point defined as follows

$$\mu_t = \begin{cases} \mu_{ti} \text{ @ } y < y_c \\ \mu_{to} \text{ @ } y > y_c \end{cases} \qquad \text{(A-16)}$$

where y_C is the smallest value of y where $\mu_{ti} = \mu_{to}$.

APPENDIX B

B.1 Baldwin-Lomax (B-L) Model

The Baldwin-Lomax(1978) turbulence model is included here for completeness inasmuch as it has become integrated into many industrial codes for direct use or as a standard from which other models are compared. Like the C-S model the B-L model also works well for attached boundary layer flows. However it incorporates features that are more advantageous than the C-S model by eliminating difficulties in the outer-layer length scale that require a knowledge of the boundary layer edge. Moreover, the inner-layer velocity scale uses the magnitude of the vorticity vector as opposed to the shearing strain. This provides 3-D capability for flows where an invariant shearing strain is not well defined. This model has the following features:

$$\mu_{ti} = \rho l^2 |\tilde{\omega}| = \rho (\kappa\, y\, D)^2 |\tilde{\omega}| \qquad \text{(B-1)}$$

where $|\tilde{\omega}|$ is the magnitude of the local vorticity vector and the damping factor D has the same functional form as in the C-S model. The vorticity term has the same form as C-S when the thin-layer assumption is invoked. Baldwin-Lomax chose local values for the fluid properties in the damping coefficient of Equation (A-8) and noted that the compressible contributions become significant only when large temperature gradients occur in the near wall region.

The outer region of the B-L model modifies the Clauser relation of C-S to give

$$\mu_{to} = 0.0268\, \rho\, y_{max}\, F_{max}\, \bar{\gamma}_o \qquad \text{(B-2)}$$

where y_{max} and F_{max} correspond to the values at the location of the maximum value in the vorticity function, $F(y) = yD|\omega|$. The modified Klebanoff intermittency factor is

$$\bar{\gamma}_0 = [\, 1 + 5.5 \left(\frac{0.3\, y}{y_{max}}\right)^6]^{-1} \qquad \text{(B-3)}$$

where one notes that δ is replaced by $y_{max}/0.3$ in Equation (5). The turbulent coefficient switch point is defined as in Equation (10). Table B.1 provides further details.

Table B.1. BALDWIN-LOMAX TURBULENCE MODEL (from Menter, 6-91)

The Baldwin-Lomax Model

The formulation for the eddy viscosity is

$$\nu_t = \begin{cases} (\nu_t)_{inner} & y \le y_{crossover} \\ (\nu_t)_{outer} & y > y_{crossover}, \end{cases} \tag{1}$$

where $y_{crossover}$ is the smallest value of y, for which the inner and the outer formulation are equal.

The inner eddy-viscosity is defined as follows:

$$(\nu_t)_{inner} = l^2|\omega| \tag{2}$$

with

$$l = ky[1 - exp(-y^+/A^+)]. \tag{3}$$

$|\omega|$ is the magnitude of the vorticity and

$$y^+ = \frac{u_\tau y}{\nu_w}. \tag{4}$$

The outer formulation is

$$(\nu_t)_{outer} = KC_{cp}F_{wake}F_{kleb}(y) \tag{5}$$

with

$$F_{wake} = min(y_{max}F_{max}; C_{wk}y_{max}u_{dif}^2/F_{max}). \tag{6}$$

The quantities y_{max} and F_{max} are determined from the function

$$F(y) = y|\omega|(1.0 - exp(-y^+/A^+)). \tag{7}$$

F_{max} is the maximum value of $F(y)$ and y_{max} is the corresponding y location. The function $F_{kleb}(y)$ is the Klebanoff intermittency function:

$$F_{kleb}(y) = \left[1 + 5.5\left(\frac{C_{kleb}y}{y_{max}}\right)^6\right]^{-1}. \tag{8}$$

The quantity u_{dif} is the difference between the maximum and the minimum total velocity in the profile. The constants used are

$A^+ = 26.0$; $C_{cp} = 1.6$; $C_{kleb} = 0.3$;
$C_{wk} = 1.0$; $k = 0.4$; $K = 0.0168$.

APPENDIX C

C.1 Johnson-King Model (J-K): One-Half Equation

The Johnson and King model (11-85) represents a nonequilibrium eddy viscosity model that is formulated by an algebraic eddy-viscosity relation and an ordinary differential equation (ODE) based on a simplification of the turbulent kinetic energy field equation. The ODE is based on the distribution of the maximum turbulent shear-stress which controls the value of the outer eddy-viscosity and ensures that lag effects are accounted for. The model has been successfully used to predict turbulent boundary layer flows including shock interactions. The model has been updated by Johnson-Coakley (11-90) to include a modification to the near wall eddy viscosity formulation as well as incorporating compressibility effects. Menter (6-91) has used the updated version of the J-K model and compared results with two-equation models as well as the Baldwin-Lomax and Baldwin-Barth (1-91) one-equation model. Table C.1 provides the modeling characteristics that include the Johnson-Coakley modifications (table was structured from Menter).

J-K attempted to develop a closure model for a limited class of flows (as opposed to a universal model) which was motivated by the ability of the C-S model to perform with known invalid assumptions of the turbulent stress dependence on local properties of the flow (Boussinesq criteria). Accordingly, the closure model without the requirement to predict the production, dissipation, and diffusion (as is done for two-equation models) was developed. For flows experiencing severe pressure gradients, it was assumed that characterizing convection effects would be essential with diffusion less dominant.

An ODE was developed that considers the maximum Reynolds stress in the stream direction that prescribes the development of $\overline{u'v'}_m$ together with an eddy viscosity distribution across the shear layer that is functionally dependent on $\overline{u'v'}_m$ (subscript m refers to the location of maximum trubulent shear stress). It should be noted that this development is in spirit to that of Norris-Reynolds (1975) and Wolfshtein (1969) where damping of the eddy viscosity (using a turbulence Reynolds number based kinetic energy characteristic velocity) is not a viscous effect but is the result of the near wall reduction of the normal fluctuations $(\overline{v'})^2$ due to pressure-strain and has been verified by direct numerical simulation (Rodi, 1-91).

J-K provided the following functional form for eddy viscosity

$$\nu_t = \nu_{to}[1 - \exp(-\nu_{ti}/\nu_{to})] \qquad \text{(C-1)}$$

where ν_{ti} and ν_{to} represent inner and outer regions of the shear layer and, in effect, can be considered a two-layer model. In Equation (C-1), ν_t is functionally dependent on ν_{to} across most of the shear layer (this is commensurate with production ≈ dissipation which is commonly used by modelers and verified using DNS and experimental data). The outer layer is used to control the rate of growth of $-\overline{u'v'}_m$. The inner-layer eddy viscosity is written as

$$\nu_{ti} = \kappa\, y\, D_{j\text{-}k}\, (\overline{u'v'}_m)^{1/2} \qquad \text{(C-2)}$$

where D_{J-K} is a damping term similar to C-S. The outer-layer is expressed as

$$\nu_{to} = \sigma\,(x)\,(0.0168)\, u_e \delta^* \gamma_0 \qquad \text{(C-3)}$$

where σ (x) represents an unknown modeling parameter (it represents the history effects to account for slow response of the Reynolds stresses to local changes). In the above, the damping term is given as

$$D_{j\text{-}k} = \left[1 - \exp\left(\frac{u_D\, y}{\nu} \Big/ A^+_{j\text{-}k}\right)\right] \qquad \text{(C-4)}$$

for

$$U_D = (\overline{u'v'}_m)^{1/2} \text{ and } A^+_{j\text{-}k} = 17 \qquad \text{(C-5)}$$

It is noted that the damping term represents a modification of the van Driest formulation to account for y dependency instead of y^2. The subscript m denotes evaluation when the Reynolds stress terms $-\overline{u'v'}$ reaches a maximum. In the outer-layer γ_o represents the Klebanoff intermittency function.

Modifications to the J-K model were made by Johnson and Coakley (11-90) that incorporated a compressibility term to the velocity scale of Equation (C-2) that consists of the density ratio $(\rho_m/\rho)^{1/2}$. Length scales are redefined to allow for the J-K model to be used for flows that are less severe than those experienced in separation. Details of these modifications are found in Table C.1 and a discussion of same in the Johnson-Coakley paper.

Table C.1. JOHNSON-KING TURBULENCE MODEL WITH JOHNSON-COAKLEY MODIFICATIONS (from Menter, 6-91)

The Johnson-King Model

The JK-model is a nonequilibrium eddy-viscosity model, which is composed of an algebraic eddy-viscosity formulation and an ordinary differential equation (ODE). The ODE is a simplified Reynolds-stress equation along the path of the maximum turbulent shear-stress. It controls the value of the outer eddy-viscosity ν_{to} and ensures that history effects are properly accounted for.

The model has recently been modified to account for a thin logarithmic region close to the wall which exists even in the presence of strong adverse pressure gradients. This new formulation was used for the present investigation (note that the compressible formulation depends on the variable density).

The eddy viscosity ν_t has the following form:

$$\nu_t = \nu_{to} \tanh(\nu_{ti}/\nu_{to})$$

with ν_{ti} and ν_{to} defined as follows:

$$\nu_{ti} = D^2 \kappa y u_s$$

$$\nu_{to} = \sigma(x)\ (0.0168 u_e \delta^* \gamma)$$

In this formulation δ^* is the displacement thickness of the boundary layer, u_e is the velocity at the edge of the boundary layer and γ is Klebanoff's intermittency function: $\gamma = \frac{1}{1+5.5(y/\delta)^6}$. The velocity scale u_s which appears in the formulation of ν_{ti} is a blending between the friction velocity u_τ and $u_m = (-\overline{u'v'}_m)^{1/2}$(the index m refers to the location of the maximum turbulent shear stress):

$$u_s = u_\tau(1-\gamma_2) + u_m \gamma_2$$

$$\gamma_2 = \tanh(y/L_c')$$

$$L_c' = \frac{u_\tau}{u_\tau + u_m} y_m$$

The damping function D is defined as follows:

$$D = 1 - exp(-\frac{u_D y}{\nu A^+})$$

where $A^+ = 17$ and $u_D = max(u_m, u_\tau)$.

The function $\sigma(x)$ is determined from the solution of the ODE for the maximum Reynolds shear stress:

$$(-\overline{u'v'}_m)^{1/2} = (-\overline{u'v'}_m)_{eq}^{1/2} - \frac{L_m \bar{u}_m}{a_1(-\overline{u'v'}_m)} \frac{d(-\overline{u'v'}_m)}{dx}$$

$$- \frac{L_m}{(-\overline{u'v'}_m)} D_m$$

In this equation L_m is the dissipation length scale, a_1 the ratio of Reynolds shear stress to turbulent kinetic energy, D_m the turbulent diffusion and $(-\overline{u'v'}_m)_{eq}$ the maximum Reynolds shear stress when convection and diffusion are zero. $(-\overline{u'v'}_m)_{eq}$ can be obtained by setting $\sigma(x) = 1$ in Eq. ( ) and replacing u_m in Eqs. ( ) and ( ) by $(u_m)_{eq}$. L_m and D_m are defined as follows:

$$\begin{aligned} L_m &= 0.4 y_m, & y_m/\delta \le 0.225 \\ L_m &= 0.09\delta, & y_m/\delta > 0.225 \end{aligned}$$

$$D_m = \frac{C_{dif}(-\overline{u'v'}_m)^{3/2}}{a_1 \delta [0.7 - (y/\delta)_m]} |1 - \sigma(x)^{1/2}|$$

The value of $\sigma(x)$ is chosen for every profile in a way, that ensures that the actual maximum shear stress:

$$-(\overline{u'v'}_m)_{act} = [\nu_t(\frac{\partial \bar{u}}{\partial y} + \frac{\partial \bar{v}}{\partial x})]_m$$

is equal to the maximum shear stress $(-\overline{u'v'}_m)_{ODE}$ computed from the ODE, Eq. ( ). This is achieved iteratively by

$$\sigma(x)^{n+1} = \sigma(x)^n \frac{(-\overline{u'v'}_m)_{ODE}}{(-\overline{u'v'}_m)_{act}}.$$

Only one iteration is performed per time step. The constants are:

$$\begin{aligned} a_1 &= 0.25 \\ C_{dif} &= 0.5 & \sigma(x) \ge 1 \\ C_{dif} &= 0.0 & \sigma(x) < 1 \end{aligned}$$

APPENDIX D

D.1 Norris-Reynolds Model (N-R)

The authors chose the turbulent kinetic energy closure concept of Prandtl for the eddy viscosity such that

$$\nu_t = \nu_t (k, \iota)$$

where k is prescribed by the turbulent kinetic energy transport equation. The length scale (ι) is algebraically specified. In addition, a closure relationship for the dissipation rate is required such that $\varepsilon = \varepsilon (k, \iota, \nu)$.

The dissipation rate ε which is a length scale in the eddy viscosity relation of Equation (11) and source a term in the kinetic energy field equation, is determined from the relation

$$\nu_t = C_\mu k^{1/2} \iota_\mu \qquad \text{(D-1)}$$

where

$$\iota_\mu = C_\iota y [1 - \exp(-C_3 R_T)] \qquad \text{(D-2)}$$

for

$$R_T = \rho k^{1/2} y/\mu \qquad \text{(D-3)}$$

The eddy viscosity that is proportional to a turbulence Reynolds number is that proposed by Prandtl and asserts that the same large eddies responsible for turbulent mixing are also those containing the bulk of the turbulent motion. The constants C_μ, C_ι and C_3 are to be determined. The one major difference in the damping term of Equation (D-2) is the use of kinetic energy velocity as opposed to the wall shear velocity in the van Driest relation. It is believed that the use of the kinetic energy as a velocity scale is one criteria for the success of simple turbulence models to predict severe pressure gradient flows (since it has been demonstrated that u_τ is no longer linear for these conditions).

Norris-Reynolds and Wolfshtein (1968) allowed for the pressure velocity term and the triple velocity correlation term to be modeled in a gradient diffusion manner such that

$$\frac{\partial}{\partial x_j}\left(\frac{1}{2}\overline{u'_i u'_i u'_j} + \overline{p' u'_i}\,\delta_{ij}/\rho\right) = \frac{\partial}{\partial x_j}(\nu\,\partial k/\partial x_i)$$

For this condition, the source term can be expressed as

$$\varepsilon = C_D k^{3/2}/\iota_\varepsilon \qquad \text{(D-4)}$$

which is based on dimensional analysis and is a result found by Kolmogorov, i.e., $\varepsilon \propto k^{3/2}/\iota$. The outer layer (of the boundary layer) should be controlled by the factor $C_D\, k^{3/2}/\iota$ which will require modification to mitigate the size of the eddies by allowing for the viscosity to be a dissipative agent for the largest eddies.

Variations on the length scale have been introduced. Wolfshtein recommended a form similar to Equation (D-2), namely

$$\iota_\varepsilon = C_\iota\, y\, [\,1 - \exp(-R_T/A_\varepsilon)] \qquad \text{(D-5)}$$

while Norris-Reynolds chose

$$\iota_\varepsilon = C_\iota\, y\, (1 + C_4/R_T)^{-1} \qquad \text{(D-6)}$$

and meets the requirement that dissipation at the wall is non-zero. The dissipation becomes the Kolmogorov function in regions away from the wall and has a functional relation $\varepsilon \propto \nu k/\iota^2$ in the near wall region. Here, one notes that $\iota \propto y$ near the wall as opposed to the van Driest equation which implies $\iota \propto y^2$.

The purpose of the van Driest damping factor is the near wall suppression of ι in order to make the eddy viscosity $\nu_t = \iota^2\,|\partial u/\partial y|$ very small in the sublayer. Accordingly, Equation (D-1) was developed in place of the van Driest damping factor for near wall dissipation. Here the exponential near wall damping factor was removed from the length scale requirement and became a direct part of the eddy viscosity specification. Moreover, the small eddy characteristics of the near wall region are retained while the proper sublayer modeling of the dissipation was achieved and provides a mean flow model that is valid all the way to the wall.

In the above, two distinct lengths have been identified. A length scale appropriate to viscosity (ι_μ) and a length scale characteristic for dissipation (ι_ε). The constants used in the length scales are as follows:

C_μ is same as k-ε (= 0.09)

C_ι is chosen for conformity to the log law

$$C_\iota = \kappa C_\mu^{-3/4} \qquad \text{(D-7)}$$

and

$$C_3 = 26/A_\mu A^+ \qquad \text{(D-8)}$$

where A^+ is equal to 26 (van Driest) and $50. \leq A\mu \leq 70$. Again A^+ can include terms to account for surface roughness and mass transfer as well as pressure gradient conditions. The remaining constants have been selected as:

$$C_D = \text{unity}$$
$$C_4 = 5.3 \qquad \text{(D-9)}$$

Rodi (1-91) noted that damping due to the exponent of Equation (D-2), as described above, is not a viscous effect but is a result of the near wall reduction due to pressure-strain that has been confirmed by direct numerical simulation (DNS). Moreover, damping of the dissipation length ι_ε, Equations (D-5) and (D-6), are not in agreement with DNS data which suggests that $\iota_\varepsilon = C_\iota y$; however, the multiplication by the damping term provides good engineering estimates for wall conditions.

APPENDIX E

E.1 Goldberg Model (6-91)

Recognizing that large-scale eddies are characterized by a development rate much different from small scale dissipative rate, a one-equation model was developed using two-time scales of turbulence. These time-scales provide length scales for diffusion (ι_μ) and dissipation (ι_ε) that are similar to those developed by Norris and Reynolds or Wolfshtein. The velocity scale is determined by solutions to the turbulence kinetic energy PDE (standard form of k-ε). The time scales for the large and small eddies (using the Kolmogorov scale) are given by

$$t_k \sim k/\varepsilon \text{ , Large Scale}$$
$$t_k \sim \sqrt{\nu/\varepsilon}, \text{ Small Scale} \qquad \text{(E-1)}$$

where υ is the kinematic molecular viscosity.

The dissipation is algebraically expressed in terms of k and a length scale throughout the boundary layer as provided by Wolfshtein i.e. Equations (D-4) and (D-5) with a condition on the y coordinate; namely

$$y = \min \{ y, C_\mu \delta/\kappa \} \qquad \text{(E-2)}$$

where δ is the boundary layer thickness and κ the von Karman constant.

Combining Eqs. (E-1) with the velocity scale k, the eddy viscosity associated with the time scales are

$$\nu_k \sim k t_k = C_\mu k^2/\varepsilon \text{ , see eq. (11)} \qquad \text{(E-3)}$$

and

$$\nu_\varepsilon \sim k\, t_\varepsilon = C_\varepsilon k \sqrt{\nu/\varepsilon}\, [1 - \exp(-A_\mu R_T)] \qquad \text{(E-4)}$$

where a damping term has been added to Eq. (E-4). The constant C_ε is obtained from comparison to the N-R results i.e. Eqs. (D-1) and (D-2) such that

$$C_\varepsilon = \sqrt{2}\, \kappa\, C_\mu^{1/4} \qquad \text{(E-5)}$$

Goldstein combined Eqs. (E-3) and (E-4) into a single expression which has the correct behavior in the near-wall region as well as away from the wall, such that

$$C_\mu f_\mu = (C_\mu + C_\varepsilon \sqrt{\nu\varepsilon}/k)\,[1 - \exp(-A_\mu R_T)] \qquad \text{(E-6)}$$

where $C_\mu f_\mu$ has limits pending on $R_T >> 1$ and $R_T << 1$. This led to an eddy viscosity expression for the entire layer given as $\upsilon_\varepsilon = c_\mu f_\mu k^2/\varepsilon$ which is the well accepted constitutive equation for k- ε models using wall damping functions. What makes the Goldstein work different from the other one-equation models is the definition of the length scales. Using the algebraic definition for the length scale (Eqs. D-4 and D-5) together with the velocity scale ($k^{1/2}$) and Eqs. (E-3) and (E-4), the length scales corresponding to large and small scale eddies become

$$l_k = \kappa C_\mu^{1/4} y\,[1 - \exp(-A_\mu R_T)] \qquad \text{(E-7)}$$

$$l_\varepsilon = \left[\frac{2\kappa^3 y}{C_\mu^{1/4} k^{1/2}}\, y\,(1 - \exp(-A_\varepsilon R_T)\right]^{1/2} [1 - \exp(-A_\mu R_T)] \qquad \text{(E-8)}$$

where provisions on y are specified by Eq. (E-2). Arguments are presented relative to scaling criteria of Eq. (E-8) as y ---> o. In particular, the behavior of the turbulence KE in the viscous sublayer that provides a density ratio with the characteristic velocity scale. This was also shown by Gorski (1-86) as well as by the Johnson and Coakley (11-90) correction to the velocity scale of the Johnson and King model. Because of the introduction of a simple multi-scale procedure and its similarity to models that have had demonstrated success, this model should be considered for further evaluation.

APPENDIX F

F.1 Baldwin-Barth Model (B-B) : One and One-Half Equation Model

The B-B turbulence model (1-91) considered a transformation of the basic physical variables in the k-ε transport equations in order to eliminate the numerical difficulties in the near wall region associated with these two-equation models. Table F.1 provides details of the turbulence structure as summarized in the Appendix of the B-B paper. The authors chose a field equation for a turbulence Reynolds number based on an eddy viscosity concept for high Reynolds number flow with the distribution away from the wall governed by $\upsilon_t = C_\mu\, k^2/\varepsilon$ [combines Equations (D-1) and (D-4)]; in particular, the turbulence Reynolds number Re_T is

$$Re_T = k^2/\upsilon\varepsilon \qquad \text{(F-1)}$$

The above is substituted into the standard k- ε equations and the results are combined to provide a one-equation model that encompasses turbulent kinetic energy and its dissipation. Equation (F-1) is rearranged to provide two regions in the shear layer consisting of an outer-layer (k_2)where production is equal to dissipation and an inner- layer (k_1)where production requires damping; namely

$$\varepsilon = k^2/\upsilon\, Re_T = (k_1 + k_2)/\upsilon\, Re_T \qquad \text{(F-2)}$$

For the outer region $\wp = \varepsilon$, and $k_1 >> k_2$, then $k^2 = \upsilon\, Re_T \wp$, and the turbulent kinetic energy becomes

$$k = (\upsilon\, Re_T\, \wp)^{1/2}\ (1 + k_2/k_1) \qquad \text{(F-3)}$$

When Equation (F-3) is substituted into the standard high Reynolds number k-ε equations, there results

$$D(\nu\, Re_T)/Dt = (C_2 - C_1)(\nu\, Re_T \wp)^{1/2} + \left(\nu + \frac{\nu_t}{\sigma_k}\right)\nabla^2(\nu\, Re_T) - \frac{1}{\sigma_\varepsilon}(\nabla \nu_t)\cdot\nabla(\nu\, Re_T) - (2 - C_1)\frac{k_2}{k_1 + k_2}(\nu\, Re_T\ \wp) - (2\ - C_2)\, k_2 \qquad \text{(F-4)}$$

The system is closed by substituting Equation (F-3) into the kinetic energy equation of the k-ε equations to give

$$Dk/Dt = -2\,(\wp/\nu Re_T)^{1/2}\, k_2 - k_2/\nu Re_T + \nabla\cdot\left(\nu + \frac{\nu_t}{\sigma_k}\right)\nabla k \qquad \text{(F-5)}$$

At this junction, the B-B approach follows a path similar to thehybridr modelers (Chen and Patel, 11-88), (Rodi, 1-91). Here, Equation (F-4) is solved for $k_2 \rightarrow 0$ for solution in the high Reynolds number region (which is most of the shear layer) and develops a length scale to accommodate damping in the near wall region. One should keep in mind that since field equations for k-ε were combined, the results represent solutions to the k- ε two-equation model for the regions away from the wall. To accommodate the near wall region, the turbulence Reynolds number is split into two factors

$$Re_T = \tilde{R}e_T \, f_3 \, (\tilde{R}e_T) \qquad \text{(F-6)}$$

where f_3 is a damping function that allows $Re_T \approx \tilde{R}e_T$ for large Reynolds numbers. Using the damping functions similar to those of van Driest or N-R, there results

$$\nu_t = \nu \, C_\mu \, f_\mu \, Re_T = \nu \, C_\mu \, f_\mu \, f_3 \, \tilde{R}e_T \qquad \text{(F-7)}$$

and

$$k^2/\nu \, Re_T = (k_1 + k_2)^2 / \nu \, f_3 \, \tilde{R}e_T \qquad \text{(F-8)}$$

where $k_1^2 = \upsilon \wp Re_T$. Using the thin-layer assumption where $\wp = \upsilon_t \, (U_y)^2$, the field equation becomes

$$D\,\tilde{R}e_T / Dt = (C_2 f_2 - C_1)(C_\mu f_\mu f_3)^{1/2} \tilde{R}e_T \frac{\partial u}{\partial y} + (\nu + \frac{\nu_t}{\sigma_k}) \frac{\partial^2 Re_T}{\partial y^2} - \qquad \text{(F-9)}$$

$$(1/\sigma_\varepsilon)(\partial \nu_t / \partial y) \, \partial (\tilde{R}e_T) / \partial y$$

which becomes the basis for the one-equation model defined in Table F.1. The damping term f_3 has to be selected to allow for k_1 to be the dominate part of k in the near wall region. Details for the selection of the damping function are provided in the B-B paper.

Menter (6-91) compared the B-B model to adverse pressure gradient experimental data as well as other turbulence models. It is not clear what velocity scale was used in the damping terms. It appears that the van Driest shear velocity was used, i.e., y^+ instead of Re_T where U_τ is used in y^+ and $k^{1/2}$ is used in Re_T. It was found that displacements (hence, pressure) were predicted with good accuracy, but could not predict profile shapes in either the inner or outer shear layer regions. Moreover, wall shear-stress distributions are similar to ones produced by the B-L model.

Table F.1. BALDWIN-BARTH ONE-EQUATION TURBULENCE MODEL (from Baldwin-Barth, 1-91)

$$B_1\frac{D(\nu\tilde{R}_T)}{Dt} = (c_{\epsilon_2}f_2 - c_{\epsilon_1})G_1\sqrt{\nu\tilde{R}_T P} + (\nu + \frac{\nu_t}{\sigma_R})G_1\nabla^2(\nu\tilde{R}_T) - \frac{1}{\sigma_\epsilon}(\nabla\nu_t)\cdot\nabla(\nu\tilde{R}_T)$$

In this equation, we use the following functions:

$$\begin{aligned}
\frac{1}{\sigma_\epsilon} &= (c_{\epsilon_2} - c_{\epsilon_1})\sqrt{c_\mu}/\kappa^2 \\
\sigma_R &= 0.25\sigma_\epsilon \\
\nu_t &= c_\mu(\nu\tilde{R}_T)D_1D_2 \\
\mu_t &= \rho\nu_t \\
D_1 &= 1 - \exp\left(-y^+/A^+\right) \\
D_2 &= 1 - \exp\left(-y^+/A_2^+\right) \\
P &= \nu_t\left(\frac{\partial U_i}{\partial x_j} + \frac{\partial U_j}{\partial x_i}\right)\frac{\partial U_i}{\partial x_j} - \frac{2}{3}\nu_t\left(\frac{\partial U_k}{\partial x_k}\right)^2 \\
f_2(y^+) &= \frac{c_{\epsilon_1}}{c_{\epsilon_2}} + (1 - \frac{c_{\epsilon_1}}{c_{\epsilon_2}})(\frac{1}{\kappa y^+} + D_1D_2)(\sqrt{D_1D_2} \\
&\quad + \frac{y^+}{\sqrt{D_1D_2}}(\frac{1}{A^+}\exp(-y^+/A^+)\,D_2 + \frac{1}{A_2^+}\exp(-y^+/A_2^+)\,D_1)) \\
G_1 &= 1 + \frac{(F_R^4 + \epsilon_0/B_2)}{(\omega^4 + B_2F_R^4 + \epsilon_0)} \\
F_R &= \frac{(\nabla\nu\tilde{R}_T)\cdot(\nabla\nu\tilde{R}_T)}{\nu\tilde{R}_T} - \frac{\kappa^2}{c_\mu}|\omega|
\end{aligned}$$

For all calculations we have used the following constants:

$$\begin{aligned}
\kappa &= 0.41, \quad c_{\epsilon_1} = 1.2, \quad c_{\epsilon_2} = 2.0 \\
c_\mu &= 0.09, \quad A^+ = 26, \quad A_2^+ = 10 \\
B_1 &= 0.4, \quad B_2 = 0.01, \quad \epsilon_0 = 10^{-10}
\end{aligned}$$

We also recommend the following boundary conditions for

1. **Solid Walls:** Specify $\tilde{R}_T = 0$.
2. **Inflow** ($\mathbf{V}\cdot\mathbf{n} < 0$): Specify $\tilde{R}_T = (\tilde{R}_T)_\infty < 1$.
3. **Outflow** ($\mathbf{V}\cdot\mathbf{n} > 0$): Extrapolate $\tilde{R}_T$ from interior values.

Since the B-B model is relatively new and untested, further work will be required prior to a full assessment. The N-R damping functions should be considered for the B-B model which incorporate kinetic energy to the 1/2 power ($k^{1/2}$) and uses a modified Kolmogorov function (for length scale) relating kinetic energy dissipation that is applicable throughout the shear layer.

APPENDIX G

Wilcox k-ω Turbulence Model (from Wilcox, 6-91)

For general compressible turbulent fluid flow, the complete sets of equations that constitute the Wilcox k-ω two-equation model and multiscale model are written in terms of Favre mass-averaged quantities as follows.

Conservation of Mass, Momentum and Energy

$$\frac{\partial \rho}{\partial t} + \frac{\partial}{\partial x_j}(\rho u_j) = 0 \qquad (1)$$

$$\frac{\partial}{\partial t}(\rho u_i) + \frac{\partial}{\partial x_j}(\rho u_j u_i) = \frac{\partial}{\partial x_j}[-p\delta_{ji} + \hat{\tau}_{ji}] \qquad (2)$$

$$\frac{\partial}{\partial t}(\rho E) + \frac{\partial}{\partial x_j}(\rho u_j E) = \frac{\partial}{\partial x_j}\left[\hat{\tau}_{ji}u_i - q_j + (\mu + \sigma^* \mu_T)\frac{\partial k}{\partial x_j}\right] \qquad (3)$$

where t is time, x_i is the position vector, u_i is velocity, ρ is density, p is pressure, μ is molecular viscosity, $\hat{\tau}_{ij}$ is the sum of molecular and Reynolds stress tensors, and q_j is the sum of molecular and turbulence heat flux vectors. In Equation (3), the quantities $E = \hat{e} + k + \frac{1}{2}u_i u_i$ and $H = h + k + \frac{1}{2}u_i u_i$ are total energy and total enthalpy, respectively, with $h = \hat{e} + p/\rho$; $\hat{e}$ and h denote internal energy and enthalpy. Also δ_{ij} is the Kronecker delta, and k is the turbulence kinetic energy that is determined by the following equations.

Turbulence Kinetic Energy, Specific Dissipation Rate

$$\frac{\partial}{\partial t}(\rho k) + \frac{\partial}{\partial x_j}(\rho u_j k) = \tau_{ij}\frac{\partial u_i}{\partial x_j} - \beta^* \rho \omega k + \frac{\partial}{\partial x_j}\left[(\mu + \sigma^* \mu_T)\frac{\partial k}{\partial x_j}\right] \qquad (4)$$

$$\frac{\partial}{\partial t}(\rho \omega) + \frac{\partial}{\partial x_j}(\rho u_j \omega) = \alpha \frac{\omega}{k}\tau_{ij}\frac{\partial u_i}{\partial x_j} - \beta \rho \omega^2 - \beta \rho \omega \hat{\xi}(2\Omega_{mn}\Omega_{mn})^{1/2} + \frac{\partial}{\partial x_j}\left[(\mu + \sigma \mu_T)\frac{\partial \omega}{\partial x_j}\right] \qquad (5)$$

The quantity ω is specific dissipation rate, τ_{ij} is Reynolds stress tensor, and μ_T is eddy viscosity. The parameters α, β, β^*, σ, σ^* and $\hat{\xi}$ are closure coefficients whose values are given below. We close the system of equations as follows.

Constitutive Relations

$$\hat{\tau}_{ij} = 2\mu\left[S_{ij} - \frac{1}{3}\frac{\partial u_k}{\partial x_k}\delta_{ij}\right] + \tau_{ij} \qquad (6)$$

$$q_j = -\left[\mu/Pr_L + \mu_T/Pr_T\right]\frac{\partial h}{\partial x_j} \qquad (7)$$

$$\mu_T = \alpha^* \rho k/\omega \qquad \omega \approx \epsilon/K \qquad (8)$$

$$S_{ij} = \frac{1}{2}\left[\frac{\partial u_i}{\partial x_j} + \frac{\partial u_j}{\partial x_i}\right] \quad . \qquad \Omega_{ij} = \frac{1}{2}\left[\frac{\partial u_i}{\partial x_j} - \frac{\partial u_j}{\partial x_i}\right] \qquad (9)$$

The quantities Pr_L and Pr_T are laminar and turbulent Prandtl numbers, respectively, and α^* is an additional closure coefficient that is specified below. We need just one additional constitutive relation for the k-ω model. Specifically, we assume the Reynolds stress tensor is proportional to the mean strain-rate tensor. The resulting relationship is as follows.

Two-Equation-Model Reynolds Stress

$$\tau_{ij} = 2\mu_T\left[S_{ij} - \frac{1}{3}\frac{\partial u_k}{\partial x_k}\delta_{ij}\right] - \frac{2}{3}\rho k \delta_{ij} \qquad (10)$$

The multiscale model computes each component of the Reynolds stress tensor separately. The model introduces two energy scales corresponding to upper and lower partitions of the turbulence energy spectrum. The quantity ρT_{ij} denotes the upper partition contribution to the Reynolds-stress tensor while ρe denotes the energy of the eddies in the lower partition. The additional equations needed for closure are as follows.

Multiscale-Model Reynolds Stress

$$\tau_{ij} = \rho T_{ij} - \frac{2}{3}\rho e \delta_{ij} \qquad (11)$$

$$\frac{\partial}{\partial t}(\rho T_{ij}) + \frac{\partial}{\partial x_k}(\rho u_k T_{ij}) = -P_{ij} + E_{ij} \qquad (12)$$

$$\frac{\partial}{\partial t}[\rho(k-e)] + \frac{\partial}{\partial x_j}[\rho u_j(k-e)] = (1 - \hat{\alpha} - \hat{\beta})\tau_{ij}\frac{\partial u_i}{\partial x_j} - \beta^* \rho \omega k(1 - e/k)^{3/2} \qquad (13)$$

$$E_{ij} = -C_1 \beta^* \omega\left[\tau_{ij} + \frac{2}{3}\rho k \delta_{ij}\right] + \hat{\alpha}P_{ij} + \hat{\beta}D_{ij} + \hat{\gamma}\rho k\left[S_{ij} - \frac{1}{3}\frac{\partial u_k}{\partial x_k}\delta_{ij}\right] + \frac{2}{3}\beta^* \rho \omega k(1-e/k)^{3/2}\delta_{ij} \qquad (14)$$

$$P_{ij} = \tau_{im}\frac{\partial u_j}{\partial x_m} + \tau_{jm}\frac{\partial u_i}{\partial x_m} \quad . \quad D_{ij} = \tau_{im}\frac{\partial u_m}{\partial x_j} + \tau_{jm}\frac{\partial u_m}{\partial x_i} \qquad (15)$$

Finally, these equations involve a number of closure coefficients whose values are given by the following equations.

Closure Coefficients

$$\beta = 3/40, \ \beta^* = 9/100, \ \sigma = 1/2, \ \sigma^* = 1/2 \qquad (16)$$

$$\alpha^* = 1, \ \alpha = \left[\beta(1 + \hat{\xi}\sqrt{\beta^*}) - \sigma\kappa^2\sqrt{\beta^*}\right]/\beta^* \qquad (17)$$

$$\hat{\alpha} = 42/55, \ \hat{\beta} = 6/55, \ \hat{\gamma} = 1/4, \ \hat{\xi} = 1 \qquad (18)$$

APPENDIX H

k-ϵ Turbulence Model
(from Speziale et al., 6-91)

For simplicity, we will restrict our analysis to incompressible turbulent flows (however, the crucial conclusions that will be drawn carry over to compressible flows). The mean velocity $\overline{\mathbf{u}}$ and mean pressure $\overline{p}$ are solutions of the Reynolds averaged Navier-Stokes and continuity equations given by

$$\frac{\partial \overline{u}_i}{\partial t} + \overline{u}_j \frac{\partial \overline{u}_i}{\partial x_j} = -\frac{\partial \overline{p}}{\partial x_i} + \nu \nabla^2 \overline{u}_i + \frac{\partial \tau_{ij}}{\partial x_j} \tag{1}$$

$$\frac{\partial \overline{u}_i}{\partial x_i} = 0 \tag{2}$$

where $\tau_{ij} = -\overline{u_i' u_j'}$ is the Reynolds stress tensor, ν is the kinematic viscosity, and the usual Einstein summation convention applies to repeated indices. We will consider the commonly used two-equation models based on an eddy viscosity where

$$\tau_{ij} = -\frac{2}{3} K \delta_{ij} + \nu_T \left(\frac{\partial \overline{u}_i}{\partial x_j} + \frac{\partial \overline{u}_j}{\partial x_i} \right) \tag{3}$$

and

$$\nu_T = C_\mu \frac{K^2}{\varepsilon} \tag{4}$$

given that $K \equiv \frac{1}{2}\overline{u_i' u_i'}$ is the turbulent kinetic energy, $\varepsilon = \nu \overline{\partial u_i'/\partial x_j \, \partial u_i'/\partial x_j}$ is the turbulent dissipation rate, and C_μ is a dimensionless constant at high turbulence Reynolds numbers. In two-equation models, transport equations are solved for any two linearly independent variables constructed from K and ε. In the $K-\varepsilon$ model, modeled transport equations for K and ε are solved; in the $K-\omega$ model, modeled transport equations for K and the reciprocal turbulent time scale $\omega \equiv \varepsilon/K$ are solved; and in the $K-\tau$ model, modeled transport equations for K and the turbulent time scale $\tau \equiv K/\varepsilon$ are solved. The exact transport equations for K and ε are as follows [8]:

$$\frac{DK}{Dt} = \tau_{ij} \frac{\partial \overline{u}_i}{\partial x_j} - \varepsilon - \mathcal{D} + \nu \nabla^2 K \tag{5}$$

$$\frac{D\varepsilon}{Dt} = \mathcal{P}_\varepsilon - \Phi_\varepsilon - \mathcal{D}_\varepsilon + \nu \nabla^2 \varepsilon \tag{6}$$

where $D/Dt = \partial/\partial t + \overline{\mathbf{u}} \cdot \nabla$. In (5) - (6),

$$\mathcal{D} = \frac{\partial}{\partial x_i} \left(\frac{1}{2} \overline{u_j' u_j' u_i'} + \overline{p' u_i'} \right) \tag{7}$$

$$\begin{aligned} \mathcal{D}_\varepsilon &= 2\nu \frac{\partial}{\partial x_i} \left(\overline{\frac{\partial p'}{\partial x_j} \frac{\partial u_i'}{\partial x_j}} \right) \\ &\quad + \nu \frac{\partial}{\partial x_j} \left(\overline{u_j' \frac{\partial u_i'}{\partial x_k} \frac{\partial u_i'}{\partial x_k}} \right) \end{aligned} \tag{8}$$

are turbulent transport terms, and

$$\begin{aligned} \mathcal{P}_\varepsilon &= -2\nu \overline{\frac{\partial u_i'}{\partial x_j} \frac{\partial u_k'}{\partial x_j} \frac{\partial \overline{u}_i}{\partial x_k}} - 2\nu \overline{\frac{\partial u_j'}{\partial x_i} \frac{\partial u_j'}{\partial x_k} \frac{\partial \overline{u}_i}{\partial x_k}} \\ &\quad - 2\nu \overline{\frac{\partial u_i'}{\partial x_k} \frac{\partial u_i'}{\partial x_j} \frac{\partial u_k'}{\partial x_j}} - 2\nu \overline{u_k' \frac{\partial u_i'}{\partial x_j} \frac{\partial^2 \overline{u}_i}{\partial x_j \partial x_k}} \end{aligned} \tag{9}$$

$$\Phi_\varepsilon = 2\nu^2 \overline{\frac{\partial^2 u_i'}{\partial x_j \partial x_k} \frac{\partial^2 u_i'}{\partial x_j \partial x_k}} \tag{10}$$

are, respectively, the production and destruction of dissipation terms.

It is a straightforward matter to show that near a wall

$$K = O(y^2), \ \varepsilon = O(1), \ \tau = O(y^2) \tag{14}$$

$$\frac{\partial \overline{u}}{\partial y} = O(1), \ \overline{u'^2} = O(y^2), \ \overline{u'v'} = O(y^3) \tag{15}$$

$$\overline{v'^2} = O(y^4), \ \overline{w'^2} = O(y^2), \ \mathcal{P} = O(y^3) \tag{16}$$

$$\mathcal{D} = O(y), \ \mathcal{P}_\varepsilon = O(y), \ \Phi_\varepsilon = O(1) \tag{17}$$

$$\mathcal{D}_\varepsilon = O(1), \ \nabla^2 K = O(1), \ \nabla^2 \varepsilon = O(1) \tag{18}$$

where $\mathcal{P} \equiv \tau_{ij} \partial \overline{u}_i / \partial x_j$ is the turbulence production.

An asymptotic analysis of the $K-\varepsilon$ model will be conducted first. In the $K-\varepsilon$ model, the eddy viscosity near a wall is taken to be of the form

$$\nu_T = C_\mu f_\mu \frac{K^2}{\varepsilon}. \tag{19}$$

The asymptotic analysis presented in this section indicates that $f_\mu = O(1/y)$ near the wall since, due to (15), ν_T must be of $O(y^3)$ in this region. Of course, sufficiently far from the wall f_μ assumes a value of 1. (C_μ is a constant which is typically taken to be 0.09). The turbulent transport term $\mathcal{D}$ in the kinetic energy equation (5) is modeled using a gradient transport hypothesis:

$$\mathcal{D} = -\frac{\partial}{\partial x_i} \left(\frac{\nu_T}{\sigma_K} \frac{\partial K}{\partial x_i} \right) \tag{20}$$

APPENDIX I

Situ and Schetz, (6-91) considered compressibility effects from the Reynolds stresses for thin shear layers. Here shear-stress is given as

$$\tau'_{xy} = -\bar{\rho}\,\overline{u'v'} - \bar{u}\,\overline{\rho'v'} - \bar{v}\,\overline{\rho'u'} - \overline{\rho'u'v'} \qquad \text{(I-1)}$$

allowing for u > > u and the neglecting the triple correlation, the shear becomes

$$\tau'_{xy} = -\bar{\rho}\,\overline{u'v'} - \bar{u}\,\overline{\rho'v'} \qquad \text{(I-2)}$$

Shang (7-74) considered the first and last terms on the RHS of eq. (I-1) to introduce compressibility. The impact of the triple correlation, as reported by Marvin Coakley (11-89), had no effect up to Mach 5, but showed some effect at higher Mach number conditions.

Situ and Schetz provided for a length scale for the scale for the second term on the RHS of equation (I-2) which together with gradient transport theory establishes an effective turbulent Schmidt number for mixtures or a turbulent Prandtl number for homogeneous gases. The Reynolds stress terms in equation (I-2) are given as

$$-\bar{\rho}\,\overline{u'v'} = \bar{\rho}\,\iota_m^2\,(\partial u/\partial y)^2 \qquad \text{(I-3)}$$

$$-u\,\overline{\rho'v'} = \iota_m^2\,\frac{u}{s}\,\frac{\partial \rho}{\partial y}\,\frac{\partial u}{\partial y} \qquad \text{(I-4)}$$

for

$$S = C_u\,\iota_u / C_\rho\,\iota_\rho \qquad \text{(I-5)}$$

$$\iota_m^2 = \text{Constant} \bullet C_u\,\iota_u^2$$

In the above, one recognizes the usual definition of the Prandtl concept, Equation (I-3), and the introduction of the new length ι_ρ due to compressibility. For thin layers

$$\mu_t = \iota_m^2 \left| \rho\,\frac{\partial u}{\partial y} + \frac{u}{s}\,\frac{\partial \rho}{\partial y} \right| \qquad \text{(I-6)}$$

where from gradient transport theory it is shown that

$$-\overline{\rho'v'} = D_t\,\frac{\partial \rho}{\partial y} = \frac{\mu_t}{Sc_t} = \iota_m^2\,\frac{\rho}{Sc_t}\,\frac{\partial u}{\partial y} \qquad \text{(I-7)}$$

and

$$-\bar{u}\,\overline{\rho'v'} \equiv \iota_m^2\,\frac{u}{Sc_t}\,\frac{\partial \rho}{\partial y}\,\frac{\partial u}{\partial y} \qquad \text{(I-8)}$$

If the turbulent Lewis number is unity, $S \cong P_{rt}$ and one can allow for $S \cong P_{rt} \cong S_{cr} \cong 0.8$.

The authors compared their work to six test cases that include compressible flow over a flat plate (M = 4.67 and 6.55), tangential slot injection (sonic jet and supersonic jet) and shock/boundary layer interacting flows. While the new model does not invoke ad-hoc techniques and success was shown to a range of test conditions, it is not clear what form of mixing length characteristics were used by the authors. Recognizing use of the original Prandtl concept as stated by the authors, they did not show if damping was used, if the length scale was proportional to y of y^2, or what form of characteristic velocity scale was used, i.e., shear velocity or a form of the kinetic energy. An inspection of the original AIAA paper (89-1821) did not reveal any further insight.

Since the method is new and has not been tested in the literature by independent sources, this work will require further evaluation. The use of the double length scale which is also provided by the hybrid modelers (i.e., ι_μ and ι_ε for viscous and diffusion effects) and the ability of the model to handle the wall jet problem warrant further investigation.